

การเตรียมโพลีเมอร์แบบแข็งโดยใช้สารประกอบเชิงซ้อนของโลหะผสมและเพนทาเอทิลีน
เฮกซามีนเป็นตัวเร่งปฏิกิริยา

นางสาวอุษอร พรหมนิมิตร

วิทยานิพนธ์นี้เป็นส่วนหนึ่งของการศึกษาตามหลักสูตรปริญญาวิทยาศาสตรมหาบัณฑิต
สาขาวิชาปิโตรเคมีและวิทยาศาสตร์พอลิเมอร์
คณะวิทยาศาสตร์ จุฬาลงกรณ์มหาวิทยาลัย
ปีการศึกษา 2554
ลิขสิทธิ์ของจุฬาลงกรณ์มหาวิทยาลัย

บทคัดย่อและแฟ้มข้อมูลฉบับเต็มของวิทยานิพนธ์ตั้งแต่ปีการศึกษา 2554 ที่ให้บริการในคลังปัญญาจุฬาฯ (CUIR)
เป็นแฟ้มข้อมูลของนิสิตเจ้าของวิทยานิพนธ์ที่ส่งผ่านทางบัณฑิตวิทยาลัย

The abstract and full text of theses from the academic year 2011 in Chulalongkorn University Intellectual Repository (CUIR)
are the thesis authors' files submitted through the Graduate School.

PREPARATION OF RIGID POLYURETHANE FOAMS USING MIXED METAL
COMPLEXES AND PENTAETHYLENEHEXAMINE AS CATALYSTS

Miss Ruchuon Promnimit

A Thesis Submitted in Partial Fulfillment of the Requirements
for the Degree of Master of Science Program in Petrochemistry and Polymer Science
Faculty of Science
Chulalongkorn University
Academic Year 2011
Copyright of Chulalongkorn University

Thesis Title PREPARATION OF RIGID POLYURETHANE FOAMS
 USING MIXED METAL COMPLEXES AND
 PENTAETHYLENEHEXAMINE AS CATALYSTS
By Miss Ruchuon Prommimit
Field of Study Petrochemistry and Polymer Science
Thesis Advisor Associate Professor Nuanphun Chantarasiri, Ph. D.
Thesis Co-advisor Duangruthai Sridaeng, Ph. D.

Accepted by the Faculty of Science, Chulalongkorn University in
Partial Fulfillment of the Requirements for the Master's Degree

.....Dean of the Faculty of Science
(Professor Supot Hannongbua, Dr.rer.nat.)

THESIS COMMITTEE

..... Chairman
(Assistant Professor Warinthorn Chavasiri, Ph. D.)

..... Thesis Advirsor
(Associate Professor Nuanphun Chantarasiri, Ph. D.)

..... Thesis Co-advirsor
(Duangruthai Sridaeng, Ph. D.)

..... Examiner
(Associate Professor Voravee P. Hoven, Ph. D.)

..... External Examiner
(Boontana Wannalarse, Ph. D.)

ถูชอร์ พรหมนิมิตร: การเตรียมโฟมพอลิยูรีเทนแบบแข็งโดยใช้สารประกอบเชิงซ้อนของ โลหะผสมและเพนทาเอทิลีนเฮกซามีนเป็นตัวเร่งปฏิกิริยา (PREPARATION OF RIGID POLYURETHANE FOAMS USING MIXED METAL COMPLEXES AND PENTA ETHYLENEHEXAMINE AS CATALYSTS) อ. ที่ปรึกษาวิทยานิพนธ์หลัก: รศ. ดร. นवलพรรณ จันทศิริ, อ. ที่ปรึกษาวิทยานิพนธ์ร่วม: ดร. ดวงฤทัย ศรีแดง, 103 หน้า.

วัตถุประสงค์หลักของงานวิจัยนี้ คือ การพัฒนาตัวเร่งปฏิกิริยาสำหรับเตรียมพอลิยูรีเทน โฟมแบบแข็ง โดยใช้สารประกอบเชิงซ้อนของโลหะ-แอมีน [$M_1(\text{pentaen})$]; ($M_1 = \text{Cu, Zn, Co, Ni}$ และ Mn) และสารประกอบเชิงซ้อนของโลหะผสม-แอมีน [$M_1(\text{pentaen}):M_2(\text{pentaen})$]; ($M_1 = \text{Cu}$ และ $M_2 = \text{Zn, Co, Ni}$ และ Mn) ซึ่งเตรียมจากเกลือแอสีเทตของโลหะกับเพนทาเอทิลีนเฮกซามีน เป็นตัวเร่งปฏิกิริยา ตัวเร่งปฏิกิริยาที่เตรียมขึ้นจะนำมาพิสูจน์เอกลักษณ์ด้วยเทคนิค ไออาร์สเปกโทรสโกปี ยูวี-วิสทิเบิลสเปกโทรสโกปี และการวิเคราะห์ธาตุ หลังจากเตรียมตัวเร่งปฏิกิริยาได้แล้ว จะนำตัวเร่งปฏิกิริยามาเตรียมพอลิยูรีเทนโฟม โดยศึกษาเวลาในการเกิดปฏิกิริยาของโฟม สมบัติทางกายภาพ และสมบัติเชิงกลของพอลิยูรีเทนโฟมเปรียบเทียบกับไดเมทิลไซโคลเฮกซิลแอมีน (DMCHA) ซึ่งเป็นตัวเร่งปฏิกิริยาอ้างอิงที่ใช้ทางการค้า หากการเปลี่ยนแปลงของหมู่ไอโซไซยานาต และอัตราส่วนระหว่างพอลิไอโซไซยานูเรตต่อพอลิยูรีเทนในพอลิยูรีเทนโฟมโดยใช้เทคนิคเอทีอาร์-ไออาร์

จากผลการทดลองพบว่าตัวเร่ง $\text{Cu}(\text{pentaen}):Zn(\text{pentaen})$ สามารถเร่งปฏิกิริยาการเกิดพอลิยูรีเทนโฟมได้ดีเทียบเท่ากับตัวเร่งปฏิกิริยาอ้างอิงที่ใช้ทางการค้า (DMCHA) และนอกจากนี้ยังพบว่าความทนทานต่อแรงกดอัด (compressive strength) ของพอลิยูรีเทนโฟมที่เร่งปฏิกิริยาด้วย $\text{Cu}(\text{pentaen}):Zn(\text{pentaen})$ มีค่าสูงกว่าโฟมที่เตรียมขึ้นด้วยตัวเร่งทางการค้า (DMCHA) โดยค่าความทนทานต่อแรงกดอัดของโฟม มีค่าเพิ่มขึ้นจาก 228.0 เป็น 321.5 kPa เมื่อความหนาแน่นของโฟมเพิ่มขึ้นจาก 40.8 เป็น 47.5 kg/m^3 จากการศึกษาพื้นฐานวิทยาของพอลิยูรีเทนโดยใช้เทคนิคสแกนนิ่งอิเล็กตรอนไมโครสโคป พบว่าโฟมที่เตรียมได้จาก $\text{Cu}(\text{pentaen}):Zn(\text{pentaen})$ มีขนาดเซลล์เล็กกว่าโฟมที่เตรียมได้จาก DMCHA ดังนั้นจึงส่งผลให้โฟมที่เตรียมจาก $\text{Cu}(\text{pentaen}):Zn(\text{pentaen})$ มีสมบัติการเป็นฉนวนทางความร้อนดีกว่าโฟมที่เตรียมจาก DMCHA

สาขาวิชา ปิโตรเคมีและวิทยาศาสตร์พอลิเมอร์...ลายมือชื่อนิสิต.....

ปีการศึกษา.....2554.....ลายมือชื่อ อ. ที่ปรึกษาวิทยานิพนธ์หลัก.....

ลายมือชื่อ อ. ที่ปรึกษาวิทยานิพนธ์ร่วม.....

5272510123 : MAJOR PETROCHEMISTRY AND POLYMER SCIENCE

KEYWORDS : MIXED METAL COMPLEX/ RIGID POLYURETHANE FOAM/
CATALYST

RUCHUON PROMNIMIT: PREPARATION OF RIGID POLYURETHANE FOAMS USING MIXED METAL COMPLEXES AND PENTAETHYLENE HEXAMINE AS CATALYSTS. ADVISOR: ASSOC. PROF. NUANPHUN CHANTARASIRI, Ph. D., CO-ADVISOR: DUANGRUTHAI SRIDAENG, Ph. D., 103 pp.

The development of catalysts for rigid polyurethane (RPUR) foam is the main objective of this research. The catalysts employed were metal-amine complexes $[M_1(\text{pentaen})]$; ($M_1 = \text{Cu, Zn, Co, Ni and Mn}$) and mixed metal-amine complexes $[M_1(\text{pentaen}):M_2(\text{pentaen})]$; ($M_1 = \text{Cu; } M_2 = \text{Zn, Co, Ni and Mn}$), which were prepared from metal acetates and pentaethylenhexamine (pentaen). FTIR, UV-vis spectroscopy and elemental analysis were used to characterize the catalysts. The metal complexes were used as the catalysts in the preparation of RPUR foams. The reaction times, physical and mechanical properties of the prepared foams were compared with that prepared using commercial catalyst, N,N-dimethylcyclohexylamine (DMCHA). ATR-IR technique was used to determine polyisocyanurate:polyurethane (PIR:PUR) ratio and isocyanate (NCO) conversion in the RPUR foam.

RPUR foams catalyzed by $\text{Cu}(\text{pentaen}):\text{Zn}(\text{pentaen})$ had a similar catalytic activity when compared with foams catalyzed by commercial catalyst (DMCHA). Furthermore, the compressive strengths of RPUR foams catalyzed by $\text{Cu}(\text{pentaen}):\text{Zn}(\text{pentaen})$ were better than that catalyzed by DMCHA. The compressive strength of RPUR foam catalyzed by $\text{Cu}(\text{pentaen}):\text{Zn}(\text{pentaen})$ increased from 228.0 to 321.5 kPa with an increasing density from 40.8 to 47.5 kg/m^3 . SEM micrographs of foam prepared from $\text{Cu}(\text{pentaen}):\text{Zn}(\text{pentaen})$ had smaller cell size than that prepared from DMCHA. Therefore, the thermal insulation properties of RPUR foam prepared from $\text{Cu}(\text{pentaen}):\text{Zn}(\text{pentaen})$ was better than that prepared from DMCHA.

Field of Study: Petrochemistry and Polymer Science Student's Signature.....

Academic Year: 2011 Advisor's Signature.....

Co-advisor's Signature.....

ACKNOWLEDGEMENTS

The author would like to express my deep gratitude to my advisor, Associate Professor Dr. Nuanphun Chantarasiri for guidance, supervision and helpful suggestion throughout the course of this research, and Dr. Duangruthai Sridaeng, co-advisor, for the valuable advice.

The author also would like to thank to Assistant Professor Dr. Warinthorn Chavasiri, Associate Professor Dr. Voravee P. Hoven and Dr. Boontana Wannalerse, for serving as chairman and member of thesis committee whose comment have been especially valuable.

Definitely, this research cannot be completed without kindness and helpful of many people. Firstly, I would like to thank Huntsman (Thailand) Co., Ltd. and The Metallurgy and Materials Science Research Institute for their chemical and SEM support, respectively. Absolutely, I am grateful to the Program of Petrochemistry and Polymer Science, Chulalongkorn University for financial support and furnishing many facilities in my research.

I sincerely thank Department of Chemistry, Chulalongkorn University and Scientific and Technological Research Equipment Center, Chulalongkorn University. In addition, I also thank members of Supramolecular Chemistry Research Unit for their encouragement and generous helps. Furthermore, many thanks are going to generous help of my friends and whose suggestion and support are throughout this research. Finally, I own deep gratitude to my family, especially my father and mother for their love and encouragement.

CONTENTS

	Page
ABSTRACT (THAI).....	iv
ABSTRACT (ENGLISH).....	v
ACKNOWLEDGEMENTS.....	vi
CONTENTS.....	vii
LIST OF TABLES.....	xi
LIST OF FIGURES.....	xiv
LIST OF SCHEMES.....	xviii
LIST OF ABBREVIATIONS.....	xix
CHAPTER I INTRODUCTION.....	1
CHAPTER II THEORY AND LITERATURE REVIEWS.....	4
2.1 Raw materials.....	4
2.1.1 Isocyanates.....	4
2.1.2 Polyols.....	7
2.1.3 Surfactants.....	9
2.1.4 Blowing agents.....	10
2.1.5 Catalysts.....	11
2.2 Reaction mechanism.....	14
2.3 Chemistry.....	17
2.3.1 Primary reaction of isocyanates.....	17
2.3.2 Secondary reaction of isocyanates.....	19
2.4 Formulations.....	20
2.5 Mechanical properties.....	21
2.6 Literature reviews.....	24
CHAPTER III EXPERIMENTAL.....	29
3.1 Chemical and raw materials.....	29
3.2 Synthetic procedures.....	30
3.2.1 Synthesis of metal-amine complexes.....	30

	Page
3.2.1.1 Synthesis of copper-pentaethylenehexamine complex [Cu(pentaen)].....	30
3.2.1.2 Synthesis of zinc-pentaethylenehexamine complex [Zn(pentaen)].....	31
3.2.2 Synthesis of mixed metal-amine complex.....	32
3.2.2.1 Synthesis of copper-zinc pentaethylenehexamine complex [Cu(pentaen):Zn(pentaen)].....	32
3.2.3 Synthesis of metal complexes in water[W_M ₁ (pentaen)].....	34
3.3.3 Rigid polyurethane (RPUR) foam preparations.....	35
3.4 Instrumentation.....	37
3.5 Physical and Mechanical properties of RPUR foam.....	39
CHAPTER IV RESULTS AND DISCUSSION	40
4.1 Synthesis of metal amine [M ₁ (pentaen)] and mixed metal-amine complexes[M ₁ (pentaen):M ₂ (pentaen)].....	40
4.2 Characterization of copper-pentaethylenehexamine complex synthesized at the mole ratio of Cu(OAc) ₂ :pentaen = 1:1.....	41
4.2.1 IR spectroscopy of Cu(pentaen) complex.....	41
4.2.2 UV-visible spectroscopy of Cu(pentaen) complex.....	42
4.2.3 Determination of metal amount in Cu(pentaen) complex by flame atomic spectrometry (FAAS).....	43
4.2.4 Elemental analysis of Cu(pentaen) complex.....	44
4.2.5 Mass spectrometry of Cu(pentaen) complex.....	44
4.3 Characterization of zinc-complex synthesized at the mole ratio of Zn(OAc) ₂ :pentaen = 1:1.....	45
4.3.1 IR spectroscopy of Zn(pentaen) complex.....	45
4.3.2 UV-visible spectroscopy of Zn(pentaen) complex.....	46
4.3.3 Determination of metal amount in Zn(pentaen) complex by flame atomic spectrometry (FAAS).....	46
4.3.4 Elemental analysis of Zn(pentaen) complex.....	47

	Page
4.3.5 Mass spectrometry of Zn(pentaen) complex.....	47
4.4 Characterization of copper:zinc-complex synthesized at the mole ratio of Cu(OAc) ₂ :Zn(OAc) ₂ :pentaen = 0.5:0.5:1.....	48
4.4.1 IR spectroscopy of Cu(pentaen):Zn(pentaen) complex.....	48
4.4.2 UV-visible spectroscopy of Cu(pentaen):Zn(pentaen) complex.....	49
4.4.3 Determination of metal amount in Cu(pentaen):Zn(pentaen) complex by flame atomic spectrometry (FAAS).....	50
4.4.4 Elemental analysis of Cu(pentaen):Zn(pentaen) complex.....	50
4.4.5 Mass spectrometry of Cu(pentaen):Zn(pentaen) complex.....	51
4.5 Preparation of rigid polyurethane (RPUR) foams.....	52
4.5.1 Preparation of RPUR catalyzed by metal complexes.....	52
4.5.2 Reaction times.....	53
4.5.2.1 An effect of mole ratio to RPUR foam properties.....	53
4.5.2.2 Effect of catalyst content on reaction time of RPUR foams.....	55
4.5.3 Apparent density.....	60
4.5.3.1 Effect of NCO indexes on foam density.....	61
4.5.3.2 Effect of catalyst quantity on foam density.....	62
4.5.3.3 Effect of blowing agent quantity on foam density.....	64
4.5.4 Foaming temperature.....	64
4.5.5 Characterization of RPUR foams.....	66
4.5.6 NCO conversion of RPUR foams.....	68
4.6 Compressive properties of RPUR foams.....	72
4.7 RPUR Foams Morphology.....	76
4.7.1 Effect of blowing agent on morphology of RPUR foam.....	77
4.8 Thermal conductivity.....	79
4.9 Thermal stability.....	79

CHAPTER V CONCLUSION	83
5.1 Conclusion.....	83
5.2 Suggestion for future work.....	84
REFERENCES	86
APPENDICES	90
APPENDIX A.....	91
APPENDIX B.....	97
VITAE	103

LIST OF TABLES

	Page
Table 2.1 Chemical Structure of TDI.....	5
Table 2.2 Chemical Structure of MDI.....	6
Table 2.3 Polyol for polyurethane manufacture.....	7
Table 2.4 Examples of commercial polyols.....	8
Table 2.5 Catalysts for use in rigid polyurethane foams manufacture.....	11
Table 3.1 Specifications of polyether polyol (Raypol [®] 4221).....	29
Table 3.2 Composition of starting materials in the preparation of metal complexes prepared at different M(OAc) ₂ :pentaen mole ratios.....	33
Table 3.3 Composition of starting materials in the preparation of mixed metal complexes at M ₁ (OAc) ₂ :M ₂ (OAc) ₂ :pentaen mole ratio of 0.5:0.5:1	33
Table 3.4 RPUR foam formulations at different NCO indexes (in part by weight unit).....	35
Table 3.5 RPUR foam formulations at different NCO indexes (in gram unit, cup test).....	36
Table 3.6 Characteristic IR bands of RPUR foam.....	37
Table 4.1 Analytical Characteristics of the FAAS method.....	43
Table 4.2 Elemental analysis (%C, %H, and %N) of Cu(pentaen).....	44
Table 4.3 Analytical Characteristics of the FAAS method.....	46
Table 4.4 Elemental analysis (%C, %H, and %N) of Zn(pentaen).....	47
Table 4.5 Analytical Characteristics of the FAAS method.....	50
Table 4.6 Elemental analysis (%C, %H, and %N) of Cu(pentaen):Zn(pentaen).....	50
Table 4.7 RPUR foams formulation catalyzed by metal complexes at different NCO indexes.....	52
Table 4.8 Reaction times of RPUR foams prepared at NCO indexes of 100 catalyzed by metal complexes prepared at different M(OAc) ₂ :pentaen mole ratios.....	54
Table 4.9 Reaction times of RPUR foams prepared at NCO indexes of 100 catalyzed by mixed metal complexes prepared at M ₁ (OAc) ₂ :M ₂ (OAc) ₂ :pentaen mole ratio of 0.5:0.5:1.....	55

	Page
Table 4.10 Reaction times of RPUR foams catalyzed by Cu(pentaen) and Zn(pentaen).....	56
Table 4.11 The reaction time of RPUR foams catalyzed by M(pentaen) and W_(pentaen) prepared at NCO index 100.....	57
Table 4.12 Maximum core temperature of PUR foam catalyzed by M(pentaen) at different NCO indexes.....	65
Table 4.13 Wavenumber of the functional groups used in calculation.....	69
Table 4.14 NCO conversions and PIR:PUR ratio of RPUR foams prepared by M(pentaen) at different NCO indexes.....	71
Table 4.15 NCO conversions and PIR:PUR ratio of RPUR foams prepared by W_M(pentaen) complexes catalyzed in water at different NCO indexes.....	72
Table 4.16 The compressive strength of RPUR foam with different cell size	78
Table 4.17 The thermal conductivity of RPUR foams at NCO index of 150 with different cell size.....	79
Table 4.18 TGA data of RPUR foam catalyzed by various metal complexes catalysts.....	80
Table 5.1 RPUR foams conclusion.....	85
Table A1 Isocyanate quantity at different NCO indexes in the above formulations.....	93
Table A2 Free NCO absorbance peak area in PMDI (MR-200) from ATR-IR.....	93
Table A3 NCO conversion of RPUR foam catalyzed by DMCHA at different NCO indexes.....	94
Table A4 NCO conversion of RPUR foam catalyzed by Cu(pentaen) at different NCO indexes.....	95
Table A5 NCO conversion of RPUR foam catalyzed by Cu(pentaen):Zn(pentaen) at different NCO indexes.....	95
Table A6 NCO conversion of RPUR foam catalyzed by Zn(pentaen) at different NCO indexes.....	95

	Page
Table A7 NCO conversion of RPUR foam catalyzed by W_Cu(pentaen) at different NCO indexes.....	96
Table A8 NCO conversion of RPUR foam catalyzed by W_Cu(pentaen):Zn(pentaen) at different NCO indexes.....	96
Table A9 NCO conversion of RPUR foam catalyzed by W_Zn(pentaen) at different NCO indexes.....	96
Table B1 Reaction times and physical properties of RPUR foams catalyzed by metal acetate and amine.....	97
Table B2 Formulations, reaction times, physical and mechanical properties of RPUR foams catalyzed by different metal complexes.....	98
Table B3 Formulations, reaction times, physical and mechanical properties of RPUR foams catalyzed by different metal complexes.....	99
Table B4 Formulations, reaction times and physical properties of RPUR foams catalyzed by different metal complexes.....	100
Table B5 Formulations, reaction times and physical properties of RPUR foams catalyzed by different complexes.....	101
Table B6 Formulations, reaction times and physical properties of RPUR foams catalyzed by different complexes.....	102

LIST OF FIGURES

	Page
Figure 2.1 The chemical structures of polymeric MDI.....	6
Figure 2.2 Structure of polyether polyol based sorbitol and sucrose used in the PUR foams.....	9
Figure 2.3 Structure of silicone surfactants used in PUR foams manufacture.....	10
Figure 2.4 Structure of commercial catalysts used in rigid polyurethane foams manufacture.....	12
Figure 2.5 Compression load deflection test rig.....	22
Figure 2.6 Schematic representation of closed cell deformation.....	22
Figure 2.7 Typical compression stress-strain curve for rigid foams.....	23
Figure 2.8 An example of metal-amine complex; Cu(pentaen) and Zn(pentaen).....	28
Figure 2.9 An example of mixed metal-amine complex; Cu(pentaen):Zn(pentaen).....	28
Figure 2.10 N, N-dimethylcyclohexyl amine (DMCHA) (ref.).....	28
Figure 3.1 RPUR foams processing.....	36
Figure 4.1 IR spectra of (a) pentaethylenehexamine (b) Cu(OAc) ₂ ; (c) Cu(pentaen) synthesized at the mole ratio of Cu(OAc) ₂ :pentaen = 1:1.....	42
Figure 4.2 UV spectra of (a) Cu(OAc) ₂ ; (b) Cu(pentaen) and (c) W_Cu(pentaen) synthesized at the mole ratio of Cu(OAc) ₂ :pentaen = 1:1.....	43
Figure 4.3 Mass spectrum of Cu(pentaen) synthesized at the mole ratio of Cu(OAc) ₂ :pentaen = 1:1.....	44
Figure 4.4 IR spectra of (a) pentaethylenehexamine; (b) Zn(OAc) ₂ ; (c) Zn(pentaen) synthesized at the mole ratio of Zn(OAc) ₂ :pentaen = 1:1.....	45
Figure 4.5 UV spectra of (a) Cu(OAc) ₂ ; (b) Zn(pentaen) and (c) W_Zn(pentaen) synthesized at the mole ratio of Zn(OAc) ₂ :pentaen =1:1.....	46

Figure 4.6	Mass spectrum of Zn(pentaen) synthesized at the mole ratio of Zn(OAc) ₂ :pentaen = 1:1.....	47
Figure 4.7	IR spectra of (a) pentaethylenehexamine; (b) Cu(OAc) ₂ ; (c); Zn(OAc) ₂ ; (d) Cu(pentaen):Zn(pentaen) synthesized at the mole ratio of Cu(OAc) ₂ :Zn(OAc) ₂ :pentaen = 0.5:0.5:1.....	48
Figure 4.8	UV spectra of (a) Zn(OAc) ₂ ; (b) Cu(OAc) ₂ (c) Cu(pentaen):Zn(pentaen) ; (d) W_Cu(pentaen):Zn(pentaen) synthesized at the mole ratio of Cu(OAc) ₂ :Zn(OAc) ₂ :pentaen = 0.5:0.5:1.....	49
Figure 4.9	Mass spectrum of Cu(pentaen):Zn(pentaen).....	51
Figure 4.10	Reaction times of RPUR foams catalyzed by M(pentaen) at NCO index of 100.....	58
Figure 4.11	Rise profiles of RPUR foams catalyzed by different metal complexes (a) DMCHA (ref.); (b) Cu(pentaen); (c) Cu(pentaen):Zn(pentaen); (d) Zn(pentaen).....	58
Figure 4.12	Maximum rise rates of RPUR foams catalyzed by different metal complexes at NCO index of 100 (a) DMCHA (ref.); (b) Cu(pentaen); (c) Cu(pentaen):Zn(pentaen); (d) Zn(pentaen).....	60
Figure 4.13	Samples for foam density measurements.....	61
Figure 4.14	Apparent density of RPUR foams catalyzed by metal complexes (a) DMCHA (ref.); (b) Cu(pentaen); (c) Cu(pentaen):Zn(pentaen); (d) Zn(pentaen) at different NCO indexes.....	62
Figure 4.15	Effect of catalyst content on RPUR foam density catalyzed by different catalysts type (a) DMCHA (ref.); (b) Cu(pentaen); (c) Cu(pentaen):Zn(pentaen); (d) Zn(pentaen) at NCO index of 130.....	63
Figure 4.16	Appearance of RPUR foam catalyzed by Cu(pentaen):Zn(pentaen) complex in various amounts at NCO index of 130.....	63
Figure 4.17	Effect of blowing agent quantities on RPUR foam density catalyzed by different catalysts (a) DMCHA (ref.); (b) Cu(pentaen); (c) Cu(pentaen):Zn(pentaen); (d) Zn(pentaen) at NCO index of 130.....	64

Figure 4.18	Temperature profiles of RPUR foams catalyzed by metal complexes (a) DMCHA (ref.); (b) Cu(pentaen); (c) Cu(pentaen):Zn(pentaen); (d) Zn(pentaen).....	66
Figure 4.19	IR spectra of starting materials and RPUR foams catalyzed by mixed metal complexes (a) polyether polyol; (b) PMDI; (c) DMCHA (ref.); (d) RPUR foams catalyzed by Cu(pentaen):Zn(pentaen).....	67
Figure 4.20	IR spectra of RPUR foams catalyzed by Cu(pentaen):Zn(pentaen) at different NCO indexes (a) 100; (b) 130; (c) 150.....	68
Figure 4.21	NCO conversions of RPUR foams catalyzed by different metal complexes.....	70
Figure 4.22	PIR:PUR of RPUR foams catalyzed by different metal complexes	71
Figure 4.23	Parallel compression stress-strain curve of RPUR foams catalyzed by different catalysts at NCO index of 150 (a) DMCHA (ref.); (b) Cu(pentaen); (c) Cu(pentaen):Zn(pentaen); (d) Zn(pentaen).....	73
Figure 4.24	Comparison of parallel compressive strength of RPUR foams between NCO indexes of 100, 130 and 150.....	74
Figure 4.25	Relationship between compressive strength and density.....	74
Figure 4.26	Comparison of compressive strength of RPUR foams between parallel and perpendicular direction of foam rising at NCO index of 150.....	75
Figure 4.27	Isotropic foam (a): spherical cells, equal properties in all directions; anisotropic foam (b): ellipsoid cells, which properties depend on direction.....	76
Figure 4.28	SEM of RPUR foams catalyzed by Cu(pentaen):Zn(pentaen) and prepared at the NCO index 150; (a) top view; (b) side view (50×).....	76
Figure 4.29	SEM of RPUR foams prepared at the NCO index of 150 and catalyzed by (a) DMCHA (ref.) ; (b) Cu(pentaen):Zn(pentaen) (top view,50×).....	77

	Page
Figure 4.30 SEM of RPUR foams prepared at the NCO index of 150, catalyzed by Cu(pentaen):Zn(pentaen) and blown by different blowing agent content (a) 1.0 (b) 2.0 (c) 3.0 pbw (top view, 50×).....	78
Figure 4.31 TGA thermograms of RPUR foams catalyzed by (a) DMCHA (ref.); (b) Cu(pentaen); (c) Cu(pentaen):Zn(pentaen); (d) Zn(pentaen) at the NCO index of 150.....	80
Figure 4.32 External appearance of RPUR foams catalyzed by metal acetates and amine.....	81
Figure 4.33 External appearance of RPUR foams catalyzed by different metal catalysts (a) DMCHA (ref.); (b) Cu(pentaen); (c) Cu(pentaen):Zn(pentaen); (d) Zn(pentaen); (e) W_Cu(pentaen); (f) W_Cu(pentaen):Zn(pentaen); (g) W_Zn(pentaen).....	82
Figure B1 Perpendicular compression stress-strain curve of RPUR foams catalyzed by different catalysts at NCO index of 150.....	97

LIST OF SCHEMES

	Page
Scheme 1.1 Diagram of metal complexes synthesis.....	2
Scheme 1.2 Diagram of mixed metal complexes synthesis.....	3
Scheme 2.1 Baker mechanism amine catalysts.....	14
Scheme 2.2 Farka mechanism amine catalysts.....	14
Scheme 2.3 Mechanism of tin (II) salts catalyst.....	15
Scheme 2.4 Mechanism of tin (IV) salts catalyst.....	16
Scheme 2.5 Mechanism of tin-amine synergism.....	17
Scheme 3.1 Synthesis of copper- pentaethylenehexamine complex [Cu(pentaen)].....	30
Scheme 3.2 Synthesis of zinc-pentaethylenehexamine complex.....	31
Scheme 3.3 Synthesis of copper-zinc pentaethylenehexamine complex.....	32
Scheme 4.1 Synthesis of metal and mixed metal- pentaethylenehexamine complexes.....	40
Scheme 4.2 Activation mechanism of metal-based catalyst on urethane formation reaction.....	59

LIST OF ABBREVIATIONS

%	percentage
ϵ	molar absorptivity
ATR-IR	Attenuated Total Reflectance-Infrared
AA	Atomic absorption
cm	centimeter
cm^{-1}	unit of wavenumber
$^{\circ}\text{C}$	degree Celsius (centigrade)
DBTDL	dibutyltin dilaurate
DMCHA	N,N-dimethylcyclohexylamine
EA	Elemental Analysis
FTIR	Fourier Transform Infrared Spectrophotometer
g	gram
h	hour
IDT	Initial Decomposition Temperature
KOH	potassium hydroxide
kg	kilogram
kV	kilovolt
M	metal
$\text{M}(\text{OAc})_2$	metal acetate
m^3	cubic meter
MDI	4,4'-methane diphenyl diisocyanate
mA	milliampere
mg	milligram
min	minute
mL	milliliter
mm	millimeter
mmol	millimole
N	newton unit
NCO	isocyanate
OHV	hydroxyl value

pbw	part by weight
PIR	polyisocyanurate
pentaen	pentaethylenehexamine
PMDI	polymeric 4,4'-methane diphenyl diisocyanate
PU	polyurethane
PUR	polyurethane
PS	polystyrene
rpm	round per minute
RPUR	rigid polyurethane
RT	room temperature
ref	reference
s	second
SEM	Scanning Electron Microscope
t	time
TEDA	triethylenediamine
TDI	toluene diisocyanate
TGA	Thermogravimetric Analysis
T _{max}	maximum core temperature
UV	ultraviolet

CHAPTER I

INTRODUCTION

Rigid Polyurethane (RPUR) foams have been used commercially for a variety of applications. Closed-cell foams are generally rigid in nature and are most suitable for thermal insulation because of their low thermal conductivity, low density, high strength-to-weight ratio, and low moisture permeability [1]. Some typical engineering applications of RPUFs are in transportation, refrigeration technology and appliances, building construction, the automotive industry, packaging and sporting goods [2].

Traditionally, polyurethanes are produced by the exothermic polymerization reaction of molecules containing two or more isocyanate groups with polyol molecules containing two or more hydroxyl groups. The functionality of the polyol or the isocyanate can be adjusted for controlling the physical and mechanical properties of polyurethanes [3].

The rigid polyurethane foams processing can be categorized into two methods which are one shot and two shot methods. For one shot method, all materials consisting of polyol, catalyst, surfactant, blowing agent and isocyanate are mixed homogeneously within one step. For two shot method, the difference is that isocyanate is added into the mixture of polyol, catalyst, surfactant and blowing agent [4-5].

The foaming reaction can be carried out with blowing agents which consist of physical and chemical blowing agents, or the mixture of both agents. There are three main reactions of polyurethane foams which lead to produce polyurethane (PUR) and polyisocyanurate (PIR) as follows [6]:

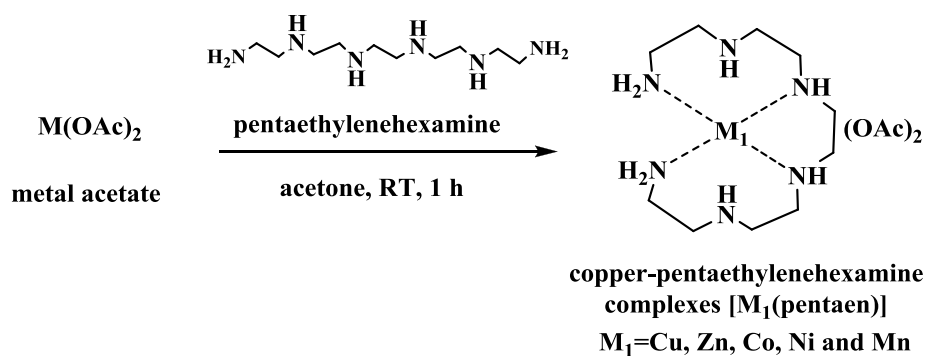
- Firstly, the reaction between isocyanate (-NCO) and hydroxyl (-OH) groups results in urethane formations.
- Secondly, the reaction between isocyanate groups and blowing agent (water) releases carbon dioxide gas.
- Finally, the reaction of three isocyanate groups in polymer chain produces isocyanurate.

However, the above reactions can not be completed without catalysts for catalytic reactions because the reaction between isocyanate with hydroxyl group is slow [7]. Therefore, In this reaction tertiary amines such as N,N-dimethylcyclohexylamine (DMCHA) and tin compounds such as dibutyltin dilaurate (DBTDL) are used as catalysts for blowing and gelling reaction, respectively. This is due to their excellent catalytic activity. However, they are toxic to human beings, strong smell and expensive. In accordance, the objective of this research is to develop new catalysts synthesized from metal and amine complexes which are less toxic, inexpensive and have weaker smell.

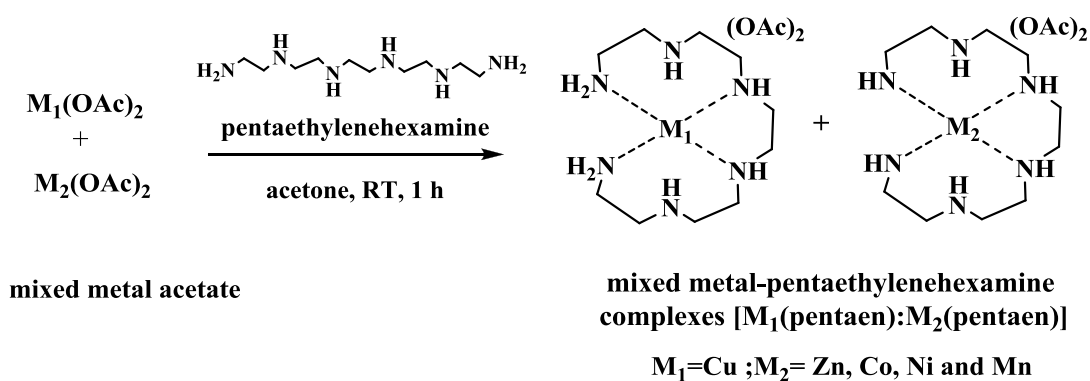
Objective and scope of the research

The proposed of this research was to prepare rigid polyurethane (RPUR) foams catalyzed by metal-amine complexes; $[M_1(\text{pentaen})]$ and mixed metal-amine complexes; $[M_1(\text{pentaen}):M_2(\text{pentaen})]$. It was expected that the synthesized metal complexes showed good solubility and good catalytic activity, which should provide the desirable physical and mechanical properties of prepared foams. Moreover, the reaction times during foam preparation, the physical and mechanical properties of foams were studied by varying catalyst types, the content of catalysts and blowing agent, and NCO indexes.

In the first part, metal-pentaethylenehexamine $[M_1(\text{pentaen})]$ complexes and mixed metal-pentaethylenehexamine $[M_1(\text{pentaen}):M_2(\text{pentaen})]$ complexes were prepared. The reactions are shown in Schemes 1.1 and 1.2, respectively. The obtained metal complexes were characterized by FTIR spectroscopy, ultraviolet-visible spectroscopy, elemental analysis and mass spectrometry.



Scheme 1.1 Diagram of metal complexes synthesis



Scheme 1.2 Diagram of mixed metal complexes synthesis

In the second part, rigid polyurethane foam preparations were catalyzed by metal complexes prepared in the first part. All of the raw materials, namely polyol, catalyst, surfactant and blowing agent (water), excluding isocyanate (PMDI), were premixed at the beginning. Then, the isocyanate was added into the mixture and mixed by mechanical stirrer. Physical and mechanical properties at various NCO indexes of the RPUR foams were determined.

During rigid polyurethane foams preparation, reaction times included cream time, gel time, tack free time and rise time were recorded. In order to evaluate the efficiency of developed catalysts, the result experimental data of synthesized catalysts was compared with the commercial catalyst, N,N-dicyclohexylamine (DMCHA), which is used as the reference catalyst.

CHAPTER II

THEORY AND LITERATURE REVIEWS

Polyurethane is formed by addition polymerization between alcohols with two or more reactive hydroxyl groups per molecules (diols or polyols) and isocyanates that have more than one reactive isocyanate group per molecule (a diisocyanate or polyisocyanate).

In manufacturing polyurethane, extremely wide range of grades and polymer stiffness from vary flexible elastomers to rigid, because specific chemical structure and the degree of crosslinking can be introduced. The type of PUR foams can vary from flexible, used in applications such as cushioning, packaging and textile industry through semi-rigid, commonly found in applications in the automotive industry, and protective packaging to rigid PUR foam, mainly used in insulation and structural applications [8].

2.1 Raw materials

For the manufacture of rigid polyurethane (RPUR) foams, two groups of at least bifunctional substances are needed as reactants; compounds with isocyanate groups, and compounds with active hydrogen atoms (polyol). The physical and chemical character, structure, and molecular size of these compounds influence the polymerization reaction, as well as final physical properties of polyurethane. In addition, additive such as catalysts, surfactants, blowing agents and fillers are used to control and modify the reaction process and performance characteristics of the polyurethane foam.

2.1.1 Isocyanates

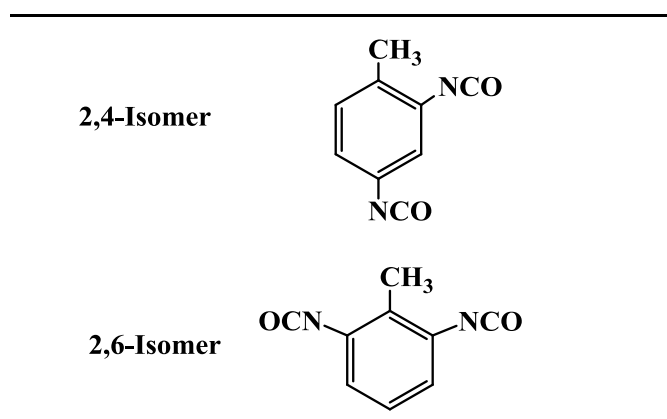
Several aromatic and aliphatic isocyanates are commercially available, the most common aromatic isocyanate used are toluene diisocyanate (TDI) and diphenylmethane diisocyanate (MDI) [7]. Aromatic isocyanates have been used for the preparation of isocyanate based foams. Aliphatic isocyanates were not used

because foaming reactions require high reactivity, and aliphatic polyisocyanates react slowly with OH groups. Variation of polyurethane properties can be achieved by variation of the types of used isocyanate [9].

2.1.1.1 Toluene diisocyanate (TDI), TDI is manufactured by phosgenation of diaminotoluene, which is obtained by the reduction of nitrotoluene. Commercial products of TDI are mixtures of 2,4- and 2,6-isomers in the weight ratio of 80:20 or 65:35. TDI with a 80:20 isomer ratio is used mainly for flexible foams. Modified TDI and undistilled TDI are mostly used for rigid polyurethane foams. The chemical structures of TDI are demonstrated in Tables 2.1 [9].

As would be expected from their chemical reactivity and substantial volatility, TDI mixtures can represent a serious toxic hazard in use, having a marked effect on the respiratory system and skin [10]. Therefore, it is pretty a difficult material to handle on site, in transport and in the laboratory and consequently its usage has been limited in favor of MDI which has a lower volatility.

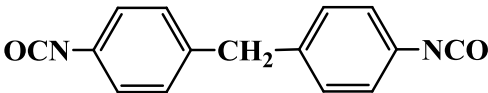
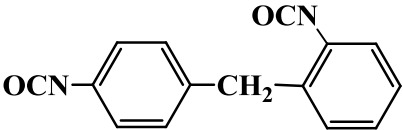
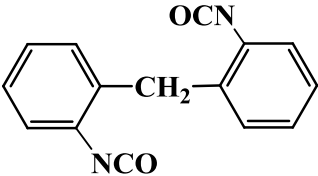
Table 2.1 Chemical Structures of TDI



2.1.1.2 4,4'-Diphenylmethane diisocyanate (MDI), or methylene diphenyl diisocyanate (MDI) based on diaminodiphenylmethane is considerably safer to use, having a much lower volatility. MDI is often used in the crude (undistilled) form. This particular isocyanate is derived by phosgenation of the diaminodiphenylmethanes form by condensation of aniline with formaldehyde [10].

MDI is available in two types, purifide monomeric and polymeric MDI. They are mainly 4,4'-isomer based and have small quantities of the 2,2'-isomer and up to 10% of the 2,4'-isomer. Pure MDI (or monomeric MDI) is obtained by the distillation of a crude reaction product and used for elastomers and coatings. Polymeric MDI is used for rigid and semi-rigid urethane foams, as well as polyisocyanurate foams. The chemical structures of MDI are demonstrated in Tables 2.2 [9].

Table 2.2 Chemical Structure of MDI

4,4-Isomer	
2,4-Isomer	
2,2-Isomer	

The undistilled MDI compositions like polymeric MDIs are made by phosgenation of polyamine mixtures. Polymeric MDI compositions have functionalities from about 2.2 to 3.0. The viscosity of polymeric MDIs increases with increasing molecular weight and polymeric isocyanate content.

Polymeric MDI, average functionality: 2.2 - 3.0

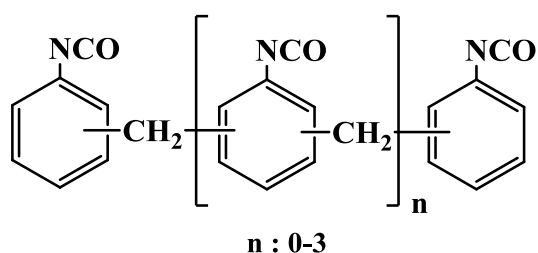


Figure 2.1 The chemical structures of polymeric MDI.

Moreover, the selection of polymeric MDI may obtain the different kinds of polyurethanes due to different range of functionality, structure and compositions.

2.1.2 Polyols

A wide range of polyols is used in polyurethane manufacture. Most of the polyols used, however, fall into two classes: hydroxyl-terminated polyether, or hydroxyl-terminated polyester. The structures of polyol play a large part in determining the properties of final polyurethane. The molecular weight and functionality of the polyol are the main factor. However, the structure of the polyol chains is also important. The characteristics of the polyol used to make the two main classes of flexible and rigid polyurethane foam are illustrated in Table 2.3 [7].

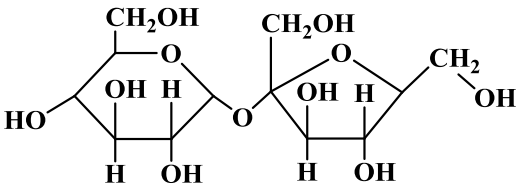
Table 2.3 Polyol for polyurethane manufacture.

Characteristic	Rigid	Flexible
	polyurethane foam	polyurethane foam
Molecular weight range	150 to 1,600	1,000 to 6,500
Functionality range	3.0 to 8.0	2.0 to 3.0
Hydroxy value range (mgKOH/g)	250 to 1,000	28 to 160

The higher molecular weight and lower functionality polyols are used in the production of flexible foams. On the contrary, rigid polyurethane (RPUR) foams need the lower molecular weight and higher functionality polyols in order to get the higher degree of crosslinking which contributes to the stiffness of polymer. It is necessary to utilize various polyols produce polyurethane with desired properties.

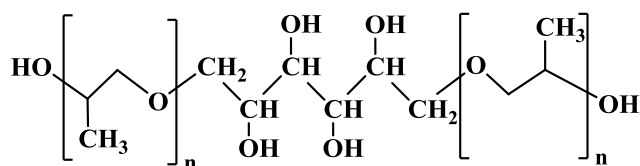
Specifications of commercial polyols include hydroxyl values which are used in stoichiometric formulation calculations. Examples are shown in Table 2.4.

Table 2.4 Examples of commercial polyols [9]

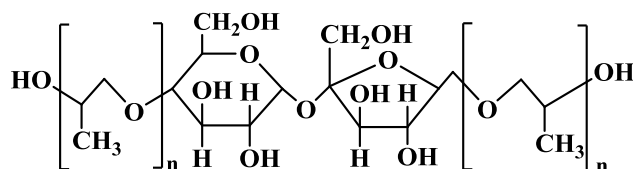
<ul style="list-style-type: none"> • Functionality = 2 	<ul style="list-style-type: none"> • Functionality = 3
$\text{HO}-\text{CH}_2-\text{CH}_2-\text{OH}$ <p>Ethylene glycol</p>	$\begin{array}{c} \text{H}_2\text{C}-\text{OH} \\ \\ \text{HC}-\text{OH} \\ \\ \text{H}_2\text{C}-\text{OH} \end{array}$ <p>Glycerol</p>
<ul style="list-style-type: none"> • Functionality = 3 	<ul style="list-style-type: none"> • Functionality = 4
$\begin{array}{c} \text{H}_2\text{C}-\text{CH}_2-\text{OH} \\ \\ \text{HC}-\text{CH}_2-\text{OH} \\ \\ \text{H}_2\text{C}-\text{CH}_2-\text{OH} \end{array}$ <p>Trimethylol propane</p>	$\begin{array}{c} \text{H}_2\text{C}-\text{OH} \\ \\ \text{HO}-\text{CH}_2-\text{C}-\text{CH}_2-\text{OH} \\ \\ \text{H}_2\text{C}-\text{OH} \end{array}$ <p>Pentaerythritol</p>
<ul style="list-style-type: none"> • Functionality = 6 	
 <p>Sucrose</p>	

2.1.2.1 Polyether polyols

In polyurethane foam production, hydroxyl-terminated polyethers (Figure 2.2) are approximately 90% of used polyols due to their low cost and ease of handling (low viscosity). Polyether-based foams have better resilience and resistance to hydrolysis than polyester-based foams. They are produced by the ring opening of alkylene oxides using a polyfunctional as starter or initiator. Ethylene or propylene oxides are the most commonly used polyols. The polyols used for making rigid foams the molecular weight is approximately 500 g/mol in order to reduce the distance between crosslinks.



Poly (propyleneoxy) sorbitol



Poly (propyleneoxy) sucrose

Figure 2.2 Structure of polyether polyol based sorbitol and sucrose used in the PUR foams

2.1.2.2 Polyester polyols

When polyether and polyester polyols are compared, the more reaction of polyester polyols tenderly produce foams with better mechanical properties due to their less soluble in organic solvents. However, they are more expensive, more viscous and therefore not easy to handle. As a consequence, they are only used in applications that require their superior properties. Polyester polyols are made by condensation reactions between diols (and triol) and dicarboxylic acid such as adipic acid, sebacic acid and m-phthalic acid.

2.1.3 Surfactants

Surfactants are essential additives used in polyurethane foam formulation. The presence of surfactants serves two purposes in polyurethane foaming. First, they stabilize the foam immediately after mixing polyol and isocyanate by lowering the surface tension of the emerging gas-liquid interface, and presumably also by emulsifying the polyol-isocyanate interface. Mechanistically, this effect arises from a preferred accumulation of surfactant molecules at interfaces. A second, equally important role of surfactants is to stabilize the polymerizing liquid-gas interface during the roughly 30 to 50 fold volume increase of rising foam. Here, the mechanism

is rather dynamic: the expanding foam continuously creates new surface area of high tension that needs to be stabilized by fast migration of surfactant towards the interface (the Marangoni effect).

Silicone surfactants are typically added in amounts of 0.4–2.0% w/w of the polyol formulation. To meet specific processing needs of different foam systems, the molecular structure may be tuned by varying the length and the composition of the polydimethylsiloxane backbone or the number, length, and composition of the pendant polyether chains [11].

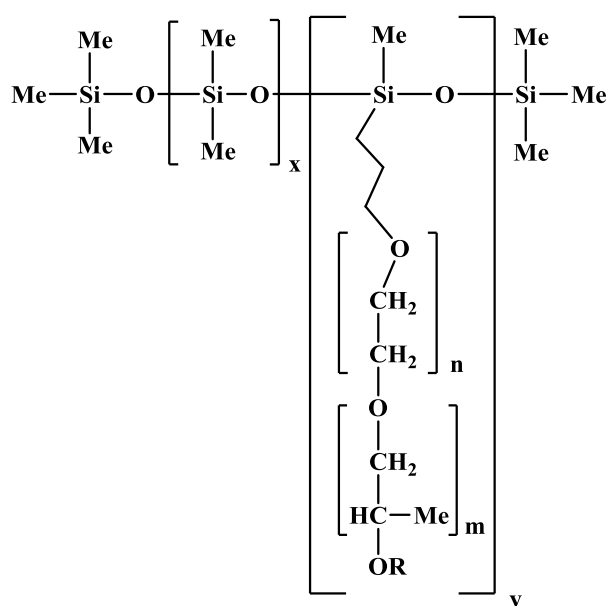


Figure 2.3 Structure of silicone surfactants used in PUR foams manufacture

2.1.4 Blowing agents

The blowing agent plays a very important role in both the manufacturing and performance of polyurethane foam. The blowing agent is the dominant factor controlling density of the foam. Besides density, it affects the cellular microstructure and morphology of the foam, which in turn define the end-use performance [11].

In RPUR foams preparation, two kinds of gas generation methods are used, is chemical and physical blowing agent, as well as their combinations. Chemical blowing agents are chemical compounds that react with isocyanate groups to generate carbon dioxide gas. A typical chemical blowing agent is water. Physical blowing

agents are liquids that have low boiling points and nonreactivity to isocyanate groups; they vaporize by the exotherm of foaming reaction [9, 11].

Water acts as a blowing agent. It produces CO₂ gas by reaction with an isocyanate. Typical water concentrations are 3-5 parts of water per 100 parts of polyester polyol. The reaction of water with an isocyanate is exothermic and results in the formation of active urea sites which form crosslinks via hydrogen bonding. To reduce the high crosslink density, auxiliary blowing agents are used to produce low density foams with a softer feel than water-blown foams and to produce closed cell flexible foams.

2.1.5 Catalysts

A number of catalysts for the reaction of isocyanate with water and with polyol and these included a range of chemical structures, such as aliphatic and aromatic tertiary amines, quaternary ammonium salts, alkali metal carboxylates, and organo-tin compounds (Table 2.5 and Figure 2.4).

Table 2.5 Catalysts for use in rigid polyurethane foams manufacture [12]

-
- **Tertiary amines**
 - Pentamethyldiethylene triamine (PMDETA)
 - Triethylenediamine (TEDA)
 - Dimethylcyclohexylamine (DMCHA)
 - **Quaternary ammonium salts**
 - 2-hydroxy propyl trimethyl ammonium (TMR)
 - **Alkali metal carboxilates**
 - Potassium acetate (K Ac)
 - Potassium octoate (K Oct)
 - **Tin compounds**
 - Stannous octoate (Sn Oct)
 - Dibutyltin dilaurate (DBTDL)
 - Dibutyltin mercaptide
-

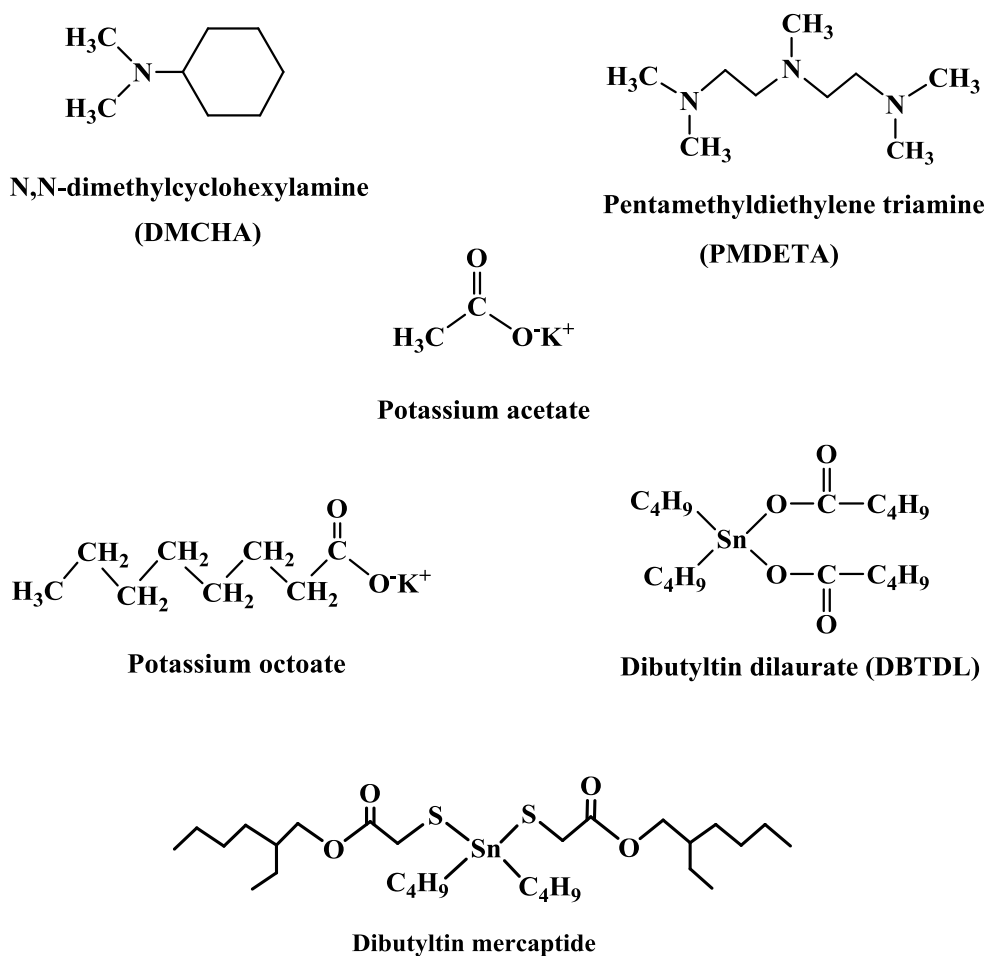


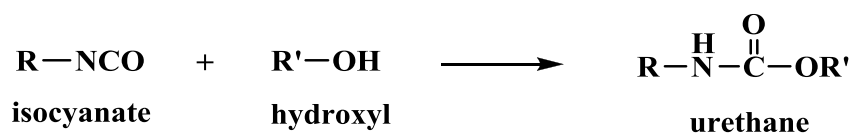
Figure 2.4 commercial catalysts used in rigid polyurethane foams manufacture

Their catalyst activity is dependent on their basicity, with steric hindrance on the active site playing a secondary role [13]. In the reactions of isocyanates catalysts play a very important role. Catalysts exert an influence upon the rates of competing reactions and have a major effect on the ultimate properties of the final foam.

Each catalyst type is specific for a particular chemical reaction. Catalyst mixtures are generally necessary to control the balance of the polymerization and the gas generation reactions which both are exothermic reactions. Getting the correct balance of polymerization and foaming is a major importance in the production of closed cell foam. A typical catalyst system would consist of a mixture of a tertiary amine and organometallic compounds. For tin compounds, the most important one is stannous octoate.

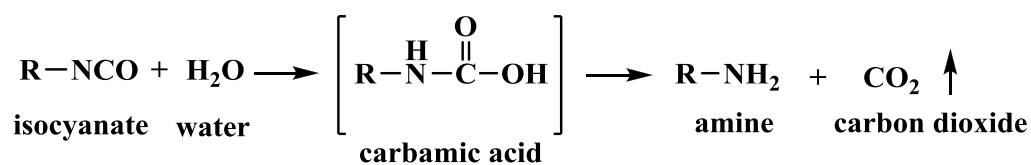
For rigid polyurethane foam preparation, two kinds of reactions, which are an isocyanate-hydroxyl reaction and an isocyanate-water reaction, are employed. Hence, two types of catalyst are necessary to balance and accelerate between gelling and blowing reaction.

Tin catalysts promote mainly isocyanate-hydroxyl reactions and they are considered "gelling catalysts" as the following equation.



"Gelling reaction"

In contrast, tertiary amine catalysts accelerate mainly the water-isocyanate reaction, which generates CO₂ and they are considered "blowing catalysts" as the belowed equation [9].



"Blowing reaction"

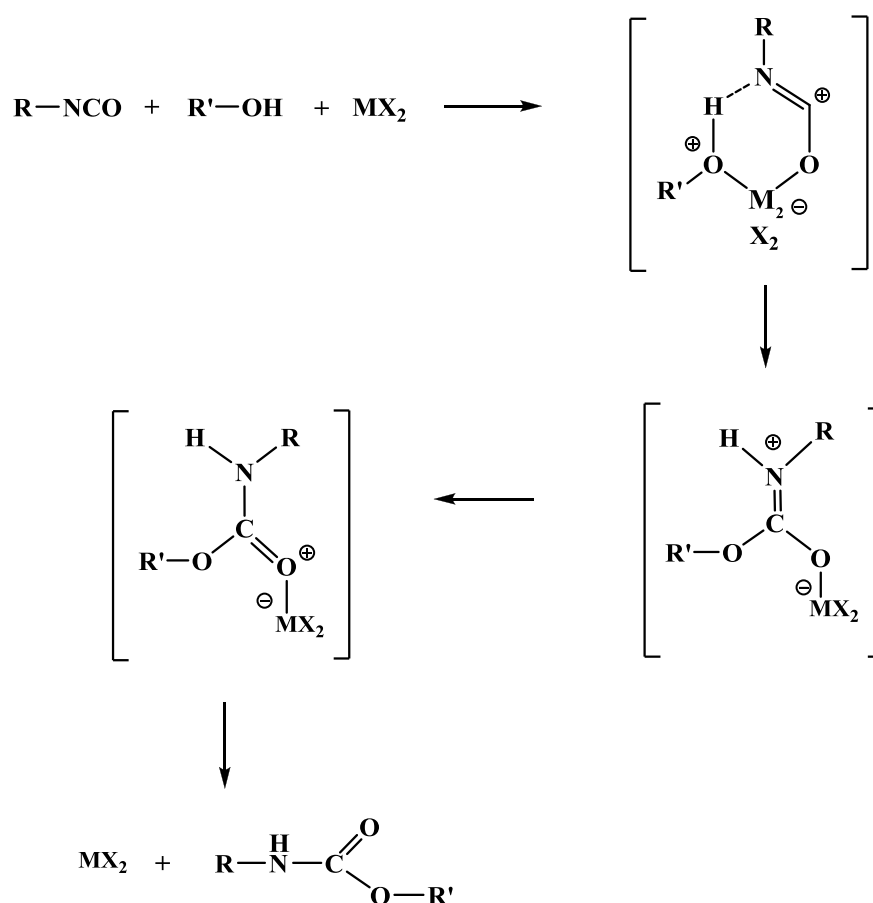
However, tertiary amines are catalyzed both the blowing and gelling reaction, whereas organo-tin catalysts catalyzed mainly isocyanate-hydroxyl reaction [10, 14].

In preparing formulations for specific processing and application needs, catalysts are thought to balance these reactions and synergistic effects of certain catalyst combinations are known as well. If the polymerization is complete before sufficient gas has been generated. A high density foam will results, i.e. virtually a solid product containing few gas cells. Thus blends of catalysts are required to balance the relative chemical reaction rates.

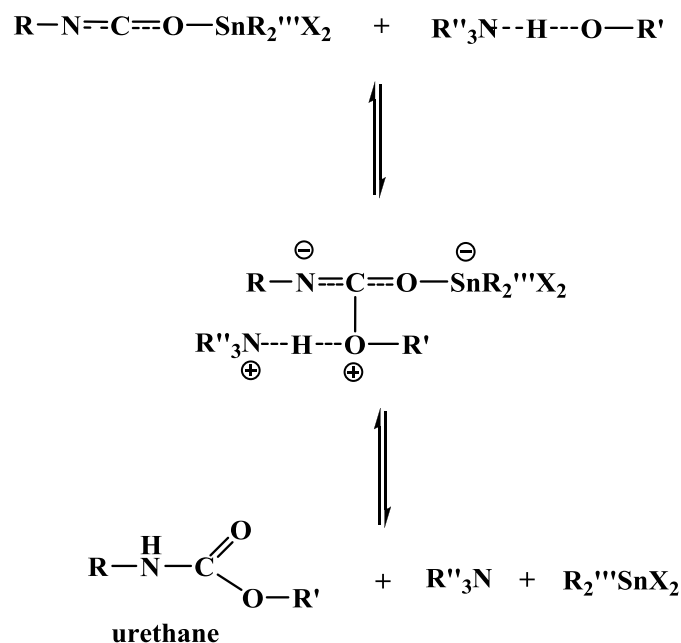
In the second mechanism, proposed by Farka (Scheme 2.2), which is supported in the more recent literature, the activation starts by the amine interacting with the proton source (polyol, water, amine) to form a complex, which then reacts with the isocyanate.

Factors that affect the catalytic activity of an amine are nitrogen atom basicity, steric hindrance, spacing of heteroatoms, molecular weight and volatility and end groups. The level of basicity is determined from the pKa value, defined as the pH at which the concentration of unprotonated and protonated forms, of an ionisable group, are equal.

2.2.2 Organotin catalysts



Scheme 2.3 Mechanism of tin (II) salts catalyst



Scheme 2.5 Mechanism of tin-amine synergism

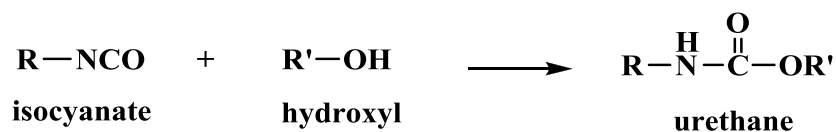
2.3 Chemistry

Polyurethane (PUR) chemistry is based on the high reactivity of the isocyanate group with any compound containing active hydrogen. Most polyurethane is formed by exothermic reaction between di- or polyfunctional isocyanates and di- or polyfunctional hydroxyl species [16]. For simplicity, the basic principle of urethane chemistry is described below using monofunctional reagents.

2.3.1 Primary reaction of isocyanates

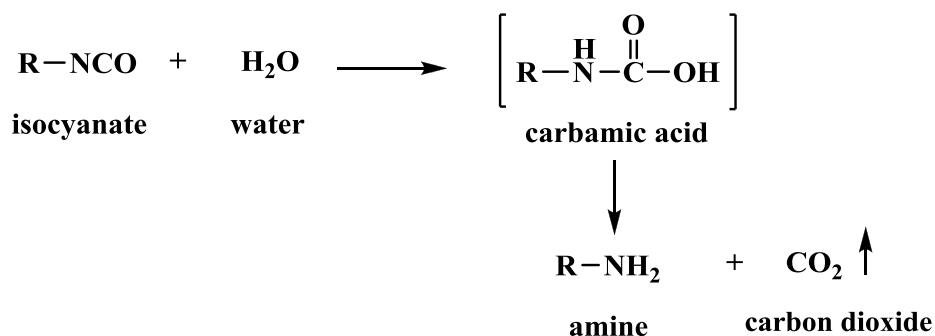
Primary isocyanate reactions produce urethane, amines, and substituted ureas, all of which still contain active hydrogen atom. In the presence of suitable catalysts at elevated temperatures, controlled secondary reactions occur which strongly influence the physical properties of the foam by introducing chain branching and crosslinking.

2.3.1.1 Reaction of isocyanate with polyol; the most important reaction in the manufacture of polyurethanes is between isocyanate and hydroxyl groups. The reaction product is a carbamate, which is called a urethane in the case of high molecular weight polymers. The reaction is exothermic and reversible going back to the isocyanate and alcohol.



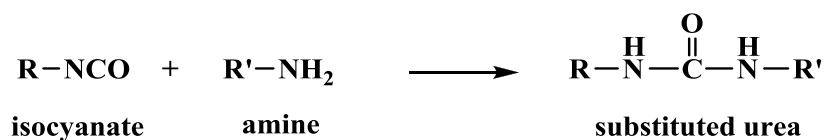
This reaction is known as the “gelling reaction”. Since it is an exothermic reaction it must be temperature controlled. The rate of polymerization is affected by the chemical structure of the isocyanate and polyol. A catalyst is used to accelerate the reaction rate.

2.3.1.2 Reaction of isocyanate with water; the reaction of isocyanates with water to produce an amine and carbon dioxide is highly exothermic. The initial reaction product is a carbamic acid, which breaks down into carbon dioxide and a primary amine [3]



This reaction is known as the “blowing reaction” because the CO₂ gas produced is used for blowing the foam which, this reaction had an effect to foam density. The reaction rate is accelerating by suitable choice of catalyst system.

2.3.1.3 Reaction of isocyanate with amines; the reaction of an isocyanate with an amine forms an urea linkage.



Reactions of unhindered isocyanates with primary amines occur approximately 100-1000 times faster than with primary alcohols [16]. The reactivity of amines increases with the basicity of the amine, and aliphatic amines react much faster than aromatic amines [3].

2.4 Formulations [7, 16]

The amount of isocyanate needed to react with polyol and other reactive components can be calculated to obtain chemically stoichiometric equivalents. This theoretical amount may be adjusted up or down dependent on the PUR system, properties required, ambient conditions and scale of production. The adjusted amount of isocyanate used is referred to as the “isocyanate index”,

$$\text{Isocyanate index} = \frac{\text{actual amount of isocyanate}}{\text{theoretical amount of isocyanate}} \times 100$$

The conventional way of calculating the ratio of the components required for PUR manufacture is to calculate the the number of part by weight of the isocyanate needed to react with 100 parts by weight of polyol and use proportionate amount of additives. The analytical data require for the calculation are the isocyanate value of the isocyanate and hydroxyl value, residual acid value and water content of the polyol and other reactive additives.

Isocyanate value (or isocyanate content) is the weight percentage of reactive -NCO groups:

$$\begin{aligned} \text{Isocyanate value} = \% \text{ NCO group} &= \frac{42 \times \text{functionality}}{\text{molar mass}} \times 100 \\ &= \frac{4200}{\text{equivalent weight}} \end{aligned}$$

Hydroxyl value (hydroxyl number; OHV)

The hydroxyl value (OHV) sometime called the hydroxyl number of the polyol, is used as a measurement of the concentration of isocyanate-reactive hydroxyl groups per unit weight of the polyol and is expressed in mg KOH/g of polyol. The hydroxyl value is also defined as the number of milligrams of potassium hydroxide equivalent to the active functions (hydroxyl content) of 1 g of the compound or polymer.

$$\begin{aligned} \text{Hydroxyl value} &= \frac{56.1 \times \text{functionality}}{\text{molar mass}} \times 1000 \\ &= \frac{56.1}{\text{equivalent weight}} \times 1000 \end{aligned}$$

Acid value is also expressed as mgKOH/g of polyol and numerically equal to OHV in isocyanate useage.

Water content; water reacts with two -NCO groups and the equivalent weight of water is thus:

$$\text{Equivalent weight} = \frac{\text{molar mass}}{\text{functionality}} = \frac{18}{2}$$

Isocyanate conversion (α), isocyanate conversion can be calculated by FTIR method [18], defined as the ratio between isocyanate peak area at time t and isocyanate peak area at time 0:

$$\text{Isocyanate conversion (\%)} = \left[1 - \frac{\text{NCO}^f}{\text{NCO}^i} \right] \times 100$$

where;

NCO^f = the area of isocyanate absorbance peak area at time t (final isocyanate)

NCO^i = the area of isocyanate absorbance peak area at time 0 (initial isocyanate)

2.5 Mechanical properties

The mechanical properties of rigid foams differ markedly from those of flexible foams. The tests used to characterize both types of foam therefore differ, as do their application areas.

Compression load deflection is used to determine the compressive stress-strain behavior, i.e. it is a measure of the load-bearing properties of the material. The test method is somewhat similar to that developed for non-cellular plastics. Test on rigid and flexible foams can be determined according to ASTM D 1621-04. A universal

testing machine fitted with a compression rig (cage) consisting of two parallel flat plates (Figure 2.5) is used for the tests.

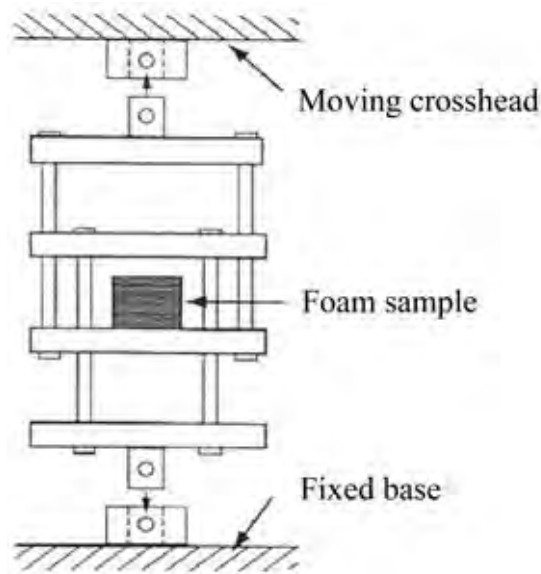


Figure 2.5 Compression load deflection test rig [16]

Compressive properties are the most important mechanical properties for RPUR foams. Compressive energy absorption characteristics and deformation characteristics of foam mainly depend on density, type of base polymer and the predominance of either open or closed cells. In simple terms, close cell foam deformation involves cell walls bending and buckling, gas compression, cell wall stretching/yielding (non-reversible). Severe compression causes cell rupture.

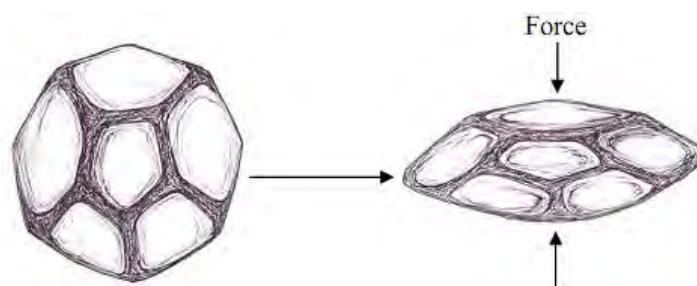


Figure 2.6 Schematic representation of closed cell deformation [16]

Closed cell rigid foams (e.g. PS and PU foams) exhibited from very limited to no yielding behavior. Consequently, gas compression and matrix strength play important roles during the mechanical deformation of rigid foams. In addition, cell

rupture often occurs during the energy absorption process. The energy absorption characteristics of foam can be represented in term of compression stress-strain curves. Figure 2.7 show typical compression stress-strain curve of rigid foams.

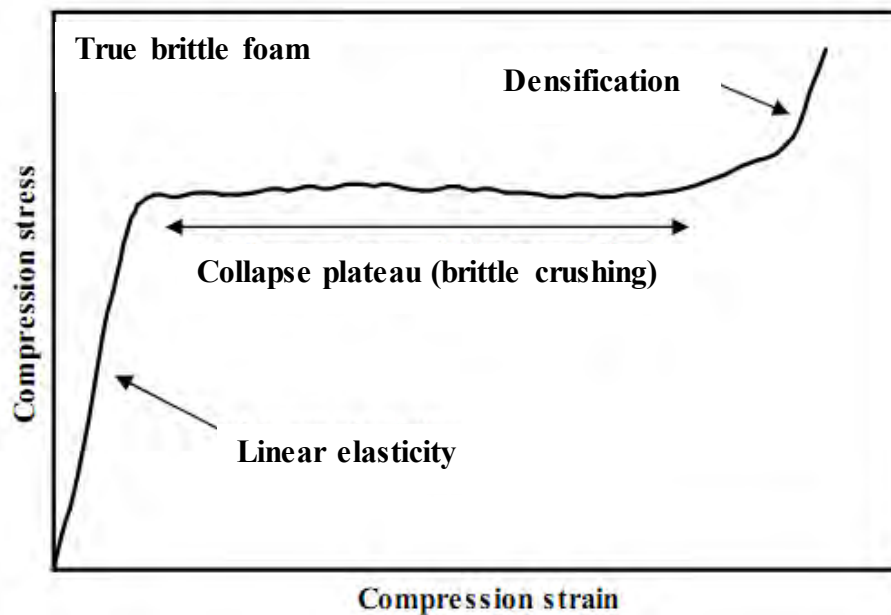


Figure 2.7 Typical compression stress-strain curve for rigid foams

For rigid foams, elements of true brittle crushing are superimposed on the elastic/plastic response. The erratic nature of the collapse plateau corresponds to intermittent rupturing of individual cells. This is due to cell rupture in rigid foams, resilience is dramatically affected. Foams can generally withstand only single impacts, for example the liners used inside riding.

The compressive strength of rigid cellular polymers is usually reported at some definite deformation (5 or 10%). The modulus is then extrapolated to 0% deformation unless otherwise stated. Structural variables that affect the compressive strength and modulus of this foam are, in order of decreasing importance, plastic phase composition, density, cell structure, and gas composition.

2.6 Literature reviews

A number of research works concerning the effect of blowing agents, surfactants and catalysts on the physical and mechanical properties of rigid polyurethane foam [19-22].

Seo and coworkers [19] prepared rigid PU foam and studied their mechanical properties. This investigation reports the mechanical, morphological, water absorption, thermal conductivity, and thermal behavior of rigid PUF varying with the density, which controls the foam architecture. Xiaobin and coworkers [20] investigated the effect of water content on rigid foams and found that water played an important role in determining the density, mechanical properties, thermal stability (TGA) and morphology of polyurethane foams. The results found that the density had effects to the mechanical properties of polyurethane foam.

Effects of silicone surfactant in rigid polyurethane foams are reported by Lim and coworkers [21]. They found that cream time, gel time and tack free time increased with the content of surfactant increasing due to the increased stability of reaction mixture and rising bubbles. Han and coworkers [22] studied the effect of surfactant on cell size of foam. The scanning electron microscopy (SEM) results indicated an optimum concentration of the silicone surfactant of about 1.5 to 2.5 pbw. The optimum of surfactant showed a smaller cell size, and therefore, demonstrated the lower thermal conductivity of the RPUR samples. From the relation between the thermal conductivity and the cell size of the foam samples, the smaller cell size improved the thermal insulation property of the RPUR foam.

Nowadays, there are stronger requirement for the development of all water-blown polyurethane foam system, because the environmentally friendly blowing agent is carbon dioxide, which is obtained in the reaction between polyisocyanurate and water, but the dimensional stability of the foams of this type is not sufficient. Studies of water-blown polyurethane foam preparation were conducted by Stirna and coworkers [23].

Normally, in polyurethane preparation, the mixed catalyst between tin and amine is used to accelerate the gelling and blowing reaction, respectively [24-26].

Singh and coworkers [24] studied effect a mixture of amine and tin catalyst to the rate of PUR foam formation. This investigation reports the amine catalyst mainly accelerated the blowing reaction, as confirmed by the faster cream time, and the tin catalyst only accelerated the gelling reaction, as confirmed by the faster gel time and tack-free time.

In the manufacture of RPUR foams, catalyst is one component has played significant role in catalytic system. Catalyst is necessary for the production of polyurethane foam. Because the reaction between isocyanate with hydroxyl group is slow [7]. Therefore, In isocyanate reactions tertiary amines and tin compounds are mainly used as catalyst, due to their excellent catalytic activity. However, tin is toxic to human beings. Accordingly, a new catalyst is necessary to replace tin catalyst. There are many works concerning the development of catalyst for polyurethane (PUR) and polyisocyanurate (PIR) foams preparation as follows:

Maris and coworkers [27] studies polyurethane catalysis by tertiary amines. They found that tertiary amines play an important role. The mechanism of tertiary amine catalysts are shown in Schemes 2.1 and 2.2. Generally, the tertiary amine coordinate to the positive electron charged carbon of the NCO group or hydrogen of the OH group and forms a transition state to activate urethane formation reaction. It is said that a tertiary amine can be tuned by maximizing its ability to form a hydrogen bond with alcohol, thereby activating the O–H bond so it can attach to the isocyanate more easily. They discussed the selection of catalyst is based on its activity as well as performance on physical foam properties. Depending on the molecular structure of the catalyst, the activity will be different. This activity relates to the catalysis of the gel and blow reaction but also the allophanate, biuret, and trimerization reactions.

In the year 2009, Sardon and coworkers [28] studied about the catalytic activity of tin and zirconium compounds in the polymerization of isophorone diisocyanate (IPDI)-based waterborne polyurethanes. Zirconium acetyl acetonate is much less toxic than the commonly used dibutyltin diacetate (DBTDA). Isophorone diisocyanate based waterborne polyurethanes was synthesized using zirconium acetyl acetonate. This catalyst had a relatively low toxicity about 10 to 20 times less toxic than comparable tin compounds.

Therefore, it was a good candidate in this application to replace the general use of tin catalysts. The results found that zirconium acetyl acetonate does not catalyze the isocyanate reaction. Nevertheless, when the zirconium compound is used in the presence of triethylamine (TEA), the reaction is conveniently catalyzed. Comparing the results obtained with zirconium and tin catalysts in presence of TEA, the zirconium compound shows a higher catalytic activity than tin catalysts. These results confirmed that zirconium catalyst was a good alternative to replace tin compounds.

Strachota and coworkers [29] studied comparison of environmentally friendly, selective polyurethane catalysts. Selected commercially available amines, including N-substituted morpholines, were evaluated as single catalyst and as catalyst mixtures for the preparation of polyurethane foam. The motivation was the search for economically and environmentally attractive replacements of “classical” catalyst like diazabicyclooctane, dibutyltindilaurate and N,N-bis(2-dimethylaminoethyl)methyl amine. Especially interesting was replacing dibutyltindilaurate, and also the possibility of using reactive catalyst derivatives that would be incorporated into polyurethane, thus reducing the content of volatile organic compounds in the polymer. The result found that the functionalized morpholine (MEO) showed a poor gelling activity when compared with the other morpholines. Its reduced mobility due to the desired incorporation into the polyurethane, as well as H-bridging is the probable reasons. Higher amounts of MEO in combination with an analogously OH-functionalized good gelation catalyst should lead to better results.

Kurnoskin [30, 31] studied the synthesized of metal-containing epoxy polymers by hardening of the diglycidyl ether of bisphenol A (DGEBA) with the chelates of metals (Cu^{2+} , Zn^{2+} , Mn^{4+} , Fe^{3+} , Ni^{2+} and Cd^{2+}) and aliphatic amines (ethylenediamine, diethylenetriamine, triethylenetetramine and cycloethylated diethylenetriamine). This is due to the aliphatic amines have high solubility. The reactivity of the complexes in reactions with DGEBA and its dependence on the structures of the chelates has been investigated. The metal-containing epoxy polymers exhibit a significant increased strength and heat resistance.

Inoue and coworkers [32] studied amine-metal complexes as an efficient catalyst for polyurethane syntheses. The reactions of aliphatic isocyanates on the polyurethane preparations are very slow. Therefore, In this reaction tertiary amines and tin compounds such as dibutyltin dilaurate (DBTDL) are mainly used as catalyst, due to their excellent catalytic activity. However, tin is toxic to human beings. In accordance, a new catalyst or catalytic system is necessary to replace tin catalyst. In this research they prepared the complexes of $M(\text{acac})_n$ [$M = \text{Mn, Fe, Co, Ni}$ and Cu] and tertiary amines are use as new catalysts for the reaction between hexamethylene diisocyanate (HDI) and polyols. They found that $\text{Mn}(\text{acac})_n$ -TEDA complex (TEDA = triethylenediamine) showed better catalytic activity than other $M(\text{acac})_n$ complexes and show nearly catalytic activity with DBTDL catalyst.

The researchers in our group, Pengjam [33] synthesized new class of catalyst for the preparation of rigid polyurethane (RPUR) foams. Metal(II)acetate-amine complexes, $M(\text{en})_2$ and $M(\text{trien})$ ($M = \text{Cu}$ and Mn en = ethylenediamine and trien = triethylenetetramine), were synthesized and used as catalysts in the preparation of RPUR foams. The catalytic activity of metal complexes and properties of RPUR foams were investigated and compared to those prepared by *N,N*-dimethylcyclohexylamine (DMCHA), which is used commercially in the preparation of RPUR foams. They found that RPUR foams catalyzed by copper complexes showed better catalytic activity than foam catalyzed by manganese complexes and a reference commercial catalyst (DMCHA).

In manufacturing of RPUR foams, the balance of gelling and blowing reactions is critical to obtain the target morphology and physical properties. Generally, a good acceleration in gelling reaction will result in a good strength of foam and a good acceleration in blowing reaction will also result in a good density of foam. Therefore, there are two kinds of catalysts normally used together, which are gelling and blowing catalysts that added to accelerate the reactions of isocyanate and establish a balance between the gelling and blowing reaction. Tin and amine were traditionally selected as gelling catalyst and blowing catalyst, respectively. However, tin catalyst is toxic to human beings, strong smell and expensive.

Consequently, in this research, metal-amine complexes are chosen catalysts to accelerate both gelling and blowing reactions instead of tin catalyst. Metal-amine and mixed metal-amine complexes were used in the preparation of RPUR foams (Figures 2.9 and 2.10). In order to evaluate the catalytic activity of metal-amine and mixed metal-amine complexes, the results were compared with dimethylcyclohexylamine (DMCHA) catalyst (Figure 2.10), which is used commercially.

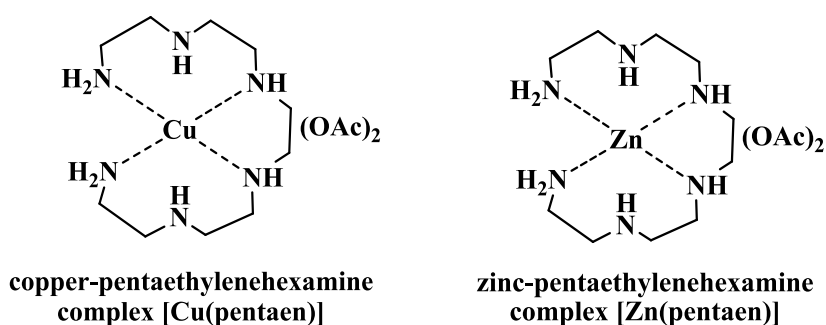


Figure 2.8 An example of metal-amine complex; Cu(pentaen) and Zn(pentaen)

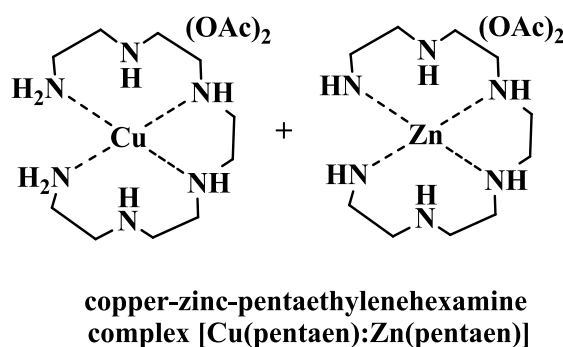


Figure 2.9 An example of mixed metal-amine complex; Cu(pentaen):Zn(pentaen)

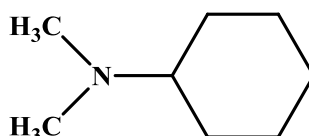


Figure 2.10 N, N-dimethylcyclohexyl amine (DMCHA) (ref.) [1]

CHAPTER III

EXPERIMENTAL

3.1 Chemicals and raw materials

3.1.1 Metal complexes synthesis

Metal acetate used were copper (II) acetate monohydrate ($\text{Cu}(\text{OAc})_2 \cdot \text{H}_2\text{O}$), zinc (II) acetate tetrahydrate ($\text{Zn}(\text{OAc})_2 \cdot 4\text{H}_2\text{O}$), manganese (II) acetate tetrahydrate ($\text{Mn}(\text{OAc})_2 \cdot 4\text{H}_2\text{O}$), nickel (II) acetate tetrahydrate ($\text{Ni}(\text{OAc})_2 \cdot 4\text{H}_2\text{O}$), Cobalt (II) acetate tetrahydrate ($\text{Co}(\text{OAc})_2 \cdot 4\text{H}_2\text{O}$) and aliphatic amine [pentaethylenhexaamine (pentaen)], were obtained from Fluka and Aldrich. Acetone was used as solvent.

3.1.2 Foam preparation

(a) Polyol

In this work polyol (Raypol[®] 4221, sucrose-based polyether polyol) was used to prepare polyurethane foam. The polyether polyol, functionality = 4.3 were supplied by Huntsman (Thailand) CO., Ltd. The specifications of polyether polyol present in Table 3.1.

Table 3.1 Specifications of polyether polyol (Raypol[®] 4221)

Specifications	Test Method	Polyether polyol
Acid number (mgKOH/g)	ASTM D 4662	0.1
Viscosity at 25 °C	ASTM D 4878	5345
Water content	ASTM D 4672	0.050
Hydroxy number	ASTM D 6342	438.39

(b) Isocyanate

Polymeric MDI (4,4'-methane diphenyl diisocyanate; PMDI, MR-200): %NCO = 30.9 (%wt.), average functionality = 2.7 were supplied by Huntsman (Thailand) CO., Ltd.

Polysiloxane (TEGOSTAB B8460, Goldschmidt) were obtained from South City Petrochem CO., Ltd. was used as a surfactant. Distilled water was used as a chemical blowing agent. Metal complexes were prepared and used as catalysts. N,N-

dimethylcyclohexylamine (DMCHA) (Huntsman (Thailand) CO., Ltd.) was used as a commercial reference catalyst.

3.2 Synthetic procedures

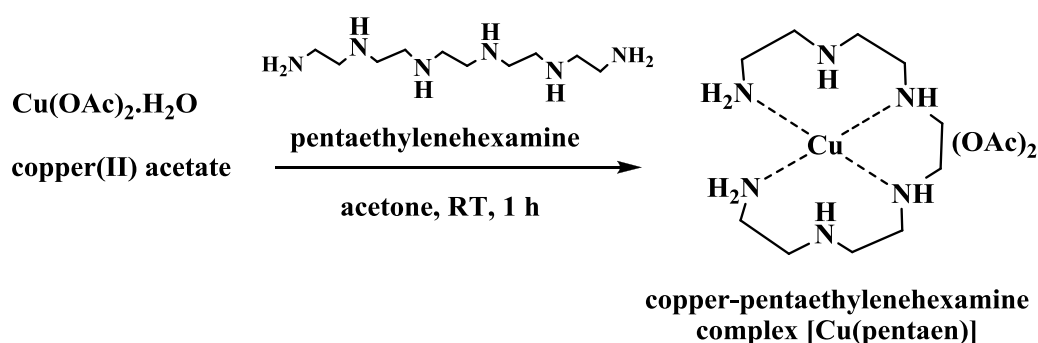
Synthesis metal-amine and mixed metal complexes for preparing RPUR foam consist of two methods. In the first method, metal-pentaethylenehexamine complexes $[M_1(\text{pentaen})]$ and mixed metal-pentaethylenehexamine $[M_1(\text{pentaen}):M_2(\text{pentaen})]$ complexes were synthesized from the reaction between metal (II) acetate and pentaethylenehexamine (pentaen) using acetone as a solvent [29]. Acetone was removed from the metal complex before using in the preparation of rigid polyurethane foam.

In the second method, the preparation of metal complexes was done in water to obtain an aqueous solution containing metal complexes. The metal complex solution was used in the preparation of rigid polyurethane foam without purification.

3.2.1 Synthesis of metal-amine complexes

3.2.1.1 Synthesis of copper-pentaethylenehexamine complex

$[\text{Cu}(\text{pentaen})]$



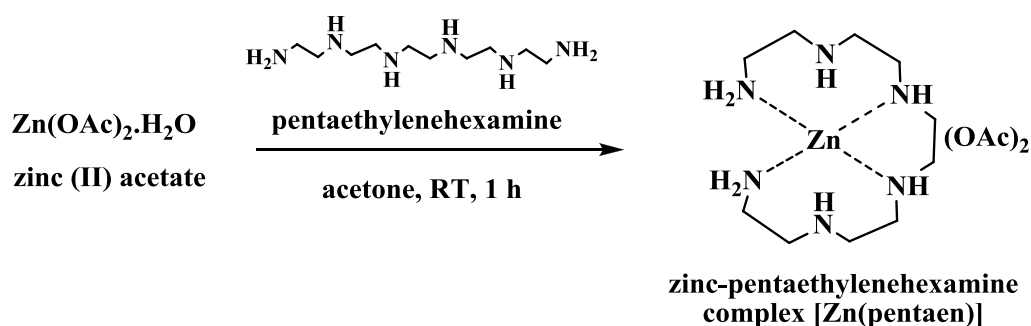
Scheme 3.1 Synthesis of copper- pentaethylenehexamine complex $[\text{Cu}(\text{pentaen})]$

The preparation of $\text{Cu}(\text{pentaen})$ was performed according to the method reported in the literature [29] as follows: a solution of pentaethylenehexamine (pentaen) (0.59 ml, 2.54 mmol) was stirred in acetone (10 mL) at room temperature for 30 minutes. After that, copper (II) acetate monohydrate (0.462 g, 2.31 mmol) was added and the reaction mixture was stirred at room temperature for 1 hour. Acetone

was removed from the reaction mixture under vacuum. Cu(pentaen) was obtained as dark blue viscous liquid (0.89 g, 89%): IR (cm^{-1}); 3403 (N-H), 2942 (C-H), 1562 (asymmetric C=O, acetate), 1408 (symmetric C=O, acetate), 1332 (C-N), 1015 (C-O). UV; $\lambda_{\text{max}}(\text{MeOH})=265$ nm, molar absorptivity (ϵ) = 4,750. Cu(pentaen) shown m/z = 436.826. Anal. Calcd. For $\text{CuC}_{14}\text{O}_4\text{H}_{34}\text{N}_6$: C 40.62; H 8.28; N 20.30; found C 40.32; H 8.48; N 19.89. AAS. Calcd. For $\text{CuC}_{14}\text{O}_4\text{H}_{34}\text{N}_6$: Cu 15.35; found Cu 15.16

3.2.1.2 Synthesis of zinc-pentaethylenehexamine complex

[Zn(pentaen)]



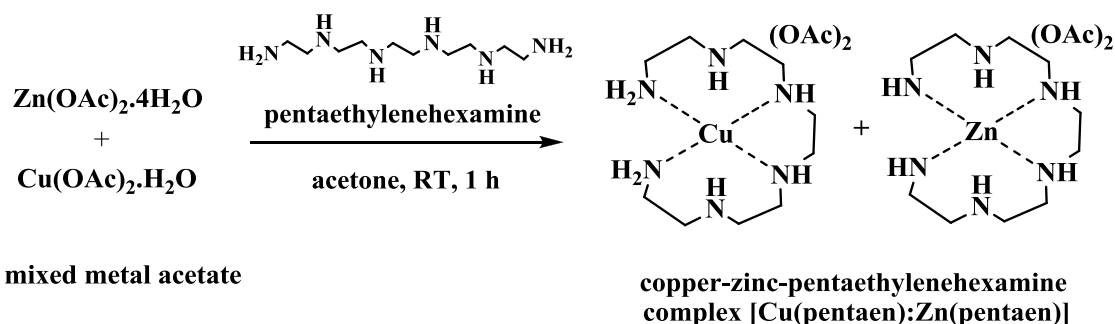
Scheme 3.2 Synthesis of zinc-pentaethylenehexamine complex

The preparation of Zn(pentaen) was done as follow: a solution of pentaethylenehexamine (0.56 ml, 2.41 mmol) was stirred in acetone (10 mL) at room temperature for 30 minutes. After that, zinc (II) acetate tetrahydrate (0.485 g, 2.30 mmol) was added and the reaction mixture was stirred at room temperature for 1 hour. The reaction mixture was dried under vacuum to remove solvent. Zn(pentaen) was obtained as yellow viscous liquid (0.75 g, 75%): IR (cm^{-1}); 3390 (N-H), 2926 (C-H), 1569 (asymmetric C=O, acetate), 1406 (symmetric C=O, acetate), 1335 (C-N), 1015 (C-O). UV; $\lambda_{\text{max}}(\text{MeOH}) = 207$ nm, molar absorptivity (ϵ) = 1,053. Zn(pentaen) shown m/z = 474.289 Anal. Calcd. For $\text{CuC}_{14}\text{O}_4\text{H}_{34}\text{N}_6$: C 40.43; H 8.24; N 20.21; found C 40.69; H 8.90; N 18.63. AAS. Calcd. For $\text{ZnC}_{14}\text{O}_4\text{H}_{34}\text{N}_6$: Zn 15.73; found Zn 14.16.

3.2.2 Synthesis mixed metal-amine complex

3.2.2.1 Synthesis of copper:zinc-pentaethylenehexamine complex

Cu(pentaen):Zn(pentaen)]



Scheme 3.3 Synthesis of copper-zinc pentaethylenehexamine complex

The preparation of Cu(pentaen):Zn(pentaen) was done as follow: a solution of pentaethylenehexamine (0.58 ml, 2.50 mmol) was stirred in acetone (10 mL) at room temperature for 30 minutes. After that, copper (II) acetate monohydrate (0.226 g, 1.13 mmol) and zinc (II) acetate tetrahydrate (0.248 g, 1.24 mmol) was added and the reaction mixture was stirred at room temperature for 1 hour. The reaction mixture was dried under vacuum to remove solvent. Cu(pentaen):Zn(pentaen) was obtained as blue viscous liquid (0.87 g, 87%): IR(cm^{-1}); 3318 (N-H), 2986 (C-H), 1565 (asymmetric C=O, acetate), 1407 (symmetric C=O, acetate), 1326 (C-N), 1039 (C-O). UV; λ_{max} (MeOH) = 264 nm, molar absorptivity (ϵ) = 4,790. Cu(pentaen) shown m/z = 436.094 and Zn(pentaen) shown m/z = 474.272 Anal. Calcd. For $\text{CuZnC}_{28}\text{O}_8\text{H}_{68}\text{N}_{12}$: C 40.52; H 8.26; N 20.25; found C 40.11; H 8.15; N 18.45. AAS. Calcd. For $\text{CuZnC}_{28}\text{O}_8\text{H}_{68}\text{N}_{12}$: Cu 7.66; Zn 7.88 found Cu 6.35; Zn 6.25.

Other metal complexes and mixed metal complexes were prepared using similar procedure as described above. Compositions of starting materials in the preparation of all metal complexes in acetone are shown in Tables 3.2 and 3.3.

Table 3.2 Composition of starting materials in the preparation of metal complexes prepared at different $M(OAc)_2$:pentaen mole ratios

Metal complexes	Wt. of $M(OAc)_2$ (g)	Weight of composition		Yield (%)	Appearance
		pentaen (mL)			
$M(OAc)_2$:pentaen =1:2					
Cu(pentaen) ₂	0.30	0.74		84	Dark blue viscous liquid
Zn(pentaen) ₂	0.321	0.72		70	Yellow viscous liquid
Co(pentaen) ₂	0.349	0.68		82	Purple-red viscous liquid
Ni(pentaen) ₂	0.349	0.68		67	Purple viscous liquid
Mn(pentaen) ₂	0.345	0.69		84	Brown viscous liquid
$M(OAc)_2$:pentaen =1:1					
Cu(pentaen)	0.462	0.59		89	Dark blue viscous liquid
Zn(pentaen)	0.485	0.56		75	Yellow viscous liquid
Co(pentaen)	0.517	0.51		86	Purple-red viscous liquid
Ni(pentaen)	0.518	0.53		72	Purple viscous liquid
Mn(pentaen)	0.513	0.52		89	Brown viscous liquid

Table 3.3 Composition of starting materials in the preparation of mixed metal complexes at $M_1(OAc)_2$: $M_2(OAc)_2$:pentaen mole ratio of 0.5:0.5:1

Metal complexes	Wt. of $M(OAc)_2$ (g)		Weight of composition		Yield (%)	Appearance
	M_1	M_2	pentaen (mL)			
Cu:Zn(pentaen)	0.226	0.248	0.58		87	Blue viscous liquid
Cu:Co(pentaen)	0.218	0.273	0.54		81	Purple-red viscous liquid
Cu:Ni(pentaen)	0.219	0.272	0.56		75	Blue viscous liquid
Cu:Mn(pentaen)	0.22	0.269	0.54		90	Brown viscous liquid

3.2.3 Synthesis of metal complexes in water [W_M(pentaen)]

3.2.2.1 Synthesis of W_Cu(pentaen) complex

Copper (II) acetate monohydrate (0.462 g, 2.31 mmol) and polysiloxane surfactant (TEGOSTAB B8460) (2.5 ml) were dissolved in 2 mL of distilled water at room temperature and the solution was stirred for 30 minutes. Pentaethylenehexamine (0.59 ml, 2.54 mmol) was then added dropwise and the solution was stirred at room temperature for 60 minutes. W_Cu(pentaen) aqueous solution was obtained as a dark blue solution. UV; λ_{\max} (MeOH) = 265 nm, molar absorptivity (ϵ) = 2,467.

3.2.2.2 Synthesis of W_Zn(pentaen) complex

Zinc acetate dihydrate (0.485 g, 2.30 mmol) and polysiloxane surfactant (TEGOSTAB B8460) (2.5 ml) were dissolved in 2 mL of distilled water at room temperature and the solution was stirred for 30 minutes. Pentaethylenehexamine (0.56 ml, 2.41 mmol) was then added dropwise and the solution was stirred at room temperature for 60 minutes. W_Zn(pentaen) aqueous solution was obtained as a yellow solution. UV; λ_{\max} (MeOH) = 207 nm, molar absorptivity (ϵ) = 840.

3.2.3 Synthesis of mixed metal complexes in water

[W_M₁(pentaen):M₂(pentaen)]

3.2.3.1 Synthesis of W_Cu(pentaen):Zn(pentaen) complex

Copper (II) acetate monohydrate (0.226 g, 1.13 mmol), zinc acetate dihydrate (0.248 g, 1.24 mmol) and polysiloxane surfactant (TEGOSTAB B8460) (2.5 ml) were dissolved in 2 mL of distilled water at room temperature and the solution was stirred for 30 minutes. Pentaethylenehexamine (0.58 ml, 2.50 mmol) was then added dropwise and the solution was stirred at room temperature for 60 minutes. W_Cu(pentaen):Zn(pentaen) aqueous solution was obtained as a dark blue solution. UV; λ_{\max} (MeOH) = 264 nm, molar absorptivity (ϵ) = 1,900.

3.3.3 Rigid polyurethane (RPUR) foam preparations

All of RPUR foam sample were synthesized with two step illustrated in Figure 3.1. The foams were prepared by mechanical mixing technique in two steps of the mixing. In the first mixing step, polyol, catalysts (metal complexes or DMCHA), surfactant and blowing agent were mixed. In the second mixing step, the isocyanate was added to the mixed polyol from first mixing then the mixture were mixed in homogeneous mixture by mechanical stirrer at 2000 rpm for 20 seconds.

The polymerization times investigated in the synthesis of rigid polyurethane foam were cream time, gel time, tack free time and rise time. The reaction times of the prepared foams were investigated and compared to those catalyzed with N,N-dimethylcyclohexylamine (DMCHA), which is used commercially. After that, the foams were kept at room temperature for 48 hours and then carrying out physical and mechanical characterization. The foam formulations are demonstrated in Tables 3.4 and 3.5. Polyurethane foams with different NCO indexes were prepared by using different catalysts.

Table 3.4 RPUR foam formulations at different NCO indexes (in part by weight unit)

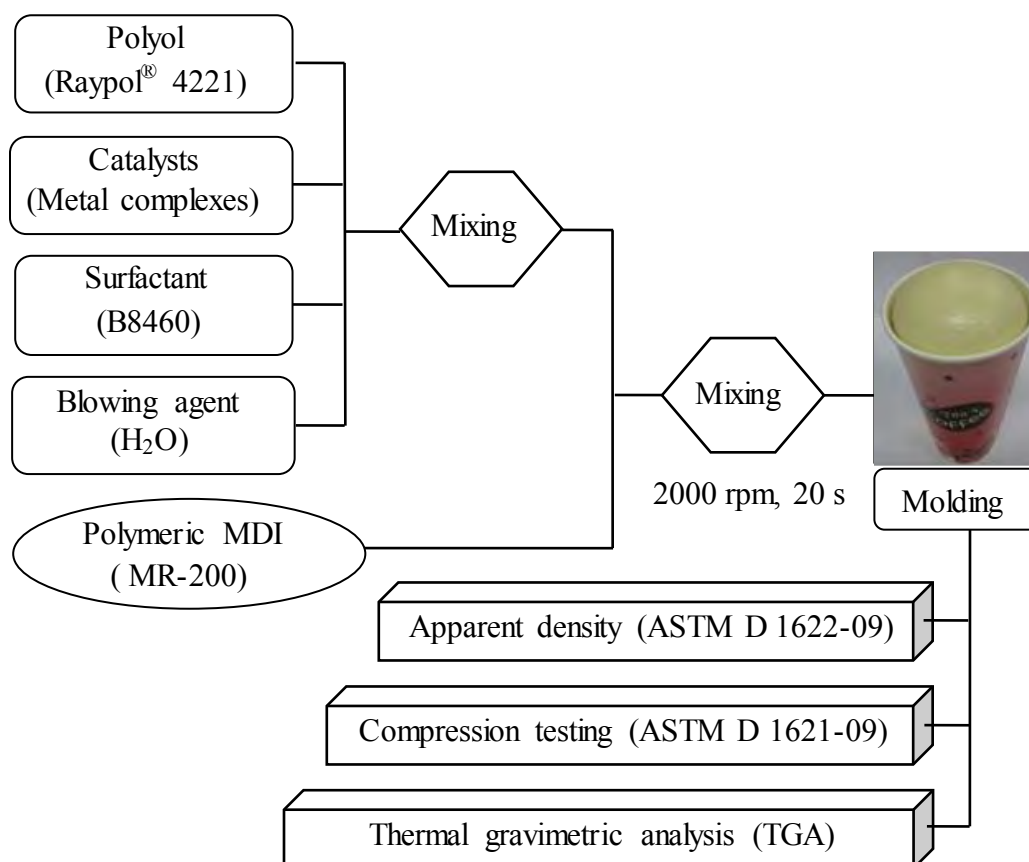
Formulations (pbw)	NCO index			
	100	130	150	170
Polyol (Raypol [®] 4221)	100	100	100	100
Catalysts (metal complexes)	1.0	1.0	1.0	1.0
Surfactant (TEGOTAB B8460)	2.5	2.5	2.5	2.5
Blowing agent (H ₂ O)	2.0	2.0	2.0	2.0
Polymeric MDI (MR-200)	137	178	205	233

Table 3.5 RPUR foam formulations at different NCO indexes (in gram unit, cup test)

Formulations (g)	NCO index			
	100	130	150	170
Polyol (Raypol [®] 4221)	10.0	10.0	10.0	10.0
Catalysts (metal complexes)	0.1	0.1	0.1	0.1
Surfactant (TEGOTAB B8460)	0.25	0.25	0.25	0.25
Blowing agent (H ₂ O)	0.20	0.20	0.20	0.20
Polymeric MDI (MR-200)	13.7	17.8	20.5	23.3

Since the rigid polyurethane foams obtained from different catalysts have similar IR spectra, therefore, only the IR data PUR foams obtained from Cu(pentaen):Zn(pentaen) catalyst is described as follows:

RPUR foam catalyzed by Cu(pentaen):Zn(pentaen); IR (IR-ATR, cm⁻¹); 3314 (N-H), 2923, 2874 (C-H), 2277 (free NCO), 1707 (C=O), 1595 (Ar-H), 1515 (N-H), 1410 (C-N isocyanurate), 1312 (C-H), 1220, 1077 (C-O urethane)

**Figure 3.1** RPUR foams processing

3.4 Instrumentation

3.4.1 Infrared spectroscopy

The Infrared (IR) spectra were recorded on a Nicolet 6700. FTIR spectrometer was used to study of functional groups on metal complexes as catalyst and foams at room temperature using a Nicolet at a resolution of 4 cm^{-1} and a total of 64 interferograms were signal averaged. It is important that the samples are pressed, reproducibly and with a constant pressure, against the IR-transmitting ATR crystal. The ATR crystal is integrated into the beam of an ATR-IR spectrometer (Nicolet 6700) in such a way that IR light is passed through the crystal by means of total reflection. ATR occurs on the measuring surface that is in contact with the foam sample. The IR bands given in Table 3.6 are used for the analysis. The measurement was controlled by Omnic software.

Table 3.6 Characteristic IR bands of RPUR foam

Functional group	Vibration mode	IR peak (cm^{-1})
NCO	NCO antisymm. Str.	2180-2310
CO	CO str.(urethane, urea, isocyanurate, allophanate, Biuret, <i>etc.</i>)	1620-1760
Isocyanurate	Ring deformation and CH_2 -deformation in PMDI	1370-1443
Amide	CN-str. (urethane, urea)	1155-1245
Reference	Non-reaction groups in polyol and isocyanate	935-1050

3.4.2 Ultraviolet-visible spectroscopy

UV-visible spectroscopy is routinely used in the quantitative determination of solutions of transition metal ions highly conjugated organic compounds. UV-Vis spectra were recorded on ultraviolet and visible spectrophotometer at room temperature. Absorption spectra were obtained on Varian Cary 50 UV-Vis

spectrophotometer. The samples were scan over range 200-500 nm at a medium speed.

3.4.3 Mass spectrometry (MS)

Mass spectrometry (MS) is an analytical technique that measures the mass-to-charge ratio of charge particles. Mass spectra were obtained on a micromass Quattro microTM API spectrometer. Electrospray can also be used in case of molecule without any ion stable sites, through the formation of proton and sodium.

3.4.4 Atomic absorption spectrometry (AAS)

Atomic absorption spectrometry (AAS) is a spectroanalytical procedure for the quantitative determination of chemical elements employing the absorption of optical radiation (light) by free atoms in the gaseous state using a flame (Perkin-Elmer : AAnalyst 100)

3.4.5 Atomic absorption spectrometry (EA)

For organic chemists, element analysis or “EA” almost always refers to %C, %H and %N analysis; the determination of the percentage weights of carbon, hydrogen and nitrogen of a sample. Elemental analysis was carried out using a Perkin-Elmer EP 2400 analyzer.

3.4.6 Digital Stopwatch

The reaction times namely, cream time, gel time tack free time and rise time were investigated by using a digital stopwatch.

3.4.7 Thermocouple

Thermocouple is a widely used type of temperatures sensor for measurement. The foaming temperatures were recorded by dual thermocouple, Digicon DP-71.

3.5 Physical and Mechanical properties of RPUR foam

3.5.1 Density

The apparent density of foams was measured according to ASTM D 1622-09, the size of specimen was 3.0 x 3.0 x 3.0 cm (length×width×thickness) and the average values of three samples were reported.

3.5.2 Scanning electron microscope (SEM)

The morphology and cell size of foams were studied using scanning electron microscope (SEM) Hitachi/ S-4800. The samples were gold coated before scanning in order to provide an electrically conductive surface. The accelerating voltage was 20 kV in order to avoid degradation of the sample.

3.5.3 Compressive testing

The compressive testing of foams in parallel and perpendicular to the foam rise direction were performed using universal testing machine (Lloyd/LRX) according to ASTM D 1621-09, the specimen size was 3.0 x 3.0 x 3.0 cm dimension, the rate of crosshead movement was fixed at 2.54 mm/min and the preload cell used was 0.10 N.

3.5.4 Thermalgravimetric analysis (TGA)

Thermalgravimetric analysis (TGA) was used to investigate the thermal stability of RPUR foam. TGA determination was performed by Netzsch STA 409C thermogravimetric analyzer. All samples were heated from 25 °C to 600 °C at heating rate of 20 °C/min under N₂ gas.

3.5.5 Thermal conductivity

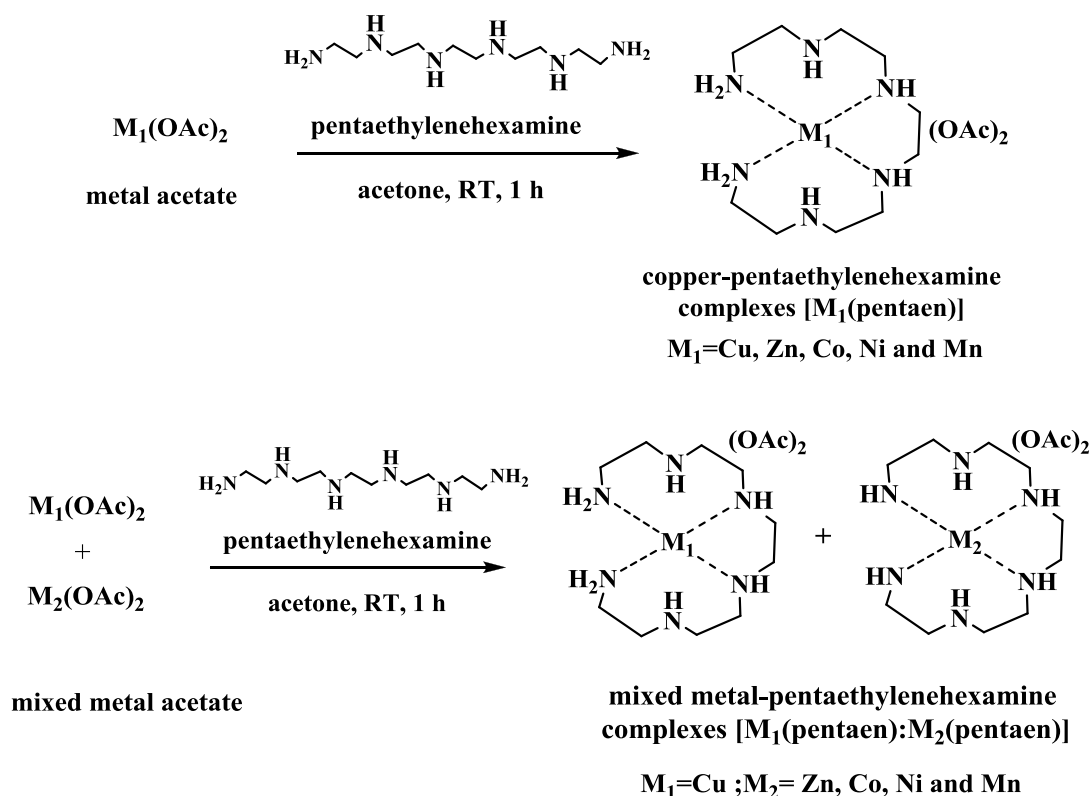
Thermal conductivity is a measure of the ability to transmit heat through the material. The size of the specimen was 5.0×5.0×2.0 cm (length×width×thickness). Analyzed by Hot Disk Thermal Constant analyzer TPS 2500 (Hot Disk AB) under room temperature condition. Disk type: Kapton Insulation (Sensor No. C7577, Radius = 2.001)

CHAPTER IV

RESULTS AND DISCUSSION

4.1 Synthesis of metal amine [$M_1(\text{pentaen})$] and mixed metal-amine complexes [$M_1(\text{pentaen}):M_2(\text{pentaen})$]

The metal and mixed-metal complexes were synthesized using two methods. In the first method, metal-pentaethylenehexamine complexes [$M_1(\text{pentaen})$] and mixed metal-pentaethylenehexamine [$M_1(\text{pentaen}):M_2(\text{pentaen})$] complexes were synthesized from the reaction between metal (II) acetate and pentaethylenehexamine (pentaen) using acetone as a solvent [30]. The mole ratios of $M(\text{OAc})_2$:pentaen were 1:2, 1:1 and 1:0.5. Acetone was removed from the metal complexes under vacuum before using in the preparation of rigid polyurethane foam.



Scheme 4.1 Synthesis of metal and mixed metal- pentaethylenehexamine complexes

In the second method, $W_M(\text{pentaen})$ and $W_M_1(\text{pentaen}):M_2(\text{pentaen})$ were synthesized using water as a solvent. It was found that the complexes formation was obtained in aqueous solution. The metal complex solution was used in the preparation of rigid polyurethane foam without purification.

4.2 Characterization of copper-pentaethylenehexamine complex synthesized at the mole ratio of $\text{Cu}(\text{OAc})_2:\text{pentaen} = 1:1$

4.2.1 IR spectroscopy of $\text{Cu}(\text{pentaen})$ complex

IR spectrum of $\text{Cu}(\text{pentaen})$ is demonstrated in Figure 4.1. They exhibited absorption band at 3403 cm^{-1} (N-H stretching), 2942 cm^{-1} (C-H stretching), 1562 cm^{-1} (C=O asymmetric stretching), 1408 cm^{-1} (C=O symmetric stretching), 1332 cm^{-1} (C-N stretching) and 1015 cm^{-1} (C-O stretching). The C=O stretching of carbonyl group in $\text{Cu}(\text{pentaen})$ appeared as absorption band at 1562 cm^{-1} (asymmetric C=O), and 1408 cm^{-1} (symmetric C=O), respectively, which were different from the typical $\text{Cu}(\text{OAc})_2$ normally appears as absorption band around at 1596 cm^{-1} (asymmetric C=O) and 1422 cm^{-1} (symmetric C=O). The absorption bands of $\text{Cu}(\text{pentaen})$ exhibited C-O stretching at 1015 cm^{-1} , respectively which shifted from typical absorption band of $\text{Cu}(\text{OAc})_2$ at 1036 cm^{-1} . It was found that the IR peak of $\text{Cu}(\text{pentaen})$ shifted from those of $\text{Cu}(\text{OAc})_2$ to lower energy because of the influence of amine coordination, which suggested that the complex was formed.

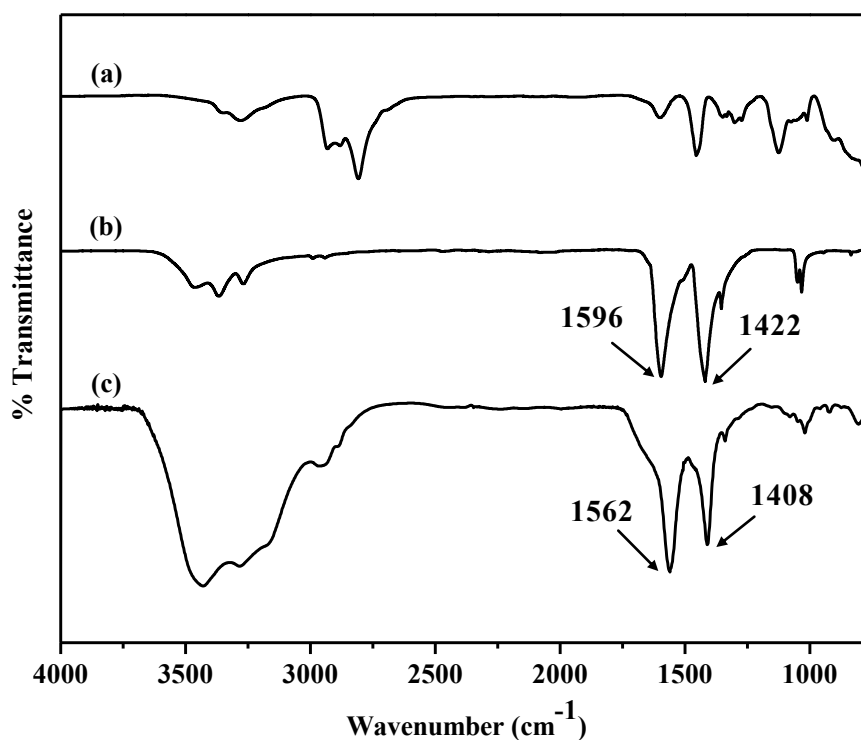


Figure 4.1 IR spectra of (a) pentaethylenhexamine (b) Cu(OAc)₂; (c) Cu(pentaen) synthesized at the mole ratio of Cu(OAc)₂:pentaen = 1:1

4.2.2 UV-visible spectroscopy of Cu(pentaen) complex

UV-visible spectrum of Cu(pentaen) (synthesized in acetone) was compared to that of W_Cu(pentaen) (synthesized in water) as illustrated in Figure 4.2. The maximum wavelength of Cu(pentaen) and W_Cu(pentaen) appeared at 265 nm. Evidently, the maximum wavelength of both Cu(pentaen) and W_Cu(pentaen) shifted from typical maximum wavelength of Cu(OAc)₂ at 244 nm, which confirmed the complex formation.

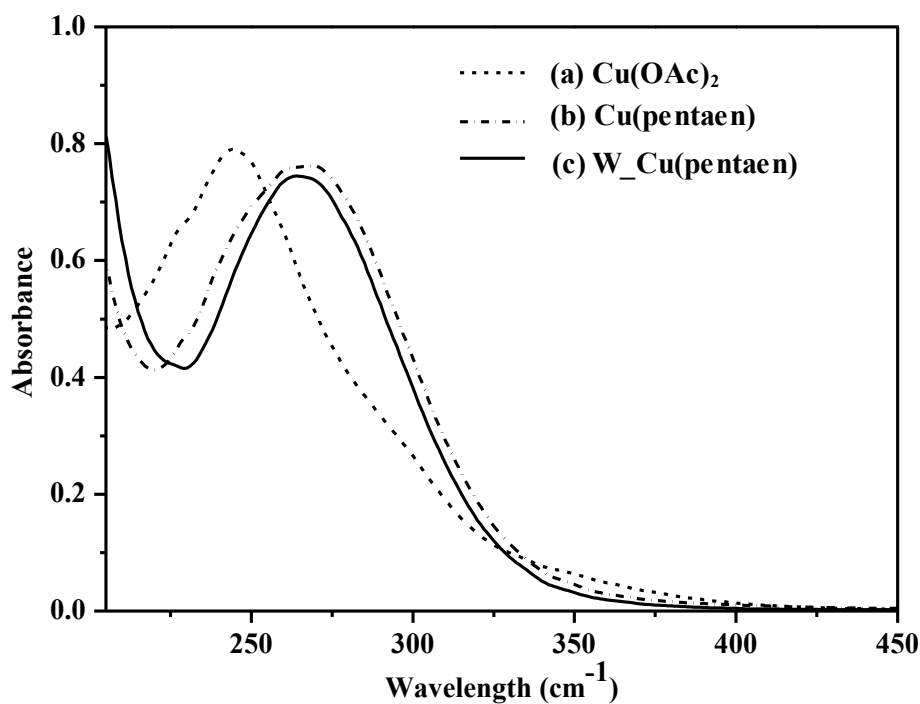


Figure 4.2 UV spectra of (a) $\text{Cu}(\text{OAc})_2$; (b) $\text{Cu}(\text{pentaen})$ and (c) $\text{W_Cu}(\text{pentaen})$ synthesized at the mole ratio of $\text{Cu}(\text{OAc})_2:\text{pentaen} = 1:1$

4.2.3 Determination of metal amount in $\text{Cu}(\text{pentaen})$ complex by flame atomic spectrometry (FAAS)

For analytical characteristics of $\text{Cu}(\text{pentaen})$ illustrated in Table 4.1 This result indicates that there is the consistency between the experimental value and the calculated value. It confirmed the structure of metal complex (Scheme 3.1).

Table 4.1 Analytical Characteristics of the FAAS method

Catalyst	Elements determined	Experimental (%)	Calculated (%)
$\text{Cu}(\text{pentaen})$	Cu	15.16	15.35

4.2.4 Elemental analysis of Cu(pentaen) complex

Elemental analysis (%C, %H and %N) of Cu(pentaen) is shown in Table 4.2. This result indicates that there is the consistency between the experimental value and the calculated value.

Table 4.2 Elemental analysis (%C, %H, and %N) of Cu(pentaen)

Catalyst	Elements determined	Experimental (%)	Calculated (%)
Cu(pentaen)	%C	40.32	40.62
	%H	8.48	8.28
	%N	19.89	20.30

4.2.5 Mass spectrometry of Cu(pentaen) complex

The molecular ion peak of Cu(pentaen) at $m/z = 436.826$ corresponding to $[\text{}^{63}\text{Cu}(\text{pentaen})+2\text{H}_2\text{O}+\text{Na}]^+$; $m/z = 436.184$ is observed in the ESI mass spectrum (Figure 4.3).

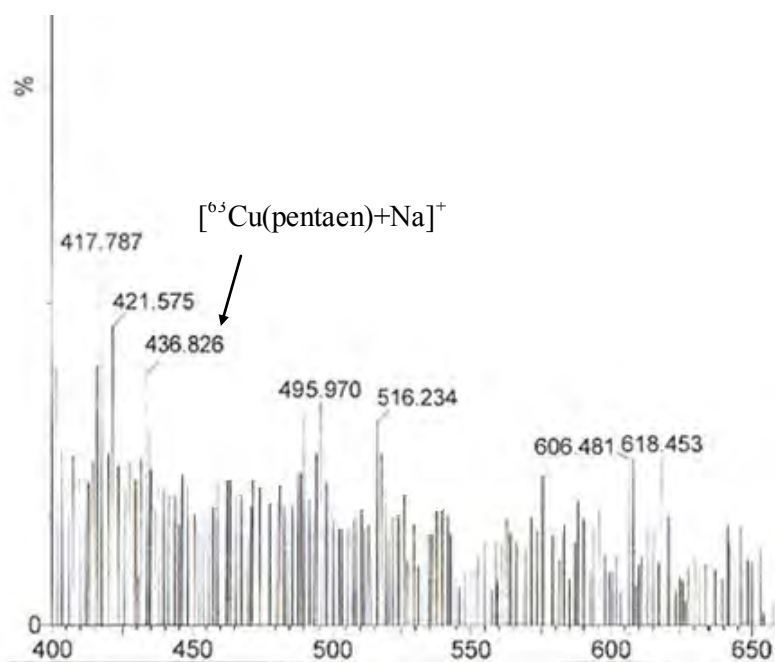


Figure 4.3 Mass spectrum of Cu(pentaen) synthesized at the mole ratio of $\text{Cu}(\text{OAc})_2:\text{pentaen} = 1:1$

4.3 Characterization of zinc-complex synthesized at the mole ratio of Zn(OAc)_2 :pentaen = 1:1

4.3.1 IR spectroscopy of Zn(pentaen) complex

Zn(pentaen) spectrum (Figure 4.4) exhibited absorption band at 3390 cm^{-1} (N-H stretching), 2926 cm^{-1} (C-H stretching), 1569 cm^{-1} (C=O asymmetric stretching), 1406 cm^{-1} (C=O symmetric stretching), 1335 cm^{-1} (C-N stretching), and 1015 cm^{-1} (C-O stretching). The C=O stretching in Zn(pentaen) appeared absorption band at 1569 cm^{-1} (asymmetric C=O), and 1406 cm^{-1} (symmetric C=O), respectively, which were different from the typical Zn(OAc)_2 normally appears as absorption band around 1541 cm^{-1} (asymmetric C=O) and 1427 cm^{-1} (symmetric C=O). The absorption bands of Zn(pentaen) exhibited of C-O stretching at 1015 cm^{-1} , respectively which shifted from typical absorption band of Zn(OAc)_2 at 1024 cm^{-1} . It was found that the IR peak of Zn(pentaen) complex slightly shifted from those of Zn(OAc)_2 , which indicated that the complexes was formed.

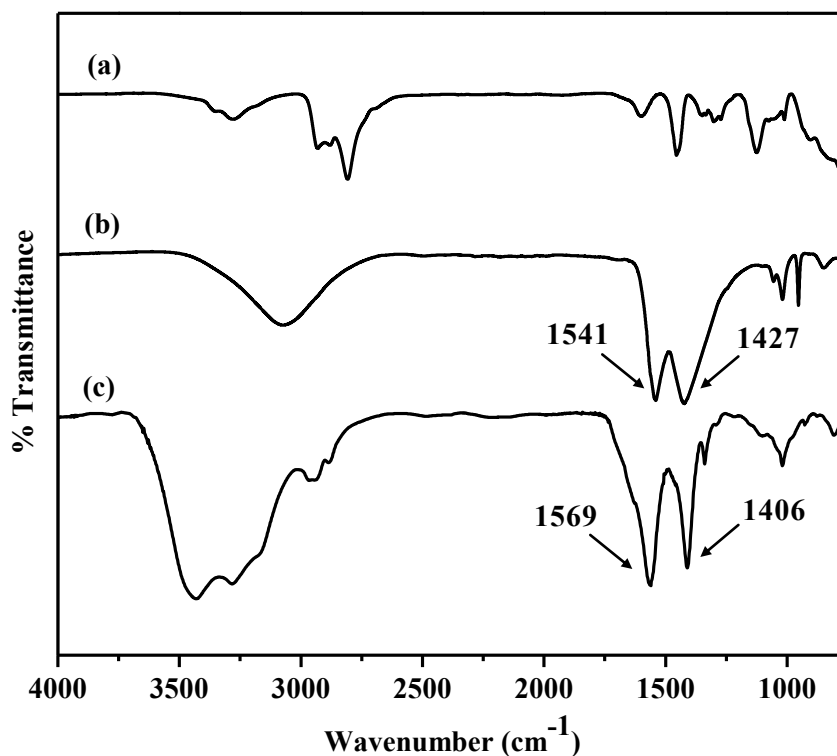


Figure 4.4 IR spectra of (a) pentaethylenehexamine; (b) Zn(OAc)_2 ; (c) Zn(pentaen) synthesized at the mole ratio of Zn(OAc)_2 :pentaen = 1:1

4.3.2 UV-visible spectroscopy of Zn(pentaen) complex

UV-visible spectra of Zn(pentaen) (synthesized in acetone) was compared to that of W_Zn(pentaen) (synthesized in water) as shown in Figure 4.5. The maximum wavelength Zn(pentaen) and W_Zn(pentaen) appeared at 207 nm. Their maximum wavelengths slightly shifted from typical maximum wavelength of Zn(OAc)₂ at 202 nm, which confirmed the complex formation.

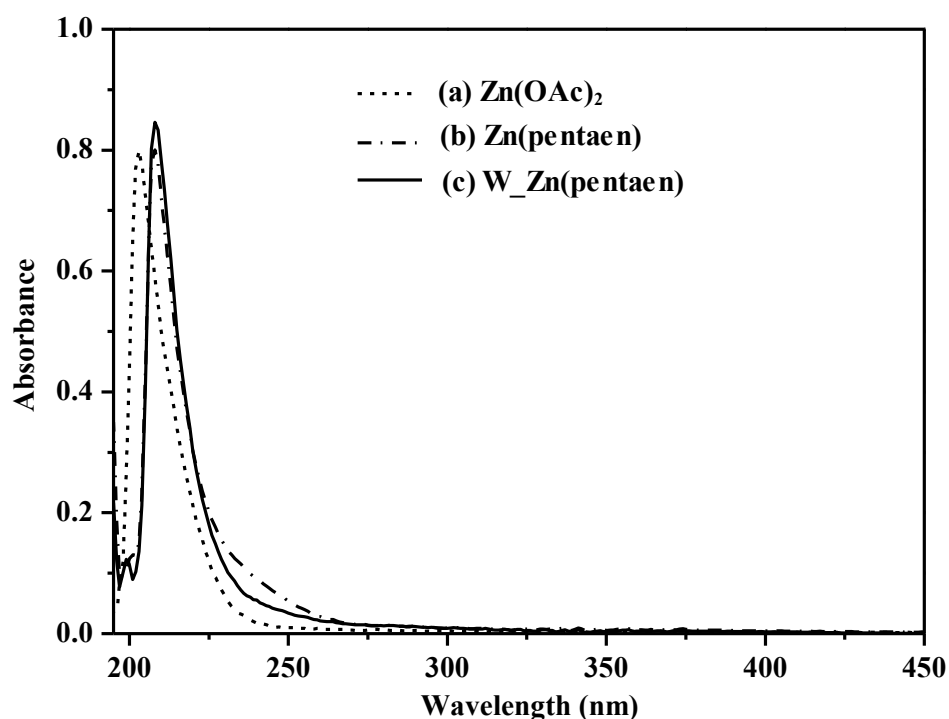


Figure 4.5 UV spectra of (a) Cu(OAc)₂; (b) Zn(pentaen) and (c) W_Zn(pentaen) synthesized at the mole ratio of Zn(OAc)₂:pentaen = 1:1

4.3.3 Determination of metal amount in Zn(pentaen) complex by flame atomic spectrometry (FAAS)

For analytical characteristics of Zn(pentaen) illustrated in Table 4.3. This result indicates that the experimental value and the calculated value were different.

Table 4.3 Analytical Characteristics of the FAAS method

Catalyst	Elements determined	Experimental (%)	Calculated (%)
Zn(pentaen)	Zn	14.16	15.73

4.3.4 Elemental analysis of Zn(pentaen) complex

Elemental analysis (%C, %H and %N) of Zn(pentaen) shown in Table 4.4. This result indicates that there was inconsistency between the experimental value and the calculated value.

Table 4.4 Elemental analysis (%C, %H, and %N) of Zn(pentaen)

Catalyst	Elements determined	Experimental (%)	Calculated (%)
Zn(pentaen)	%C	40.69	40.43
	%H	8.90	8.24
	%N	18.63	20.21

4.3.5 Mass spectrometry of Zn(pentaen) complex

The molecular ion peak of Zn(pentaen) at $m/z = 474.289$ corresponding to $[^{64}\text{Zn}(\text{pentaen})+2\text{H}_2\text{O}+\text{Na}]^+$; $m/z = 473.204$ is observed in the ESI mass spectrum (Figure 4.6).

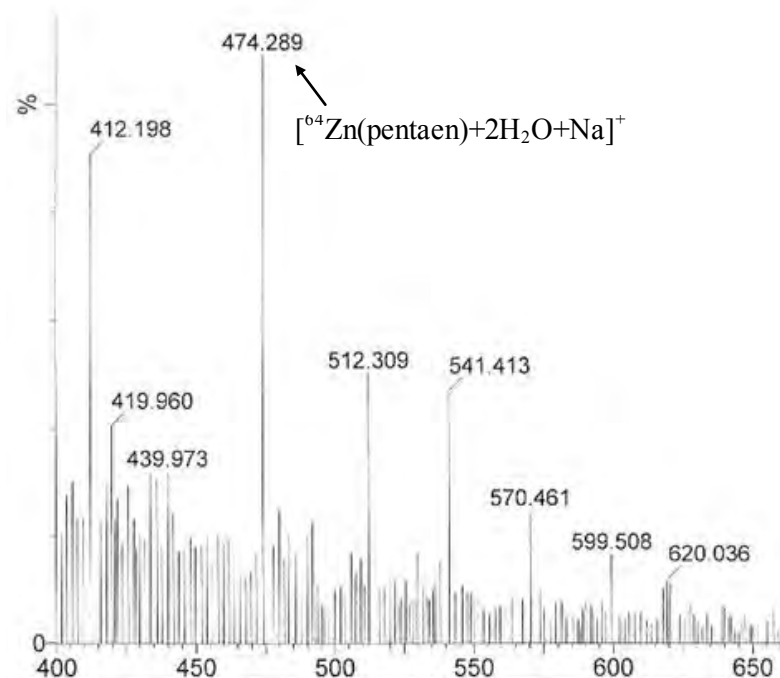


Figure 4.6 Mass spectrum of Zn(pentaen) synthesized at the mole ratio of $\text{Zn}(\text{OAc})_2:\text{pentaen} = 1:1$

4.4 Characterization of copper:zinc-complex synthesized at the mole ratio of $\text{Cu}(\text{OAc})_2:\text{Zn}(\text{OAc})_2:\text{pentaen} = 0.5:0.5:1$

4.4.1 IR spectroscopy of $\text{Cu}(\text{pentaen}):\text{Zn}(\text{pentaen})$ complex

IR spectra of $\text{Cu}(\text{pentaen}):\text{Zn}(\text{pentaen})$ is demonstrated in Figure 4.7. They exhibited absorption band at 3415 cm^{-1} (N-H stretching), 2935 cm^{-1} (C-H stretching), 1565 cm^{-1} (C=O asymmetric stretching), 1407 cm^{-1} (C=O symmetric stretching), 1335 cm^{-1} (C-N stretching) and 1015 cm^{-1} (C-O stretching). The C=O stretching of carbonyl group in $\text{Cu}(\text{pentaen}):\text{Zn}(\text{pentaen})$ appeared as absorption band at 1565 cm^{-1} (asymmetric C=O), and 1407 cm^{-1} (symmetric C=O), respectively, which were different from the typical $\text{Cu}(\text{OAc})_2$ and $\text{Zn}(\text{OAc})_2$ normally appears as absorption band around at $1596, 1541\text{ cm}^{-1}$ (asymmetric C=O) and $1422, 1427\text{ cm}^{-1}$ (symmetric C=O) respectively. The absorption bands of $\text{Cu}(\text{pentaen}):\text{Zn}(\text{pentaen})$ exhibited C-O stretching at 1015 cm^{-1} which shifted from typical absorption band of $\text{Cu}(\text{OAc})_2$ and $\text{Zn}(\text{OAc})_2$ at $1036, 1024\text{ cm}^{-1}$. It indicated that the complex was formed.

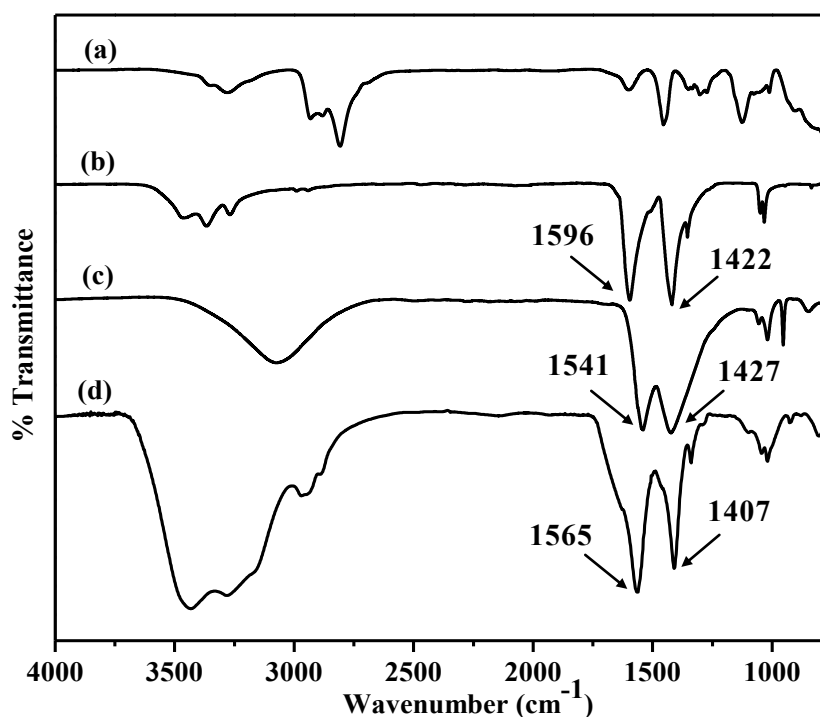


Figure 4.7 IR spectra of (a) pentaethylenehexamine; (b) $\text{Cu}(\text{OAc})_2$; (c); $\text{Zn}(\text{OAc})_2$; (d) $\text{Cu}(\text{pentaen}):\text{Zn}(\text{pentaen})$ synthesized at the mole ratio of $\text{Cu}(\text{OAc})_2:\text{Zn}(\text{OAc})_2:\text{pentaen} = 0.5:0.5:1$

4.4.2 UV-visible spectroscopy of Cu(pentaen):Zn(pentaen) complex

UV-visible spectra of Cu(pentaen):Zn(pentaen) (synthesized in acetone) and W_Cu(pentaen):Zn(pentaen) (synthesized in water) were compared as illustrated in Figure 4.8. The maximum wavelength of Cu(pentaen):Zn(pentaen) and W_Cu(pentaen):Zn(pentaen) both appeared at 264 nm. Evidently, their maximum wavelengths shifted from typical maximum wavelength of Cu(OAc)₂ at 244 nm which confirmed the complex formation.

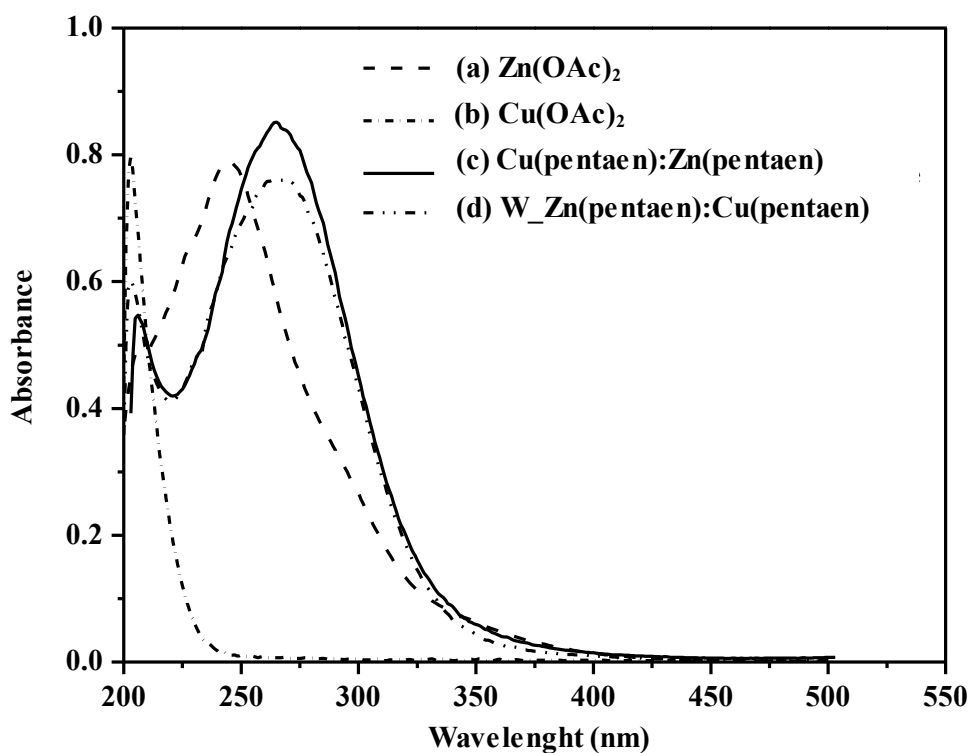


Figure 4.8 UV spectra of (a) Zn(OAc)₂; (b) Cu(OAc)₂ (c) Cu(pentaen):Zn(pentaen) ; (d) W_Cu(pentaen):Zn(pentaen) synthesized at the mole ratio of Cu(OAc)₂:Zn(OAc)₂:pentaen = 0.5:0.5:1

4.4.3 Determination of metal amount in Cu(pentaen):Zn(pentaen) complex by flame atomic spectrometry (FAAS)

For analytical characteristics of Cu(pentaen):Zn(pentaen) illustrated in Table 4.5, the results indicated that there was inconsistency between the experimental value and the calculated value. This might be due to the different sensitivity of each metal.

Table 4.5 Analytical Characteristics of the FAAS method

Catalyst	Elements determined	Experimental (%)	Calculated (%)
Cu(pentaen)	Cu	6.35	7.66
Zn(pentaen)	Zn	6.25	7.88

4.4.4 Elemental analysis of Cu(pentaen):Zn(pentaen) complex

Elemental analysis (%C, %H and %N) of Cu(pentaen):Zn(pentaen) is shown in Table 4.6. This result indicates that there was inconsistency between the experimental value and the calculated value.

Table 4.6 Elemental analysis (%C, %H, and %N) of Cu(pentaen):Zn(pentaen)

Catalyst	Elements determined	Experimental (%)	Calculated (%)
Cu(pentaen):Zn(pentaen)	%C	40.11	40.52
	%H	8.15	8.26
	%N	18.45	20.25

4.4.5 Mass spectrometry of Cu(pentaen):Zn(pentaen) complex

The positive-ion ESI mass spectrum of Cu(pentaen):Zn(pentaen) showed the molecular ion peak at $m/z = 436.094$ corresponding to the form of $[\text{}^{63}\text{Cu}(\text{pentaen}) + \text{Na}]^+$; $m/z = 436.184$ and $m/z = 474.272$ corresponding to the form of $[\text{}^{64}\text{Zn}(\text{pentaen}) + 2\text{H}_2\text{O} + \text{Na}]^+$; $m/z = 473.204$ as demonstrated in Figure 4.9.

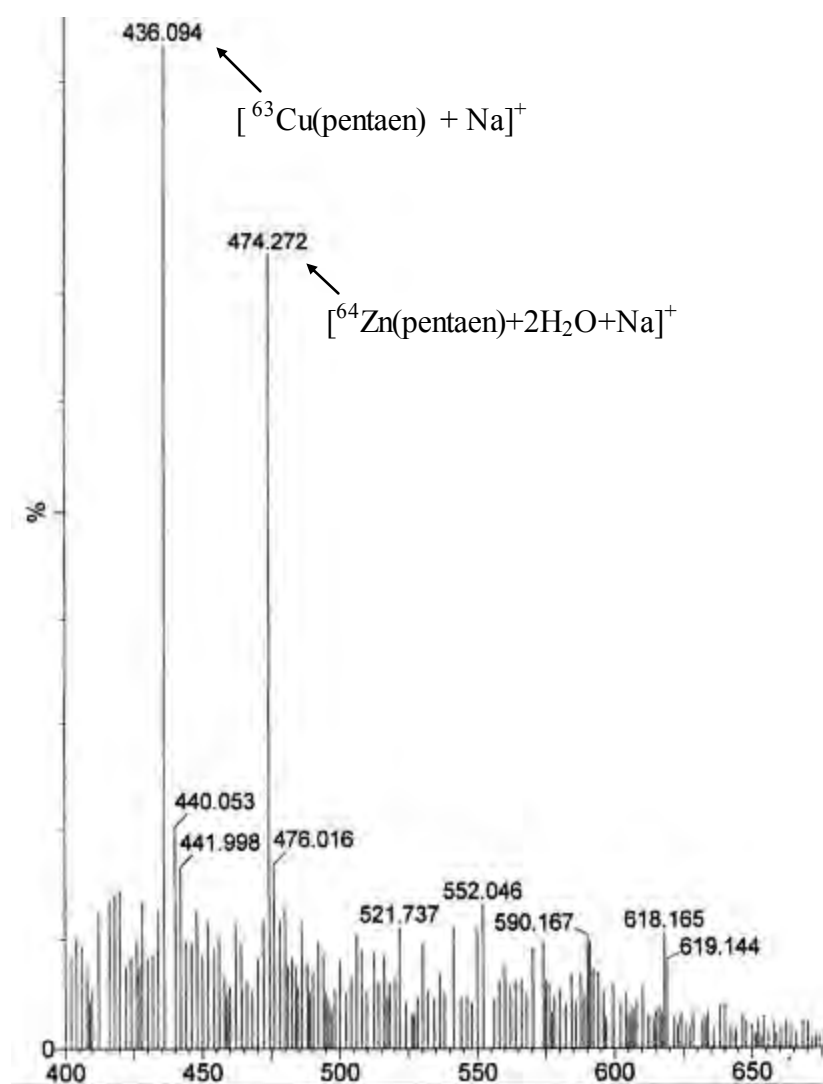


Figure 4.9 Mass spectrum of Cu(pentaen):Zn(pentaen)

4.5 Preparation of rigid polyurethane (RPUR) foams

4.5.1 Preparation of RPUR catalyzed by metal complexes

The ratio $M_1(\text{pentaen})$ and $M_1(\text{pentaen}):M_2(\text{pentaen})$ employed in the synthesis of metal complexes was varied were 1:2, 1:1 and 1:0.5. The rigid polyurethane foams catalyzed by metal $M_1(\text{pentaen})$; ($M_1 = \text{Cu, Zn, Co, Ni and Mn}$) and mixed metal $M_1(\text{pentaen}):M_2(\text{pentaen})$; ($M_1 = \text{Cu, } M_2 = \text{Zn, Co, Ni and Mn}$) were prepared by mechanical mixing technique in two steps of the mixing. In the first step, was prepared by mixing polyol, catalysts (metal complexes or DMCHA), surfactant and blowing agent (water) were mixed in 700 mL paper cup. In the second step, the isocyanate (polymeric MDI) was added to the mixed polyol from first mixing, then the mixture were mixed to obtained homogeneous mixture by mechanical stirrer at 2000 rpm for 20 seconds.

During the reaction, cream time, gel time, tack free time and rise time were measured. After that, the foams were kept at room temperature for 48 hours before carrying out physical and mechanical characterization. In this work, the content of polyol, catalyst, surfactant (B8460), and blowing agent (water) were fixed. The polymeric MDI was varied according to NCO indexes of 100, 130, 150 and 170 and RPUR foams were prepared by using different catalysts at the same 1.0 pbw. The foam formulation of RPUR foams is illustrated in Tables 4.7.

Table 4.7 RPUR foam formulations catalyzed by metal complexes at different NCO indexes

Formulations (pbw*)	NCO index			
	100	130	150	170
Raypol [®] 4221	100	100	100	100
Catalyst (metal complexes or DMCHA)	1.0	1.0	1.0	1.0
Surfactant (B8460)	2.5	2.5	2.5	2.5
Water (blowing agent)	2.0	2.0	2.0	2.0
PMDI (MR-200)	137	178	205	233

*pbw: part by weight or 1 gram in 100 grams of polyol

4.5.2 Reaction times

The metal complexes were used as the catalyst in the formulation of rigid polyurethane foams. The reaction time, namely cream time, gel time, tack free time and rise time were investigated and compared to a commercial reference catalyst (dimethylcyclohexylamine, DMCHA).

The reaction times measured were cream time (which is the start of bubble rise and hence color of the mixture becomes cream-like from dark brown due to the introduction of bubbles or blowing reaction) [2], gel time (which is the time of foam mixture begin to gel or gelling reaction), tack free time (which is the time of the foam could not tack with other materials or crosslinking reaction) and rise time (which is the time of the foam stop rising).

4.5.2.1 An effect of mole ratio to RPUR foam properties.

The data in Table 4.8 demonstrate that the reduction of amine in $M(OAc)_2$:pentaen ratio from 1:2 to 1:1 had an effect to both reaction time and external appearance of foam. The reaction time was shorter and external appearance was better when amine was reduced in foam preparation. This is due to $M(OAc)_2$:pentaen ratio of 1:2 had steric hindrance during the polyurethane reaction. Moreover, Metal and amine had a different catalytic mechanism. However, when mole ratio of $M(OAc)_2$:pentaen was 1:0.5 catalyst was not soluble in starting material. Therefore, there was no the result data of 1:0.5 mole ratio with in Table 4.8.

As the results, it could be concluded that the catalytic activity of the metal complex catalyst with the $M(OAc)_2$:pentaen mole ratio of 1:1 better than those with the mole ratio of 1:2. Especially, Cu(pentaen) and Zn(pentaen) perform as the good catalysts due to the shortest time when they were used in foam preparation.

Table 4.8 Reaction times of RPUR foams prepared at NCO indexes of 100 catalyzed by metal complexes prepared at different $M(\text{OAc})_2$:pentaen mole ratios

Catalysts	Cream time (min)	Gel time (min)	Tack free time (min)	Rise time (min)	Volume (V)	External appearance
$M(\text{OAc})_2$:pentaen =1:2						
Cu(pentaen) ₂	0:35	0:59	3:54	4:18	6/8V	
Zn(pentaen) ₂	0:31	1:04	4:19	4:03	6.5/8V	Brittle
Co(pentaen) ₂	0:37	1:12	8:56	7:43	5.5/8V	foam
Ni(pentaen) ₂	0:34	1:11	12:57	9:33	5.5/8V	
Mn(pentaen) ₂	0:36	1:21	10:45	8:55	5.5/8V	
$M(\text{OAc})_2$:pentaen =1:1						
Cu(pentaen)	0:28	0:45	2:08	2:20	7/8V	
Zn(pentaen)	0:25	0:57	3:58	3:42	7.5/8V	Good
Co(pentaen)	0:30	1:06	7:55	6:55	6/8V	foam
Ni(pentaen)	0:31	0:59	10:55	8:55	6/8V	
Mn(pentaen)	0:30	1:07	9:25	8:01	6/8V	

Cu(pentaen) performed as a good catalyst, however, it was difficult to dissolve in starting material (polyol). Zn(pentaen) had less catalytic activity than Cu(pentaen) but Zn(pentaen) could be easily dissolved in polyol. Therefore, mixed metal complex catalysts, $M_1(\text{pentaen}):M_2(\text{pentaen})$, was studied. The reaction time of RPUR foam catalyzed by mixed metal complexes is shown in Table 4.9. It was found that Cu(pentaen):Zn(pentaen) showed better catalytic activity than DMCHA and better than other $M_1(\text{pentaen}):M_2(\text{pentaen})$ catalysts.

Table 4.9 Reaction times of RPUR foams prepared at NCO indexes of 100 catalyzed by mixed metal complexes prepared at $M_1(OAc)_2:M_2(OAc)_2$:pentaen mole ratio of 0.5:0.5:1

Catalysts	Cream time (min)	Gel time (min)	Tack free time (min)	Rise time (min)	Volume (V)
DMCHA (ref.)	0:22	0:32	3:07	2:21	7.5/8V
Cu(pentaen):Zn(pentaen)	0:27	0:53	2:51	3:07	7.5/8V
Cu(pentaen):Co(pentaen)	0:29	0:58	3:30	3:34	6/8V
Cu(pentaen):Ni(pentaen)	0:30	1:01	4:20	3:54	6/8V
Cu(pentaen):Mn(pentaen)	0:31	1:08	4:30	4:02	6/8V

4.5.2.2 Effect of catalyst content on reaction time of RPUR foams

The effect of catalyst content on the reaction time of RPUR foam is shown in Table 4.10. The results indicated that the reaction time of foams increased with increasing of catalyst content. Interestingly, It was found that the increasing of Cu(pentaen) content promotes the gelling reaction, relatively, which was confirmed by faster gel time and tack-free time. However, the increasing of Zn(pentaen) content promotes the blowing reaction, relatively, which was confirmed by faster cream time [24-26]. Therefore, it could be concluded that Cu(pentaen) is a gelling catalyst and Zn(pentaen) is a blowing catalyst.

Table 4.10 Reaction times of RPUR foams catalyzed by Cu(pentaen) and Zn(pentaen) prepared at M(OAc)₂:pentaen mole ratio of 1:1

Catalyst type at NCO index 130						
Catalyst	Cu(pentaen)			Zn(pentaen)		
Content (pbw)	Cream Time (min)	Gel Time (min)	Tack free Time (min)	Cream Time (min)	Gel Time (min)	Tack free Time (min)
0.25	0:33	1:37	4:57	0:30	2:03	8:32
0.5	0:31	1:12	3:50	0:28	1:31	6:02
1.0	0:29	0:50	2:19	0:26	1:05	4:14

In Table 4.11, the reaction times of RPUR foams catalyzed by metal complexes synthesized in acetone, M(pentaen), are compared to those catalyzed by metal complexes synthesized in water, W_(pentaen). The obtained results are also compared with commercial catalysts (DMCHA).

In the preparation of RPUR foams, W_(pentaen) gave slightly shorter reaction time and lower density than M(pentaen). Therefore, the preparation of W_(pentaen) in water had advantage because foam formulation contained water as a blowing agent. The preparation of W_(pentaen) spent less time than M(pentaen). This is because acetone had to be removed from M(pentaen) before use.

Both Cu(pentaen) and Zn(pentaen) were good catalyst since reaction time were short, however, RPUR foams prepared by Cu(pentaen) foam had less volume and had higher density than those prepared by Zn(pentaen). This results indicated that Cu(pentaen) catalyzed gelling reaction, which was the reaction between isocyanate and hydroxyl group, to form urethane groups very well. Moreover, Zn(pentaen) was a good catalyst in blowing reaction, which normally had an effect to foam density due to the released CO₂. Therefore, when Cu(pentaen):Zn(pentaen) was used as a catalyst, Cu(pentaen) performed as a gelling catalyst that increased RPUR foam high strength [27, 34] and Zn(pentaen) performed as a blowing catalyst that increased the foam volume.

Table 4.11 The reaction time of RPUR foams catalyzed by M(pentaen) and W_(pentaen) prepared at NCO index 100.

Catalysts types	Cream time (min)	Gel time (min)	Tack free time (min)	Rise time (min)	Density (kg/m³)	Volume (V)
DMCHA (ref.)	0:22	0:32	3:07	2:21	39.7	7.5/8V
Cu(pentaen)	0:28	0:45	2:08	2:25	42.4	7/8V
Cu(pentaen):Zn(pentaen)	0:27	0:53	2:51	3:07	40.8	7.5/8V
Zn(pentaen)	0:25	0:57	3:58	3:42	38.6	7.5/8V
W_Cu(pentaen)	0:26	0:39	1:47	2:03	41.8	7/8V
W_Cu(pentaen):Zn(pentaen)	0:25	0:47	2:30	2:48	40.1	7.5/8V
W_Zn(pentaen)	0:23	0:50	3:41	3:30	37.8	7.5/8V

The reaction time of RPUR foams catalyzed by metal complexes demonstrated in Figure 4.10. It indicated that Cu(pentaen) and Cu(pentane):Zn(pentane) showed better catalytic activity than the commercial reference catalyst (DMCHA, dimethylcyclohexylamine). As a result, tack free time was shorter than rise time when using Cu(pentaen) and Cu(pentaen):Zn(pentane) as catalyst. This result was good for foam preparation since the foam continued to rise when the polymerization reaction was almost completed. After the reaction was completed, the foam would not collapse.

Furthermore, rise profile of RPUR foams prepared from Cu(pentaen), Cu(pentaen):Zn(pentaen) and Zn(pentaen) showed similar trend to that of DMCHA (Figure 4.11). DMCHA is a tertiary amine-based catalyst and has strong catalytic activity towards both blowing and gelling reactions [27]. The metal complexes showed longer initial time than DMCHA and exhibited a fast rise curve in the latter stage.

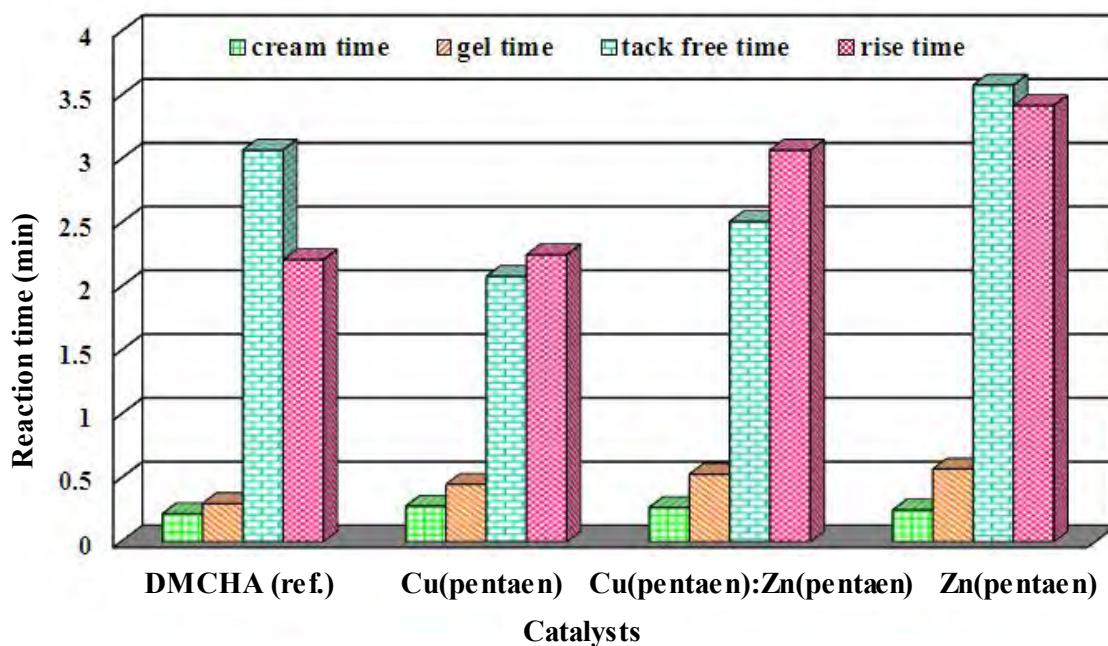


Figure 4.10 Reaction times of RPUR foams catalyzed by M(pentaen) at NCO index of 100

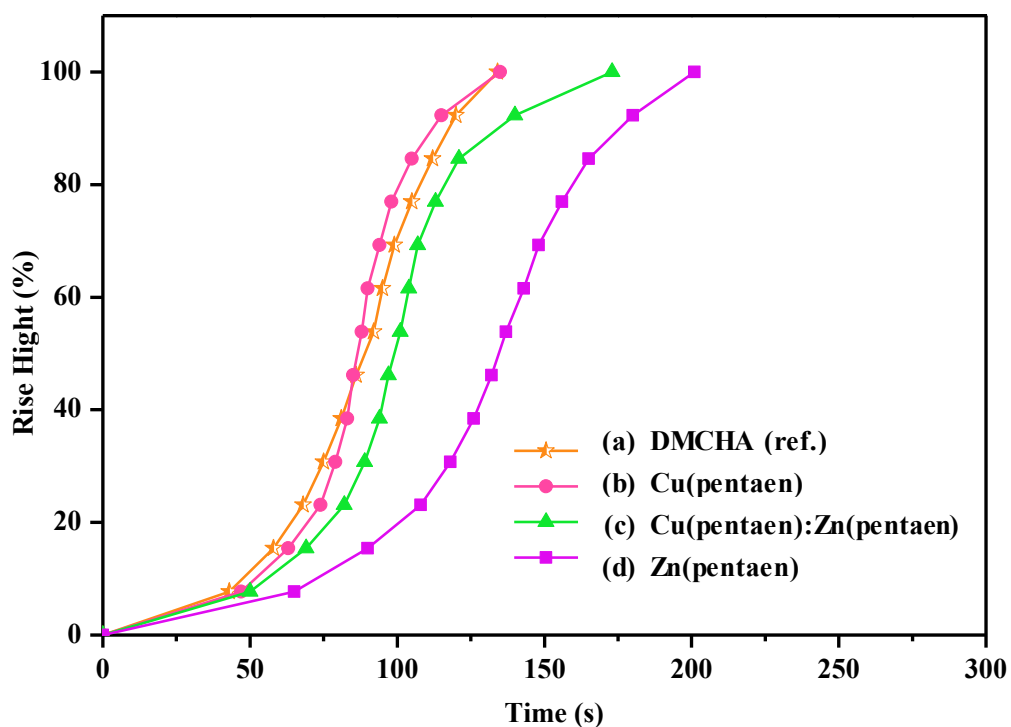
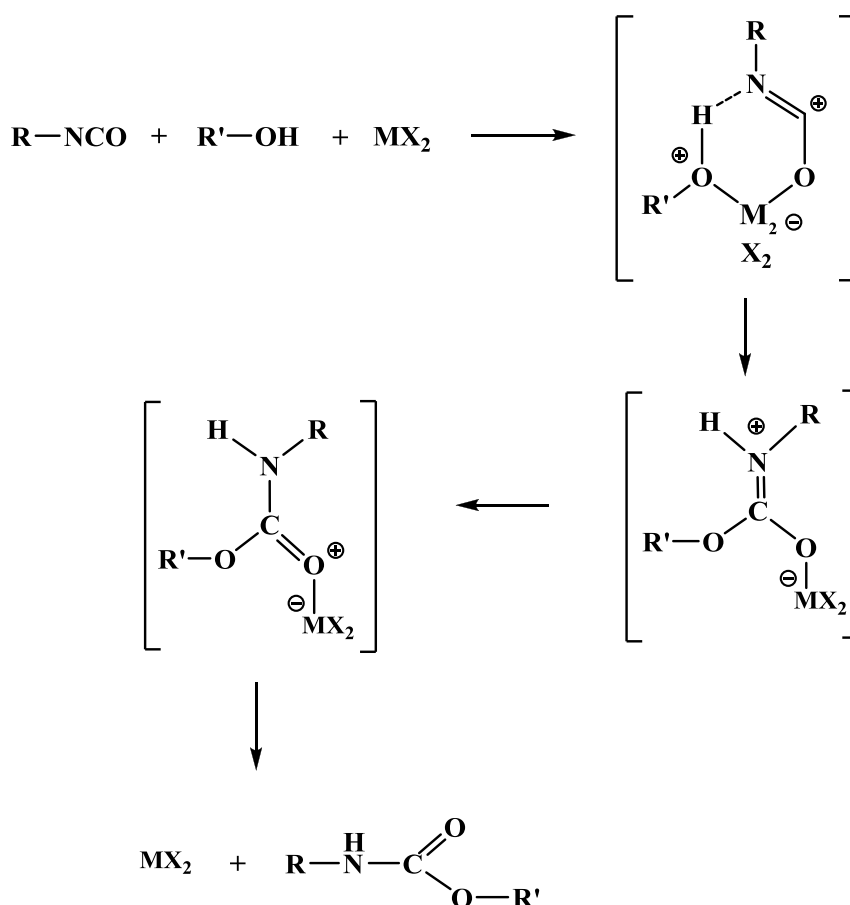


Figure 4.11 Rise profiles of RPUR foams catalyzed by different metal complexes (a) DMCHA (ref.); (b) Cu(pentaen); (c) Cu(pentaen):Zn(pentaen); (d) Zn(pentaen)

The reaction mechanism of RPUR foams catalyzed by metal-based catalyst is shown in Schemes 4.2. It is proposed that M (pentaen) and M_1 (pentaen): M_2 (pentaen) could catalyze RPUR foam polymerization by this mechanism. Therefore, the metal complexes acted as a Lewis acid, primarily coordinated to the oxygen atom of the NCO group and activated the electrophilic nature of the carbon [27] and amine interacting with the proton of hydroxyl group in polyol, which then reacts with the isocyanate. While, the tertiary amine coordinates to the positive electron charged carbon of the NCO group or hydrogen of the OH group and forms a transition state to activate urethane formation reaction (Schemes 2.1 and 2.2). Tertiary amine can be tuned by maximizing its ability to form a hydrogen bond with alcohol, thereby activating the O–H bond so it can attach to the isocyanate more easily.



Scheme 4.2 Activation mechanism of metal-based catalyst on urethane formation reaction

The maximum rise rates were calculated by differential at secondary stage of rise profile which gives maximum slope as illustrated in Figure 4.12. It was demonstrated that the RPUR foams catalyzed by Cu(pentaen) showed higher maximum rise rate than that DMCHA. Cu(pentaen):Zn(pentaen) catalyst showed similar catalytic activity with DMCHA catalyst. This results indicated that the RPUR foams catalyzed by Cu(pentaen) and Cu(pentaen):Zn(pentaen) showed good catalytic activity. Although Zn(pentaen) complexes had lowest catalytic activity than those catalyst but also showed good blowing reaction which showed high maximum rise rate.

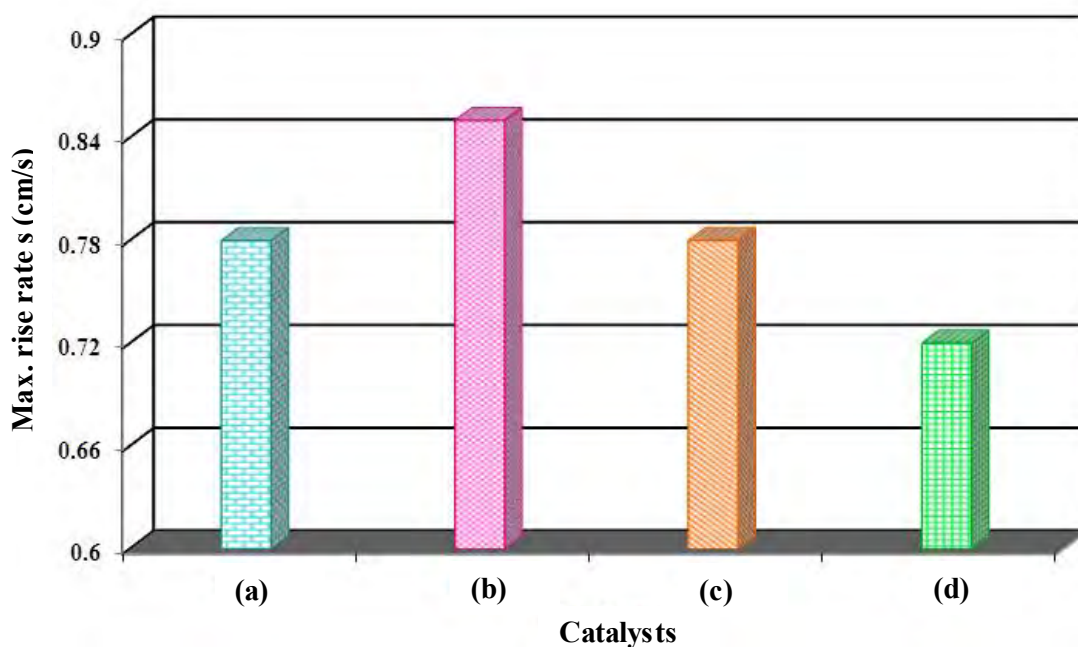


Figure 4.12 Maximum rise rates of RPUR foams catalyzed by different metal complexes at NCO index of 100 (a) DMCHA (ref.); (b) Cu(pentaen); (c) Cu(pentaen):Zn(pentaen); (d) Zn(pentaen)

4.5.3 Apparent density

The apparent density of RPUR foams were measured according to ASTM D 1622. After foam preparation, RPUR foams were kept in room temperature for 48 hours, and then the foams were cut into cubic shape with 3.0 cm x 3.0 cm x 3.0 cm dimensions before apparent density of foams were measured as shown in Figure 4.13.

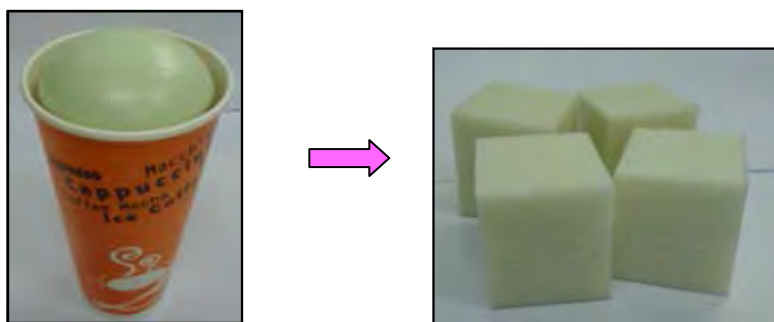


Figure 4.13 Samples for foam density measurements

4.5.3.1 Effect of NCO indexes on foams density

To investigate the effect of NCO indexes on the density of RPUR foams, the NCO index was varied from 100 to 170. These results indicated that the apparent density of RPUR foams increased with increasing the content of NCO indexes (Figure 4.14) because the excess of isocyanate in PUR system could undergo further polymerization to provide crosslinked structure [6]. RPUR foams prepared from metal complexes had suitable density when prepared at the NCO index of 100-170. If RPUR foams were prepared over the NCO index of 170, the foam would be brittle. Therefore, the density could not be measured.

In comparison between the density of foams prepared from metal complexes and DMCHA, it indicated that RPUR foams catalyzed by Cu(pentaen) and Cu(pentaen):Zn(pentaen) showed higher density than those catalyzed by DMCHA. However, foams prepared from Zn(pentaen) complexes showed apparent density lower than those prepared from DMCHA. This result indicated that Zn(pentaen) was a good catalyst in blowing reaction which this reaction had an effect to foam density due to the released CO₂. Density of RPUR foams catalyzed by Cu(pentaen) and Cu(pentaen):Zn(pentaen) complexes at NCO indexes 100-150 was in range of 40-50 kg/m³, which was the desirable density for foam applications [3, 15].

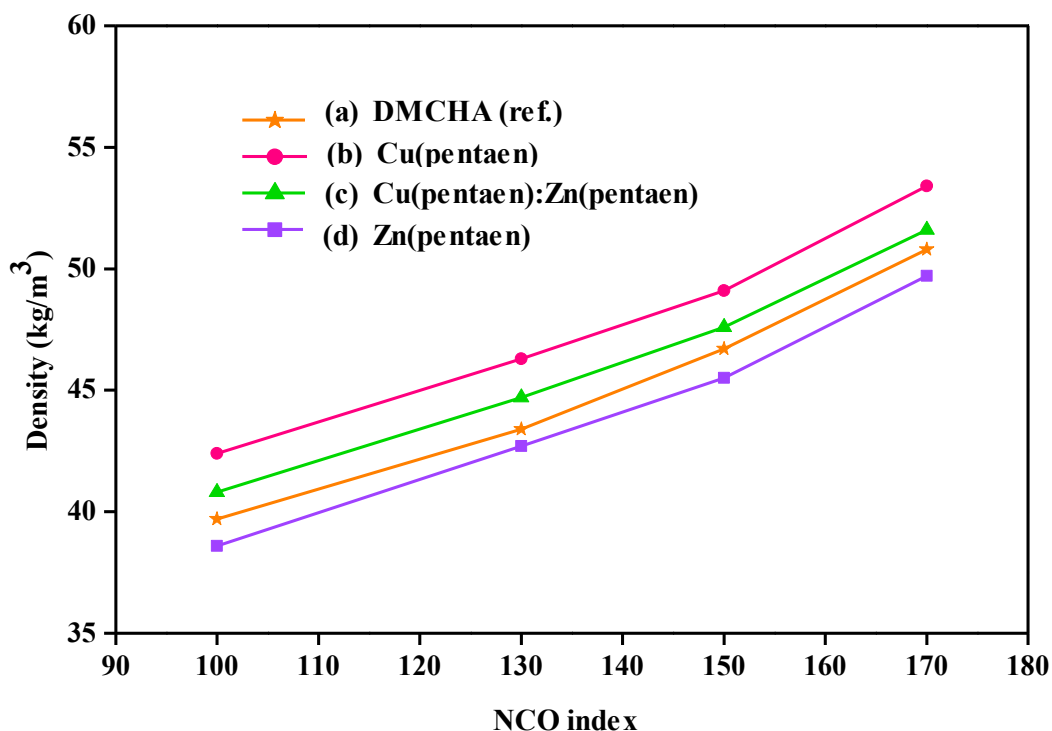


Figure 4.14 Apparent density of RPUR foams catalyzed by metal complexes (a) DMCHA (ref.); (b) Cu(pentaen); (c) Cu(pentaen):Zn(pentaen); (d) Zn(pentaen) at different NCO indexes

4.5.3.2 Effect of catalyst quantity on foam density

The effect of catalyst quantity on RPUR foam density catalyzed by DMCHA, Cu(pentaen), CuZn(pentaen) and Zn(pentaen) is shown in Figure 4.15. It was found that the foam density decreased with increasing the content of catalyst in foam formulation since more blowing reactions could occur when increasing amount of catalyst. The result indicated that the foam prepared at catalyst quantity of 0.25 part by weight (pbw) showed the lowest blowing reaction when compared with those prepared from 0.50, 1.0 and 2.0 pbw of catalyst (Figure 4.16). Although high catalyst quantities resulted in good blowing reaction, however, the cell size of RPUR foam was not uniform. There were several cells which are obviously larger than the others. In addition, the high quantity of catalyst resulted in the decreasing of foam density, which was not suitable for applying in foam manufacturing.

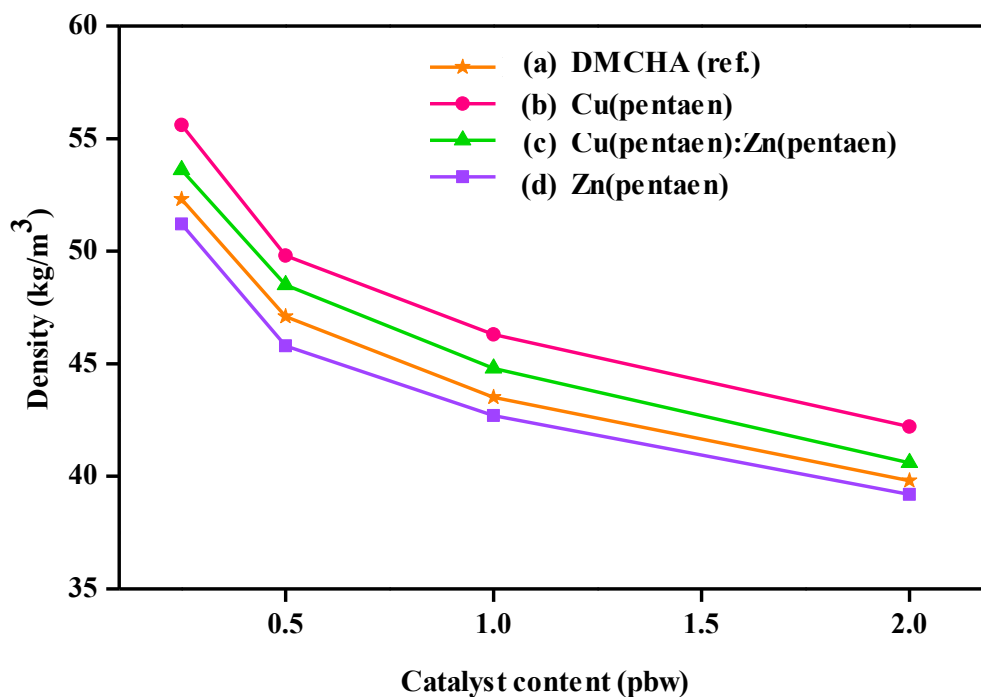


Figure 4.15 Effect of catalyst content on RPUR foam density catalyzed by different catalysts type (a) DMCHA (ref.); (b) Cu(pentaen); (c) Cu(pentaen):Zn(pentaen); (d) Zn(pentaen) at NCO index of 130

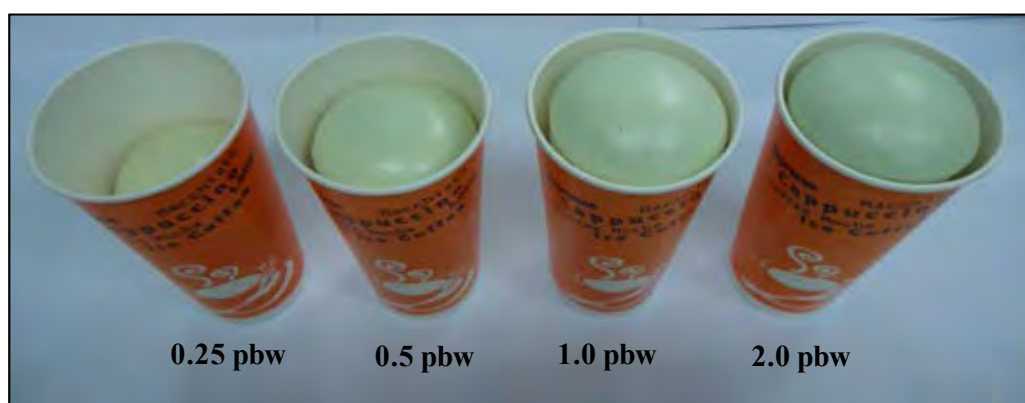


Figure 4.16 Appearance of RPUR foam catalyzed by Cu(pentaen):Zn(pentaen) complex in various amounts at NCO index of 130.

4.5.3.3 Effect of blowing agent quantity on foam density

In Figure 4.17, the effect of the content of blowing agent on RPUR foams density at NCO index 130 is demonstrated. It was found that the apparent density of RPUR foams decreased with increasing of blowing agent content. Since blowing agent (water) could react with isocyanate group to generate CO_2 gas and the temperature of foam was higher due to exothermic reaction, therefore the blowing agent of 3.0 pbw released more CO_2 and made the foam volume increased than that of 1.0 pbw. Therefore, the foams prepared at blowing agent of 1.0 pbw showed higher apparent density than those prepared from 3.0 pbw.

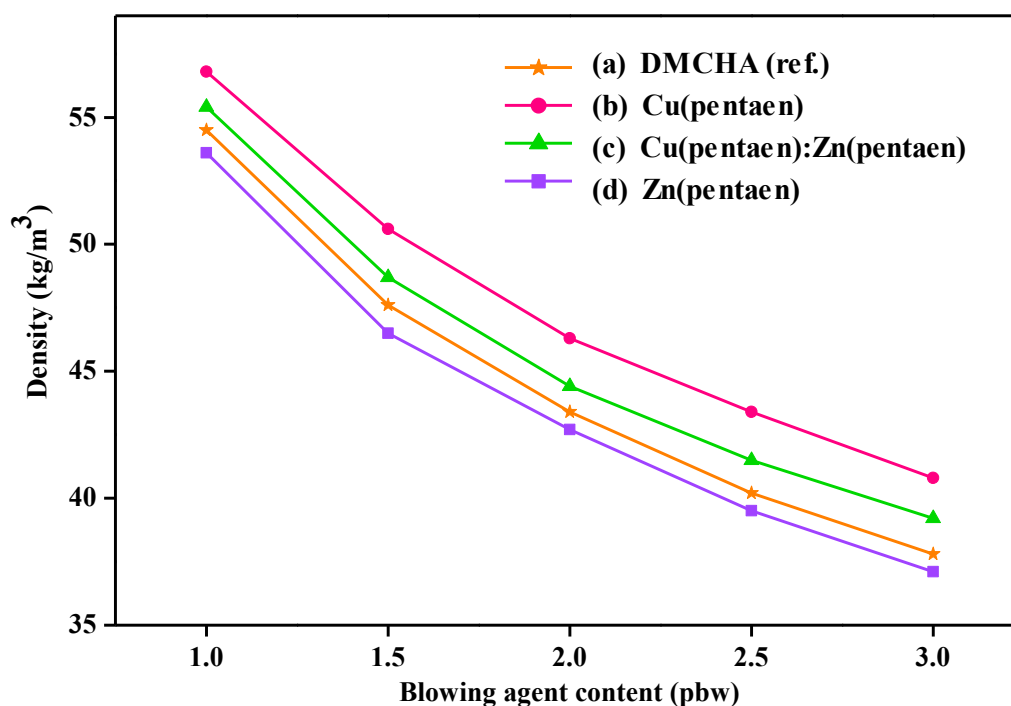


Figure 4.17 Effect of blowing agent quantities on RPUR foam density catalyzed by different catalysts (a) DMCHA (ref.); (b) Cu(pentaen); (c) Cu(pentaen):Zn(pentaen); (d) Zn(pentaen) at NCO index of 130.

4.5.4 Foaming temperature

The effect of isocyanate index on the foaming temperature of RPUR foams is shown in Table 4.12. This result indicated that the foaming temperature increased with increasing isocyanate (NCO) index from 100 to 150 due to the released heat

from reaction between isocyanate and water. At isocyanate index less than 150, less isocyanate was present to react with water and thus less heat was released leading to a lower foaming temperature [34]. The maximum core temperature of foams from metal complexes was in the range of 121-137 °C.

Table 4.12 Maximum core temperature of PUR foam catalyzed by M(pentaen) at different NCO indexes

Catalysts	NCO indexes	Maximum core temperature (°C)	Starting times (min) at T _{max}
DMCHA	100	121	330 (5:30)
	130	126	360 (6:00)
	150	132	390 (6:30)
Cu(pentaen)	100	124	315 (5:15)
	130	128	330 (5:30)
	150	133	360 (6:00)
Cu(pentaen):Zn(pentaen)	100	125	330 (5:30)
	130	129	345 (5:45)
	150	133	390 (6:30)
Zn(pentaen)	100	127	375 (6:15)
	130	132	285 (6:30)
	150	136	420 (7:00)

The temperature profiles of RPUR foam prepared from different catalysts at NCO index of 100 were investigated (Figure 4.18). It was found that the profiles of foams prepared from metal complexes were the same as that prepared with DMCHA. The RPUR foams prepared from DMCHA, Cu(pentaen) and Cu(pentaen):Zn(pentaen) catalyst showed shorter time at initial profile than Zn(pentaen) which they showed faster gel times. However, Zn(pentaen) had longer gel time than other catalyst. This is because Zn(pentaen) accelerated blowing reaction.

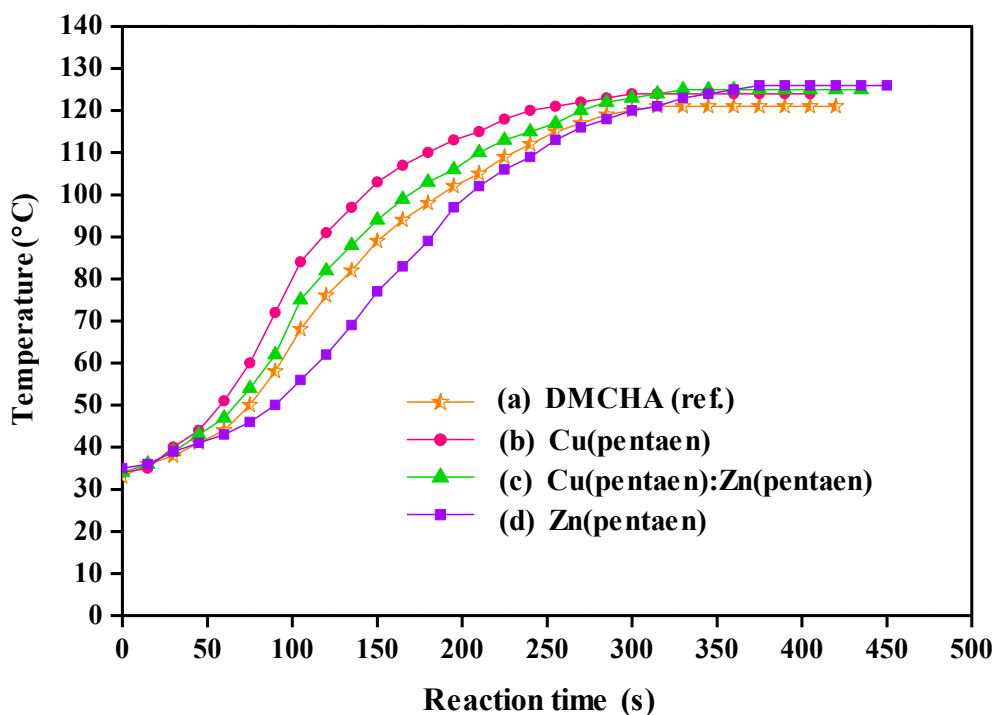


Figure 4.18 Temperature profiles of RPUR foams catalyzed by metal complexes (a) DMCHA (ref.); (b) Cu(pentaen); (c) Cu(pentaen):Zn(pentaen); (d) Zn(pentaen)

4.5.5 Characterization of RPUR foams

Figure 4.19 illustrated the IR spectra of starting materials, namely polyol, polymeric MDI (PMDI isocyanate) and their corresponding RPUR foams. From the IR spectrum of (a) polyol, the broad band at about 3402 cm^{-1} was the characteristic stretching vibration of hydroxyl groups, which indicated vibration of hydroxyl groups. The isocyanate stretching of (b) PMDI (2277 cm^{-1}) observed high intensity of free NCO absorption band.

Also, isocyanate groups at 2277 cm^{-1} in PMDI disappeared, which indicate that isocyanate group were completely consumed by the reactions with hydroxyl groups and water.

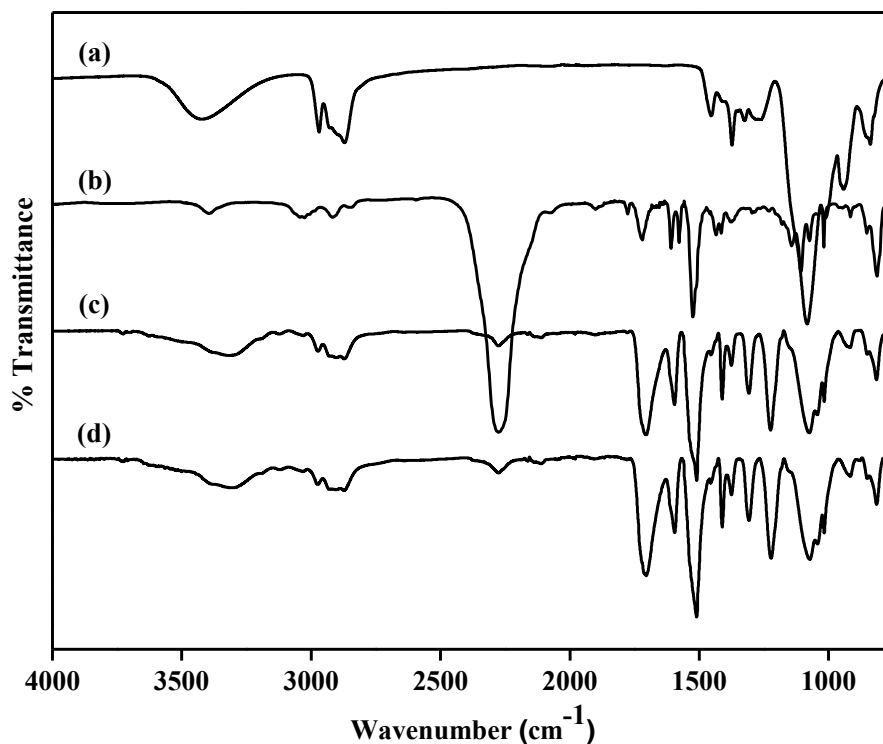


Figure 4.19 IR spectra of starting materials and RPUR foams catalyzed by mixed metal complexes (a) polyether polyol; (b) PMDI; (c) DMCHA (ref.); (d) RPUR foams catalyzed by Cu(pentaen):Zn(pentaen)

On the contrary, from the IR spectra of RPUR foams, (c) and (d), the absorption bands at 3392, 1714, 1518, 1220 cm^{-1} showed the urethane and disubstituted urea that were formed through the polymerization of isocyanate groups, hydroxyl groups and water. The bands at 3392 and 1714 cm^{-1} were the characteristic stretching vibrations of amine group (N-H) and carbonyl group (C=O) of urethane and urea linkages, respectively, while the band at 1220 cm^{-1} was associated with the characteristic stretching vibration of C-N-H bond of urethane and urea. The band at 1518 cm^{-1} could be attributed to N-H bending vibration and C-N stretching vibration of urethane and urea groups [34].

4.5.6 NCO conversion of RPUR foams

FTIR spectroscopy was employed to investigate the polymerization of RPUR foam system. IR spectra of polymeric MDI, polyether polyol and RPUR foams are demonstrated in Figure 4.19. It indicated that the absorption band of isocyanate could be observed at 2277 cm^{-1} . Therefore, the NCO conversion was determined from FTIR spectra. When higher NCO index was used in the foam formulation, high intensity of free NCO absorption band could be observed in RPUR foam as shown in Figure 4.20.

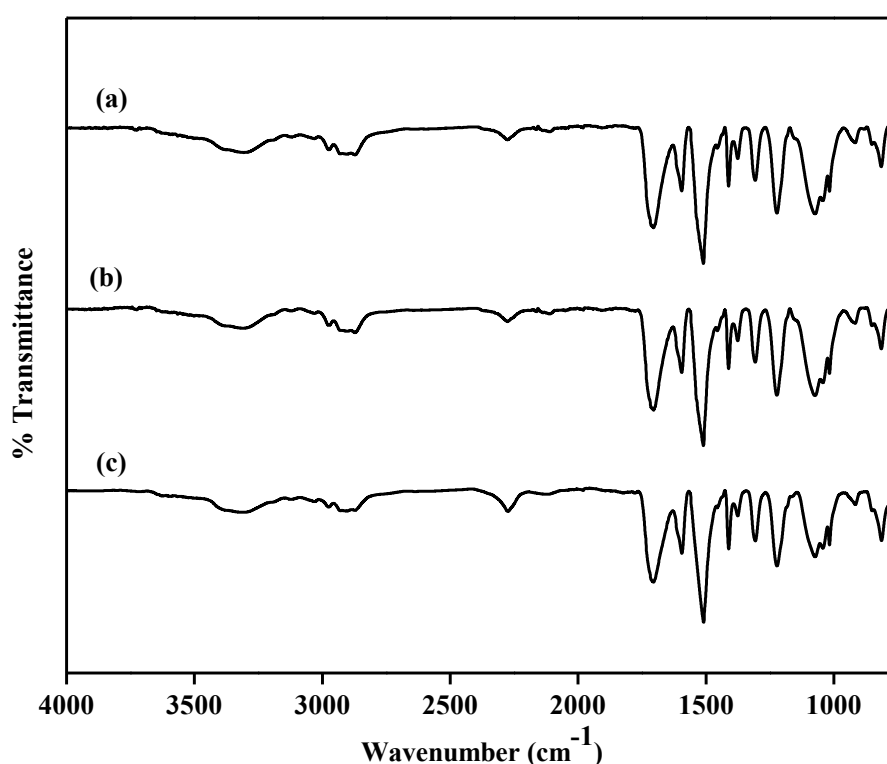


Figure 4.20 IR spectra of RPUR foams catalyzed by Cu(pentaen):Zn(pentaen) at different NCO indexes (a) 100; (b) 130; (c) 150

The NCO conversion defined as the ratio between isocyanate peak area at time t and isocyanate peak area at time 0 as shown in following equation [36-38]:

$$\text{Isocyanate conversion (\%)} = \left[1 - \frac{\text{NCO}^f}{\text{NCO}^i} \right] \times 100$$

where;

NCO^f is the area of isocyanate absorbance peak area at time t (spectra (c) and (d) in Figure 4.19)

NCO^i is the area of isocyanate absorbance peak area at initial time 0 (spectra (b) in Figure 4.19)

Quantity of free NCO in RPUR foams were normalized by aromatic ring absorption band at 1595 cm^{-1} .

Polyisocyanurate:polyurethane (PIR:PUR) ratio was calculated from the peak area of isocyanurate and urethane at 1415 and 1220 cm^{-1} , respectively (Table 4.13).

Table 4.13 Wavenumber of the functional groups used in calculation [6]

Functional groups	Wave number (cm^{-1})	Chemical structure
Isocyanate	2277	$\text{N}=\text{C}=\text{O}$
Phenyl	1595	Ar-H
Isocyanurate	1415	PIR
Urethane	1220	-C-O-

The results of NCO conversion of RPUR foams catalyzed by metal complexes at NCO indexes 100, 130 and 150 are demonstrated in Figure 4.21. This result indicated that NCO conversion decreased by increasing the content of NCO indexes. The excess isocyanate could not undergo trimerization to provide isocyanurate group. Therefore metal complex catalysts were not specific toward of isocyanurate formation. Although, the NCO conversion decreased with increasing the content of NCO index, the conversion was 98-99 %.

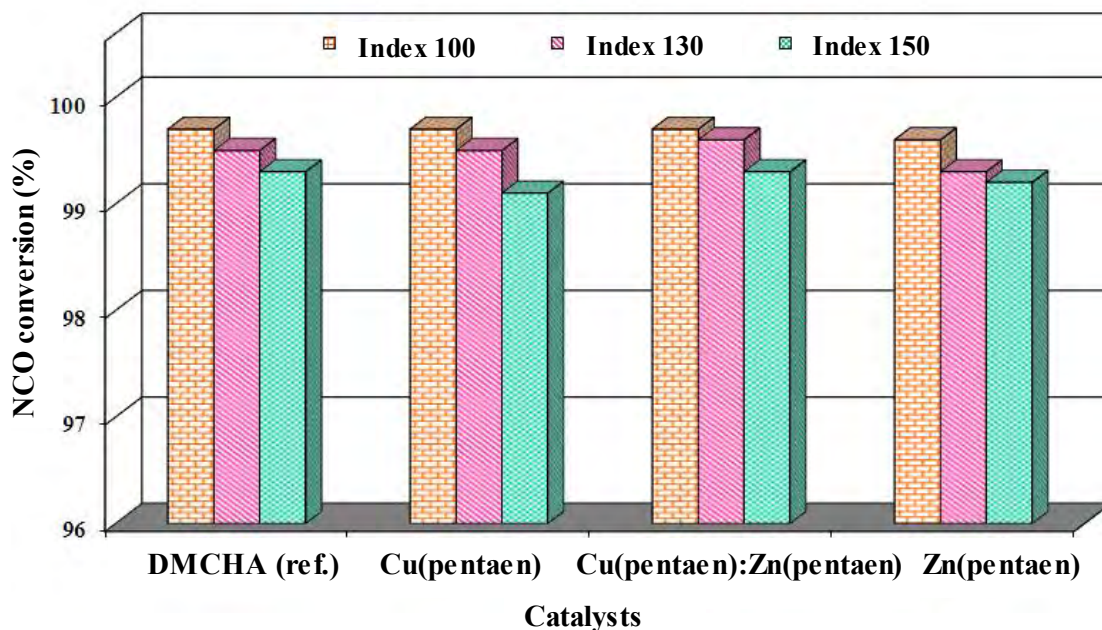


Figure 4.21 NCO conversions of RPUR foams catalyzed by different metal complexes

The ratio of polyisocyanurate:polyurethane (PIR:PUR) in RPUR foams prepared from different catalysts is shown in Figure 4.22. From these results, PIR:PUR of all RPUR foam slightly increased with increasing the content of NCO index. Therefore, this result indicated that metal complexes were not good catalyst for polyisocyanurate formation. It could be concluded that metal complexes were good catalysts for polyurethane formation and blowing reaction but they were not good catalysts for trimerization reaction. In Tables 4.14 and 4.15, the summarized NCO conversion and PIR:PUR ratio of RPUR foams catalyzed by metal complexes is illustrated as follows.

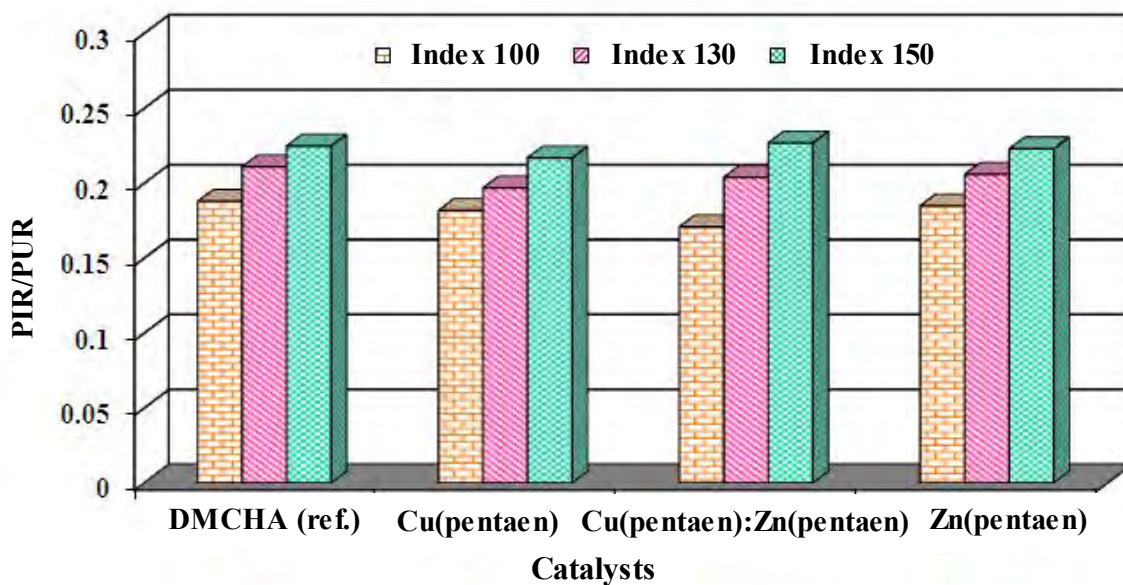


Figure 4.22 PIR:PUR of RPUR foams catalyzed by different metal complexes

Table 4.14 NCO conversions and PIR:PUR ratio of RPUR foams prepared by M(pentaen) at different NCO indexes

Catalysts	NCO indexes	NCO conversion (%)	PIR/PUR
DMCHA (ref.)	100	99.7	0.188
	130	99.5	0.211
	150	99.3	0.225
Cu(pentaen)	100	99.7	0.182
	130	99.5	0.197
	150	99.0	0.217
Cu(pentaen):Zn(pentaen)	100	99.7	0.171
	130	99.6	0.204
	150	99.3	0.227
Zn(pentaen)	100	99.6	0.185
	130	99.3	0.206
	150	99.2	0.223

Table 4.15 NCO conversions and PIR:PUR ratio of RPUR foams prepared by W_M(pentaen) complexes catalyzed in water at different NCO indexes

Catalysts	NCO indexes	NCO conversion (%)	PIR/PUR
DMCHA (ref.)	100	99.7	0.184
	130	99.4	0.212
	150	99.0	0.228
W_Cu(pentaen)	100	99.6	0.190
	130	99.3	0.220
	150	98.9	0.225
W_Cu(pentaen):Zn(pentaen)	100	99.4	0.189
	130	99.2	0.196
	150	98.8	0.206
W_Zn(pentaen)	100	99.4	0.189
	130	99.2	0.196
	150	98.8	0.206

4.6 Compressive properties of RPUR foams

Compressive strength of RPUR foams is an important parameter which determines its application. RPUR foams subjected to compressive stress at 10% strain. The compression stress-strain curves of RPUR foams catalyzed by metal complexes are shown in Figure 4.23. The curves revealed three stages of deformation; initial linear behavior, linear plateau region and finally, densification. The initial slope was used to calculate the compressive modulus of foam and intersection point between the initial slope and plateau slope was used to determine the compressive strength [39]. It was observed that slope of the initial linear are the same for all RPUR foams. The shape of plateau region depends on the cell morphology of RPUR foam. For linear plateau, cell deformation occurs as combination of cell bending and collapse.

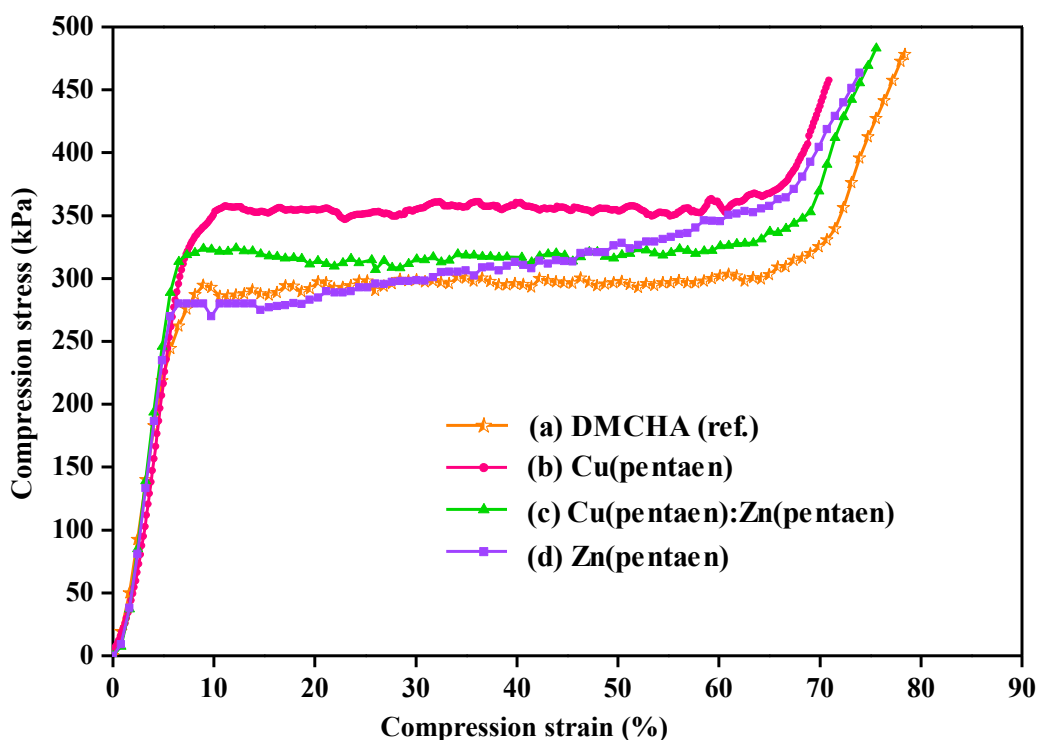


Figure 4.23 Parallel compression stress-strain curve of RPUR foams catalyzed by different catalysts at NCO index of 150 (a) DMCHA (ref.); (b) Cu(pentaen); (c) Cu(pentaen):Zn(pentaen); (d) Zn(pentaen)

Parallel compressive strength of RPUR foams at NCO indexes of 100, 130 and 150 is shown in Figure 4.24. It demonstrated that the compressive strength of RPUR foam was increased by increasing NCO index from 100 to 150, respectively. RPUR foams catalyzed by Cu(pentaen):Zn(pentaen) showed higher compressive strength than the foam prepared from a commercial reference catalyst (DMCHA) at both NCO indexes of 100, 130 and 150.

This phenomenon could be explained that the foams prepared by higher NCO index normally had higher than the foam prepared by lower NCO index. In Figure 4.25 illustrated that the compressive strength of RPUR foam catalyzed by Cu(pentaen):Zn(pentaen) increased from 228.0 to 321.5 kPa with an increasing density from 40.8 to 47.5 kg/m³. This is due to the cell size decreased with increased density [19]. Therefore it indicated that the mechanical properties of foams mainly depend on the density [25, 40-41].

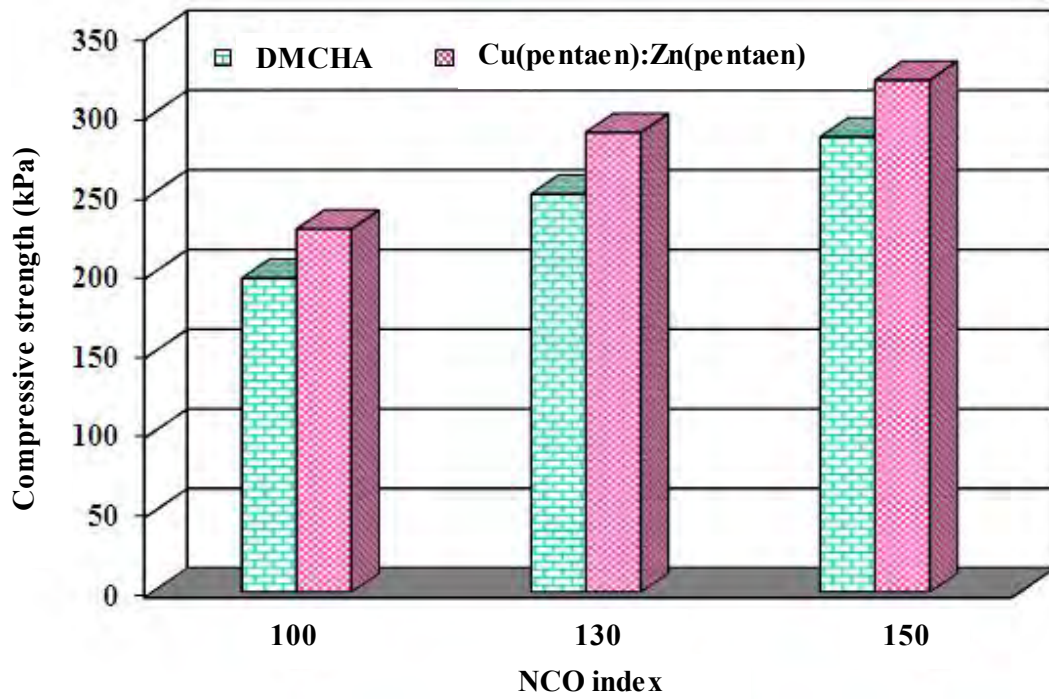


Figure 4.24 Comparison of parallel compressive strength of RPUR foams between NCO indexes of 100, 130 and 150

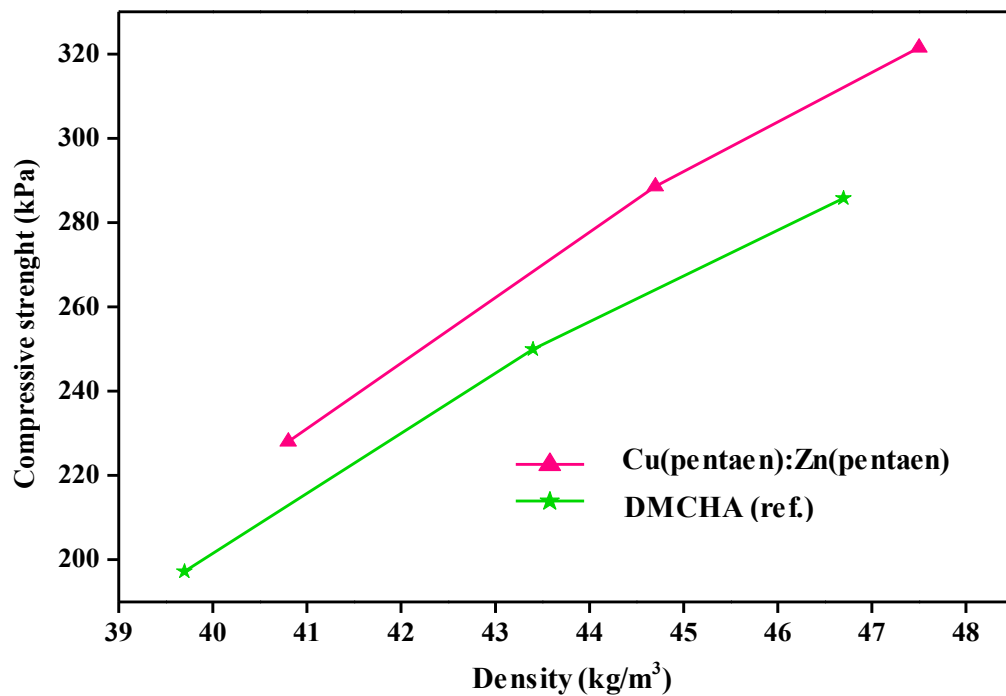


Figure 4.25 Relationship between compressive strength and density

In Figure 4.26, compressive strength of RPUR foams catalyzed by metal complexes in parallel and perpendicular direction of foam rising is demonstrated. From the results, it was observed that the parallel compressive strength of foams was higher than that of perpendicular compression direction. This is due to perpendicular, the foam cells were elongated in the direction of the rise [42]. The compressive properties depend on direction of measurement, all foams were anisotropic foams. In general, a high compressive strength in one direction occurred at the expense of the compressive strength in the other directions which were could be explained by the foam cell model as illustrated in Figure 4.27.

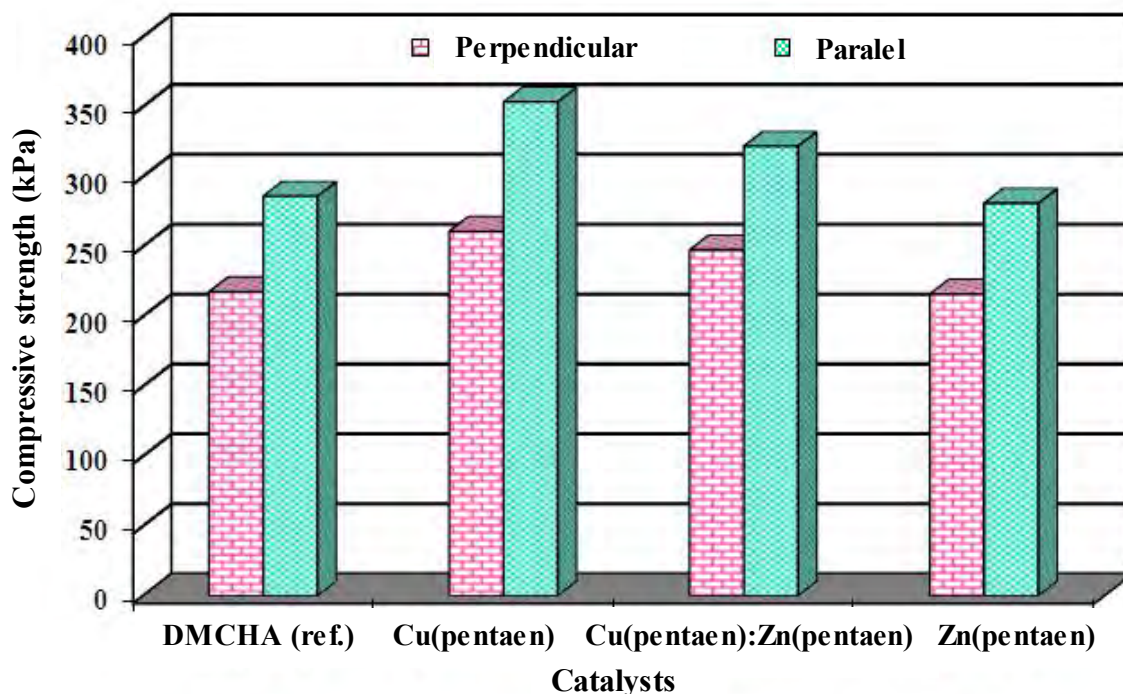


Figure 4.26 Comparison of compressive strength of RPUR foams between parallel and perpendicular direction of foam rising at NCO index of 150

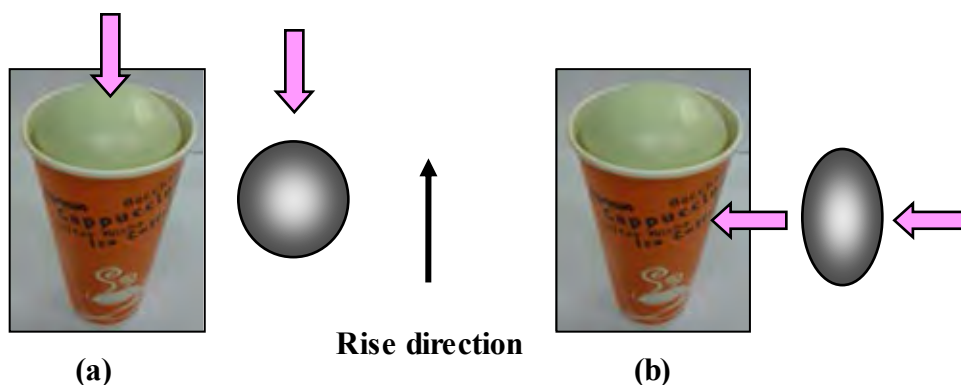


Figure 4.27 Isotropic foam (a): spherical cells, equal properties in all directions; anisotropic foam (b): ellipsoid cells, which properties depend on direction [1]

4.7 RPUR Foams Morphology

Morphology of RPUR foam catalyzed by Cu(pentaen):Zn(pentaen) in parallel and perpendicular of foam rising is demonstrated in Figure 4.28. It was observed that cell morphology showed spherical cell and elongated cell in (a) parallel and (b) perpendicular direction, respectively. It was illustrated the foams were anisotropic materials which were confirmed by compressive strength and cell morphology results.

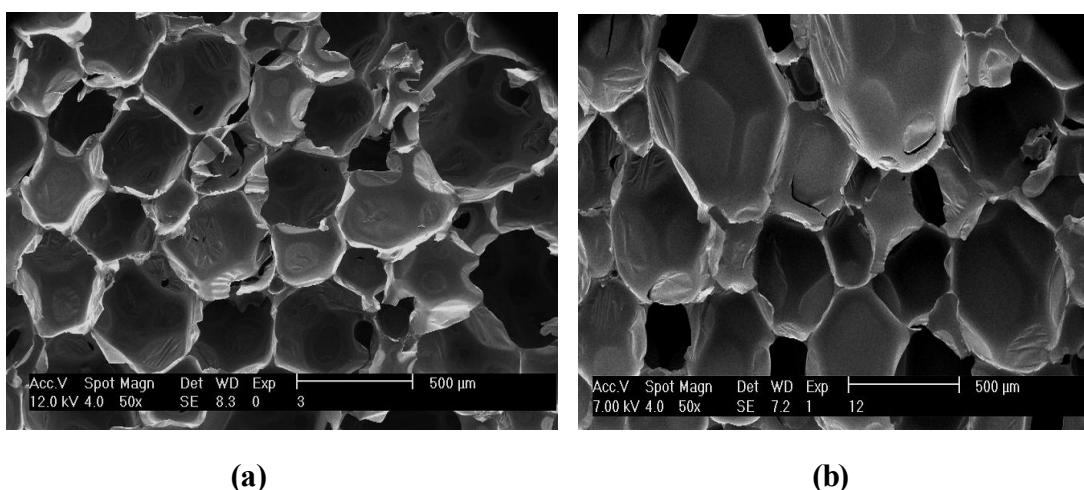


Figure 4.28 SEM of RPUR foams catalyzed by Cu(pentaen):Zn(pentaen) and prepared at the NCO index 150; (a) top view; (b) side view (50x)

SEM micrographs of RPUR foams prepared from both DMCHA and Cu(pentaen):Zn(pentaen) catalysts shown in Figure 4.29. It was observed that closed-cell foams. Then RPUR foam catalyzed by Cu(pentaen):Zn(pentaen) had more uniform and smaller cell size (cell size = 409.9 μm) when compared with RPUR foam catalyzed by DMCHA (cell size = 497.5 μm). This result indicated that the small cell size provided more strength to the RPUR foam [43]. Therefore, the foam catalyzed by Cu(pentaen):Zn(pentaen) had higher compressive strength than that prepared from DMCHA.

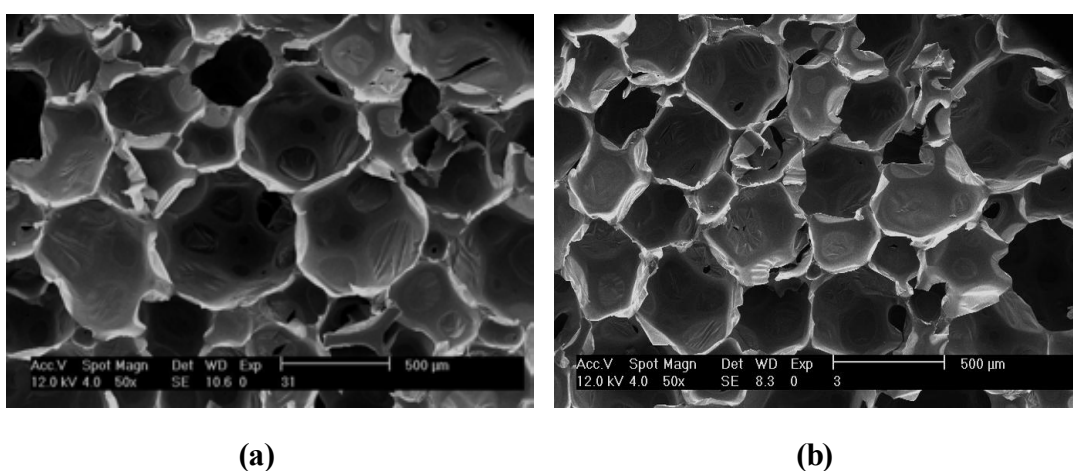


Figure 4.29 SEM of RPUR foams prepared at the NCO index of 150 and catalyzed by (a) DMCHA (ref.) ; (b) CuZn(pentaen) (top view, 50 \times)

4.7.1 Effect of blowing agent on morphology of RPUR foams.

Generally, the mechanical properties not only depend on density of foams, but also relate to the cell size and morphology of foams. Thus, in the present study, the morphology of foam with different blowing agent content, which were observed in the free-rising direction which scanning electron microscopy (SEM), are shown in Figure 4.30. As seen in figure, the higher was the blowing agent content, the larger was the average cell size of foams. As blowing agent content increased from 1.0 to 3.0 pbw the cell size increased from 367.4 to 513.2 μm , respectively [19-20]. This is due to the fact that the increase in the blowing agent content generating more bubbles combined with one another, therefore, the cell size of foam increased with the increase in the blowing agent content [20, 24].

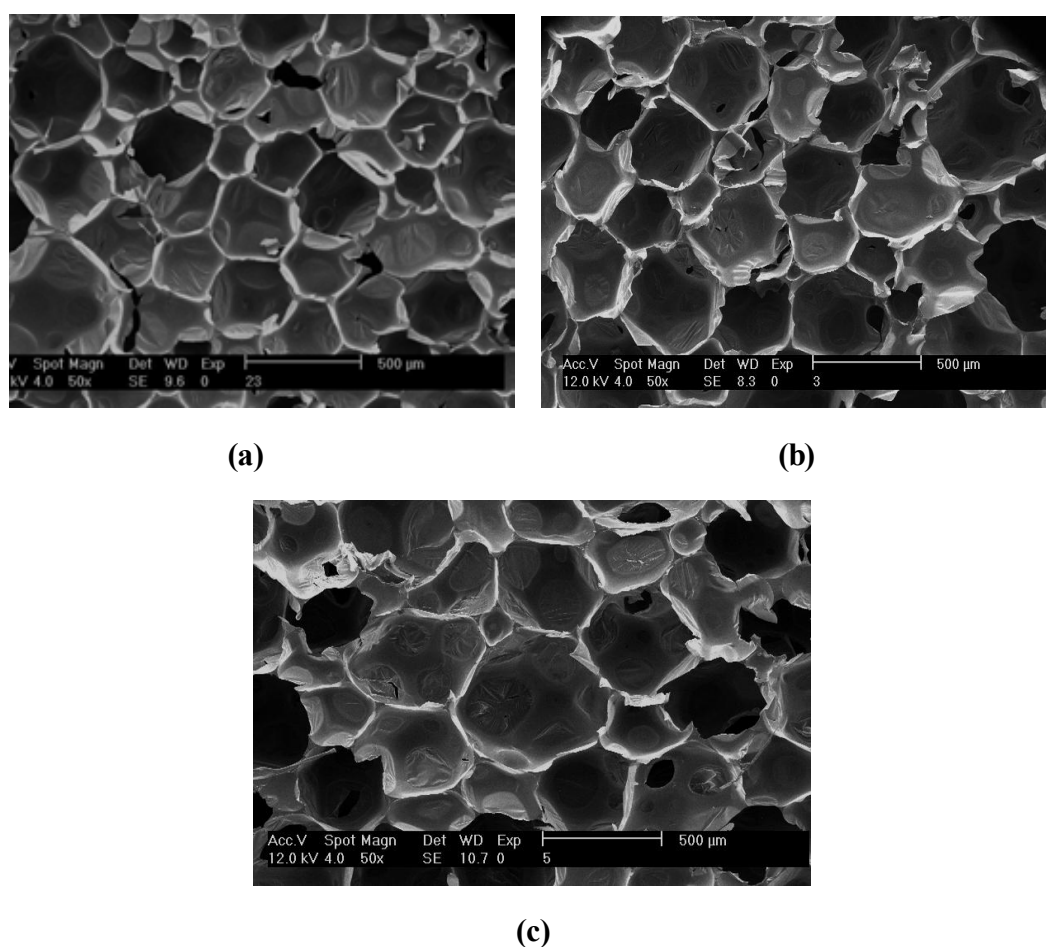


Figure 4.30 SEM of RPUR foams prepared at the NCO index of 150, catalyzed by Cu(pentaen):Zn(pentaen) and blown by different blowing agent content (a) 1.0 (b) 2.0 (c) 3.0 pbw (top view, 50×)

According to the relationship between cell size and mechanical properties, the compressive strength will be higher when RPUR foams have smaller cell size and more uniform [34, 44]. This result was confirmed by Table 4.16. The average cell size of foam increased from 367.4 to 513.2 μm and the compressive strength decreasing from 433.2 to 230.8 kPa.

Table 4.16 The compressive strength of RPUR foam with different cell size

Blowing agent content	Cell size (μm)	Compressive strength (kPa)
1.0 pbw	367.4	433.2
2.0 pbw	409.9	321.5
3.0 pbw	513.2	230.8

4.8 Thermal conductivity

Thermal conductivity is ability to transmit heat through the foam matrix. The thermal insulation properties of RPUR foams are mostly expressed in terms of their K-factor. As the K value decreased the thermal insulation properties of RPUR foams are increase.

Thermal conductivity of foams is usually controlled by its density and cell size [21-22, 45]. Thermal conductivity of RPUR foams catalyzed by DMCHA and Cu(pentaen):Zn(pentaen) were investigated. In Table 4.17 shows the effect of density and cell size on the thermal conductivity of foam. It indicates that as the density of foam increases (smaller cell size), the thermal conductivity slightly decreases. It may be due to the decreased radiant heat transfer via trapped gases in lower foam cells in the higher density of RPUR foams [19]. Therefore, It could be concluded that the smaller cell size improved the thermal insulation property of the RPUR foam [21-22].

Table 4.17 The thermal conductivity of RPUR foams at NCO index of 150 with different cell size.

Catalyst types	Density (kg/m ³)	Cell size (μm)	Thermal conductivity (W/m K)
DMCHA (ref.)	46.7	497.5	0.0377
Cu(pentaen):Zn(pentaen)	47.5	409.9	0.0363

4.9 Thermal stability

Thermal stability of RPUR foams catalyzed by DMCHA, Cu(pentaen), Cu(pentaen):Zn(pentaen) and Zn(pentaen) at NCO index of 150 were investigated by thermalgravimetric analysis under nitrogen atmosphere. Their thermograms are shown in Figure 4.31 and Table 4.18. TGA thermograms of all RPUR foams showed the decomposition of foams in one step.

The initial composition temperature (IDT), which is the temperature at 5% weight loss was found in the range of 283.4-285.7 °C. This step was attributed to decomposition of urethane [46]. The residual weights at 600 °C were in the range of 32.2-34.6 %. RPUR foams catalyzed by DMCHA, Cu(pentaen), Zn(pentaen) and

Cu(pentaen):Zn(pentaen) showed their maximum decomposition temperature (T_{\max}) values in the range of 336.1-337.6 °C. The foams prepared from all metal complexes catalysts showed similar thermal decomposition with that prepared from DMCHA catalyst. This indicated that the metal complexes showed similar catalytic reaction with that of DMCHA.

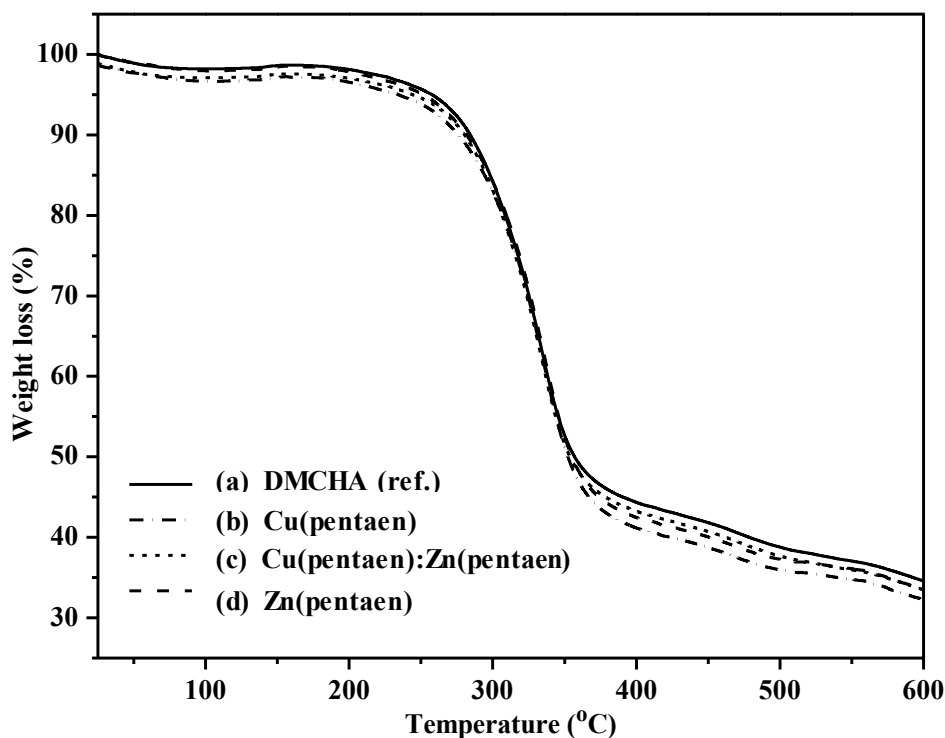


Figure 4.31 TGA thermograms of RPUR foams catalyzed by (a) DMCHA (ref.); (b) Cu(pentaen); (c) Cu(pentaen):Zn(pentaen); (d) Zn(pentaen) at the NCO index of 150

Table 4.18 TGA data of RPUR foam catalyzed by various metal complexes catalysts

RPUR catalyzed by various catalysts	IDT (°C)	Weight residue (%) at different temperatures (°C)					T_{\max} (°C)
		200	300	400	500	600	
		DMCHA (ref.)	285.7	98.1	84.2	44.3	
Cu(pentaen)	283.4	96.5	82.9	41.2	36.0	32.2	336.3
Cu(pentaen):Zn(pentaen)	284.6	97.0	83.1	43.2	37.7	33.5	336.4
Zn(pentaen)	284.8	97.8	84.2	42.5	37.3	33.5	337.6

For comparison, RPUR foams catalyzed by starting materials (Figure 4.32) showed bad appearance, brittle foam and had a long time of processing time. It was indicated that starting materials were unsuitable catalytic reaction.

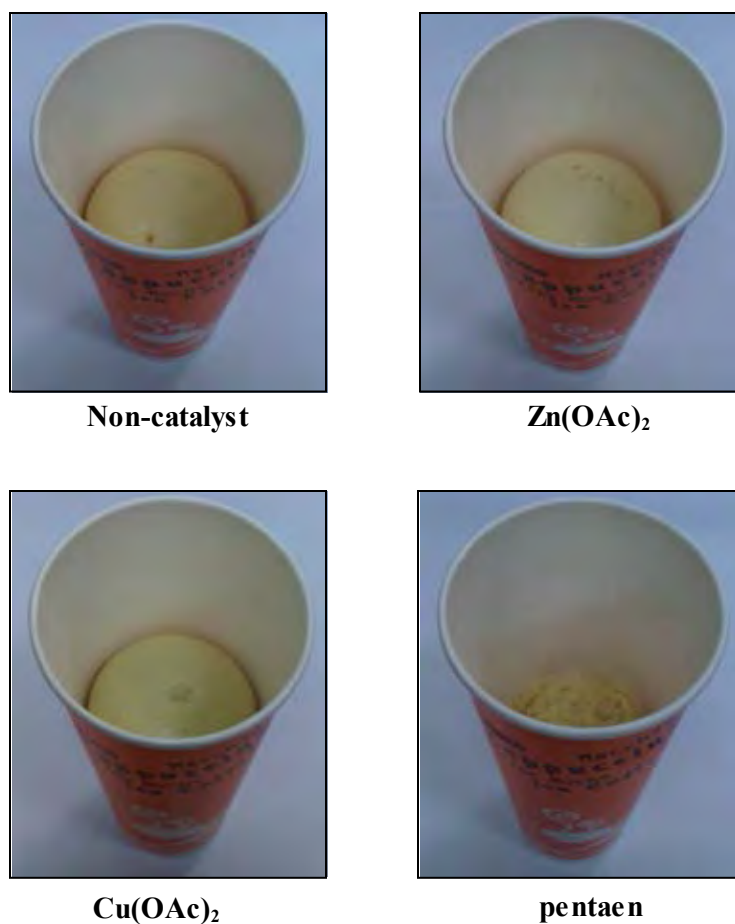


Figure 4.32 External appearance of RPUR foams catalyzed by $M(OAc)_2$ and amine

RPUR foams catalyzed by Cu(pentaen), Cu(pentaen):Zn(pentaen), Zn(pentaen) and DMCHA catalysts (Figure 4.33) showed good blowing reaction and good foam.



(a) DMCHA (ref.)



(b) Cu(pentaen)



(c) Cu(pentaen):Zn(pentaen)



(d) Zn(pentaen)



(e) W_Cu(pentaen)



(f) W_Cu(pentaen):Zn(pentaen)



(g) W_Zn(pentaen)

Figure 4.33 External appearance of RPUR foams catalyzed by different metal catalysts (a) DMCHA (ref.); (b) Cu(pentaen); (c) Cu(pentaen):Zn(pentaen); (d) Zn(pentaen); (e) W_Cu(pentaen); (f) W_Cu(pentaen):Zn(pentaen); (g) W_Zn(pentaen)

CHAPTER V

CONCLUSION

5.1 Conclusion

Metal-amine and mixed metal-amine complexes, namely $M_1(\text{pentaen})$ and $M_1(\text{pentaen}):M_2(\text{pentaen})$ were synthesized and used as catalysts for rigid polyurethane foam preparation. They were characterized by means of FT-IR, UV-vis, MS spectrometry and elemental analysis.

Use of $\text{Cu}(\text{pentaen}):\text{Zn}(\text{pentaen})$ as catalyst for foam preparation had the following advantages. $\text{Cu}(\text{pentaen})$ performed as a gelling catalyst that increased RPUR foam high strength and $\text{Zn}(\text{pentaen})$ performed as a blowing catalyst that increased the foam volume. Interestingly, the mixed metal complexes using balance gelling and blowing reaction.

RPUR foams catalyzed by $\text{Cu}(\text{pentaen}):\text{Zn}(\text{pentaen})$ had a similar catalytic activity when compared with foams catalyzed by commercial catalyst (DMCHA). From the reaction time, $\text{Cu}(\text{pentaen}):\text{Zn}(\text{pentaen})$ had tack free time shorter than rise time. This resulted in the foam dimension stability since the foam would not collapse after that the reaction was completed.

Apparent density of RPUR foams increased with increasing of the NCO content. The foams prepared at the NCO indexes of 100 and 150 had the apparent density about of 40.0 and 49.0 kg/m^3 , respectively. The density of foams prepared from $\text{Cu}(\text{pentaen})$ and $\text{Cu}(\text{pentaen}):\text{Zn}(\text{pentaen})$ complexes were suitable for foam applications. ATR-IR spectroscopy was used to determine the NCO conversion and polyisocyanurate (PIR): polyurethane (PUR) ratio. It was found that NCO conversion of RPUR foams decreased with increasing of the NCO content. PIR: PUR ratio slightly increased with increasing of NCO content in foam formulations. Thus, this result indicated that the metal complexes could not catalyze the PIR formation.

SEM micrographs of RPUR foams catalyzed by Cu(pentaen):Zn(pentaen) had the cell size smaller than that prepared from DMCHA. Therefore, the compressive strength of RPUR foam catalyzed by Cu(pentaen):Zn(pentaen) were higher than the foam prepared from DMCHA catalyst. The compressive strength of RPUR foam catalyzed by Cu(pentaen):Zn(pentaen) increased from 228.0 to 321.5 kPa with an increasing density from 40.8 to 47.5 kg/m³. This indicated that compressive strength mainly depended on the foam density. Compressive strength of foams in parallel direction of foam rising was higher than that in perpendicular direction which indicated that RPUR foams were anisotropic materials.

Morphology of RPUR foams was obtained by SEM. The average cell size of RPUR foams increased from 367.4 to 513.2 μm when increasing the blowing agent content from 1.0 to 3.0 pbw. This result showed the decreasing of both density and compressive strength of RPUR foams.

From the relation between thermal conductivity and cell size of RPUR foams, smaller cell size improved the thermal insulation property of the RPUR foam. This is due to the decreased radiant heat transfer via trapped gases in lower foam cells in RPUR foam. Therefore, RPUR foams catalyzed by Cu(pentaen):Zn(pentaen) provided a good the thermal insulation properties than DMCHA.

All data of RPUR foam are concluded in Table 5.1.

5.2 Suggestion for future work

The suggestion for future work is to develop the synthesis of mixed metal complexes in water. They might be developed to be used as catalysts in the water-based polyurethanes.

Table 5.1 RPUR foams conclusion

Parameters	Conclusions			
	metal-amine complexes synthesized in acetone			
Reaction times	DMCHA	Cu(pentaen)	Cu(pentaen): Zn(pentaen)	Zn(pentaen)
Cream time (min)	0:22	0:28	0:27	0:25
Gel time (min)	0:32	0:45	0:53	0:57
Tack free time (min)	3:01	2:08	2:51	3:58
Rise time (min)	2:21	2:25	3:07	3:42
Catalytic reaction	Blowing and Gelling	Gelling	Blowing and Gelling	Blowing
Catalytic activity	Cu(pentaen) > Cu(pentaen):Zn(pentaen) = DMCHA > Zn(pentaen)			
Density (kg/m³)	NCO index = 100		NCO index = 150	
	38.0 - 42.0		44.0 - 49.0	
Parallel Compressive strength (kPa)	Cu(pentaen):Zn(pentaen) > DMCHA-RPUR foam			
	NCO index = 100		NCO index = 150	
DMCHA	217.5		285.8	
Cu(pentaen): Zn(pentaen)	228.0		321.5	
Parallel testing > perpendicular testing	Anisotropic materials			
Thermal insulation properties	Cu(pentaen):Zn(pentaen)-RPUR foam better than DMCHA-RPUR foam			
	Thermal conductivity (W/m K)			
DMCHA	0.0377 (W/m K)		Cell size = 497.5 (µm)	
Cu(pentaen): Zn(pentaen)	0.0363 (W/m K)		Cell size = 409.9 (µm)	

REFERENCES

- [1] Oertel, G. *Polyurethane handbook*. New York: Hanser Publishers, 1985.
- [2] Kim, S. H. and Kim, B. K. Effect of Isocyanate Index on the Properties of Rigid Polyurethane Foams Blown by HFC 365mfc. *Polym. Adv. Technol.* 19 (2008): 1729-1738.
- [3] Randall, D. and Lee, S. *The polyurethane book*. London: Jonh Wiley & Sons, 2002.
- [4] Lim, H.; Kim, S. H. and Kim, B. K. Effects of the Functionality of Polyol in Rigid Polyurethane Foams. *J. Appl. Polym. Sci.* 110 (2008): 49-54.
- [5] Lim, H.; Kim, S. H. and Kim, B. K. Effects of the hydroxyl value of polyol in rigid polyurethane foams. *Polym. Adv. Technol.* 19 (2008): 1729-1738.
- [6] Modesti, M.; Lorenzetti, A.; Simioni, F. and Checchin, M. Influence of different flame retardants on fire behaviour of modified PIR/PUR polymers. *Polym. Degrad. Stabil.* 74 (2001): 475-479.
- [7] Wood, G. *The ICI polyurethane book*. 2nd Edition. London: Jonh Wiley & Sons, 1990.
- [8] Mondal, P. and Khakhar, D. V. Hydraulic Resistance of Rigid Polyurethane Foams. II. Effect of Variation of Surfactant, Water, and Nucleating Agent Concentration on Foam Structure and properties. *J. Appl. Polym. Sci.* 93 (2004): 2830-2837.
- [9] Ashida, K. *Handbook of Polyurethane and Related Foams*. New York, Taylor & Francis Group, 2007
- [10] Hapburn, C. *Handbook of Polyurethane Elastomers*, Elsevier, Oxford, 1991.
- [11] Lee, S.T. and Ramesh N.S. *Polymeric foams*. New York: CRC Press, 2004.
- [12] Eaves D. *Handbook of Polymer Foams*. Rapra Technology Limited, UK, 2004.
- [13] Wegener, G.; Brandts, M.; Duda, L.; et al. Trends in industrial catalysis in the polyurethane industry. *Appl. Catal.* 221 (2001): 303-335.
- [14] Mondal, P. and Khakhar, D. V. Hydraulic Resistance of Rigid Polyurethane Foams. III. Effect of Variation of the Concentration of Catalysts on Foam Structure and Properties. *J. Appl. Polym. Sci.* 93 (2004): 2838-2843.

- [15] Landrock, H. *Handbook of plastic foams*. USA: Noyes Publications, 1995.
- [16] Pentrakoon, D. and Ellis, J.W. *An introduction to plastic foams*. Chulalongkorn University Press, 2005.
- [17] Ionescu M. *Handbook of Chemistry and Technology of Polyols for Polyurethanes*. Rapra Technology Limited, UK, 2005.
- [18] Modesti, M. and Lorenzetti, A. An experimental method for evaluating isocyanate conversion and trimer formation in polyisocyanurate-polyurethane foams. *Eur. Polym. J.* 37 (2001): 949-954.
- [19] Thirumal, M., S., H. and Kim, B. K.; et al. Effect of Foam Density on the Properties of Water Blown Rigid Polyurethane Foams. *J. Appl. Polym. Sci.* 108 (2008): 1810-1817.
- [20] Xiaobin, LI., Hongbin, CAO., and Yi, Zhang. Structures and physical properties of rigid polyurethane foams with water as the sole blowing agent. *Sci. Ed. J.* 49 (2008): 363-370.
- [21] Han, M. S.; Choi S. J.; Kim, J. M.; et al. Effects of Silicone Surfactant on the Cell Size and Thermal Conductivity of Rigid Polyurethane Foams by Environmentally Friendly Blowing Agents. *Macromol. Res.* 17 (2009) 44-50.
- [22] Lim, H.; Kim, S. H. and Kim, B. K. Effects of silicone surfactant in rigid polyurethane foams. *Express. Polym. Lett.* 2 (2008): 194-200.
- [23] Stirna, U. and Cabulis, U. Water-blown polyisocyanurate foams from vegetable oil polyols. *J. Cell. Plast.* 44 (2008): 139-159.
- [24] Singh, H. Sharma, T. P. and Jain, A. K. Reactivity of the Raw Materials and Their Effects on the Structure and Properties of Rigid Polyurethane Foams. *J. Appl. Polym. Sci.* 106 (2007): 1014-1023.
- [25] Seo, W. J.; Park, J. H.; Sung Y. T.; Hwang D. H.; Kim W. N. and Lee H. S. Properties of Water-Blown Rigid Polyurethane Foams with Reactivity of Raw materials.. *J. Appl. Polym. Sci.* 93 (2004): 2334-2342.
- [26] Choe, K. H.; Lee, D. S.; Seo, W. J.; and Kim, W. N. Properties of Rigid Polyurethane Foams with Blowing Agents and Catalyst. *Polym. J.* 36 (2004): 368-373.

- [27] Maris, R. V.; Tamano, Y.; Yoshimura, H. and Gay, K. Polyurethane catalysis by tertiary amines. *J. Cell. Plast.* 41 (2005): 305-322.
- [28] Shardon, H.; Irusta L. and Fernández-Berridi M. J. Synthesis of isophorone diisocyanate (IPDI) based waterborne polyurethanes: Comparison between zirconium and tin catalysts in the polymerization process. *Prog. Org. Coat.* 66 (2009): 291-295.
- [29] Strachota, A.; Strachotova, B. and Spirkova, M. Comparison of environmentally friendly, selective polyurethane catalysts. *Mater. Manuf. Process.* 23 (2008): 566-570.
- [30] Kurnoskin, A. V. Metalliferous epoxy chelate polymers: 1. synthesis and properties. *Polymer.* 34 (1993): 1060-1067.
- [31] Kurnoskin, A. V. Metalliferous epoxy chelate polymers: 2. influence of structural fragments on properties. *Polymer*, 34 (1993): 1068-1076.
- [32] Inoue, Sh. I.; Nagai, Y. and Okamoto, H. Amine-manganese complexes as a efficient catalyst for polyurethane syntheses. *Polym. J.* 34 (2002): 298-301.
- [33] Pengjam, W. Saengfak, B. Ekgasit, S. and Chantarasiri, N. Copper–Amine Complexes as New Catalysts for Rigid Polyurethane Foam Preparations, *J. Appl. Polym. Sci.*, in press.
- [34] Yan, Pang, H. Yang, X. Zhang, R and Liao, B. Preparation and Characterization of Polyurethane Foams from Liquefied Cornstalk Polyol. *J. Appl. Polym. Sci.* 110 (2008): 1099-1111.
- [35] Tu, Y. C.; Fan, H., Suppes, G. J. and Hsieh, F. H. Physical Properties of Water-Blown Rigid Polyurethane Foams Containing Epoxidized Soybean Oil in Different Isocyanate Indices. *J. Appl. Polym. Sci.* 114 (2009): 2577-2583.
- [36] Romero, R. R.; Robert, A.; Grigsby, J. R.; Ernest, L.; Rister, J. R.; Pratt, J. K. and Ridgway, D. A study of the reaction kinetics of polyisocyanurate foam formulations using real-time FTIR. *J. Cell. Plast.* 41 (2005): 339-359.
- [37] Cateto, C. A.; Barreiro, M. F. and Rodrigues, A.E. Monitoring of lignin-based polyurethane synthesis by IR-ATR. *Ind. Crop. Prod.* 27 (2008): 168-174.
- [38] Jones, S. A.; Scott, K. W.; Willoughby, B. G. and Sheard, E. A. Monitoring of polyurethane foam cure. *J. Cell. Plast.* 38 (2002): 285-299.

- [39] Saha, M. C.; Kabir, M. E. and Jeelani, S. Enhancement in thermal and mechanical properties of polyurethane foam infused with nanoparticles, *Mat. Sci. Eng.* 479 (2008): 213–222.
- [40] Seo, W. J.; Jung H. C.; Hyun, J. C.; Kim, W. N.; et al. Mechanical, Morphological and Thermal Properties of Rigid Polyurethane Foams Blown by Distilled Water. *J. Appl. Polym. Sci.* 90 (2003): 12-21.
- [41] Saint-Michel, F.; Chazeau, L.; Cavaille, J.-Y. and Chabert, E. Mechanical properties of high density polyurethane foams: I. Effect of the density. *Compos. Sci. Technol.* 66 (2006): 2700–2708.
- [42] Goto, A.; Yamashita, K.; Nonomura, Ch. and Yamaguchi, K. Modeling of cell structure in polyurethane foam. *J. Cell. Plast.* 40 (2004): 481-488.
- [43] Hawkins, M. C.; O’Toole, B. and Jackovich, D. Cell morphology and mechanical properties of rigid polyurethane foam. *J. Cell. Plast.* 41 (2005): 267-285.
- [44] Yin, B.; Li, Z.-M.; Quan, H.; Yang, M.-B.; Zhou, Q.-M. and Tian, Ch.-R.; Wang J.-H. Morphology and mechanical properties of nylon-10,10-filled rigid polyurethane foams. *J. Elast. Plast.* 36 (2004); 333-349.
- [45] Thimural, M.; Khastgir, D.; Singha, N. K. and Manjunath, B. S. Effect of a Nanoclay on the mechanical, Thermal and Flame Retardant Properties of Rigid Polyurethane Foam. *J. Macromol. Sci.* 46 (2009): 704-712.
- [46] Trovati, G.; Sanches, E. A.; Neto, S. C.; et al. Characterization of Polyurethane Resins by FTIR, TGA and XRD. *J. Appl. Polym. Sci.* 115 (2009): 263-268.

APPENDICES

Appendix A

NCO index and NCO conversion Calculations

NCO index calculation

#Example Calculate the parts by weight (pbw) of pure PMDI (MR-200), molar mass = 366.99, functionality = 2.7 at an isocyanate indexes of 100, 130, 150 and 170 required to react with the following formulation:

Formulation (pbw)	Part by weight (g)
Raypol [®] 4221 (OHV = 440 mgKOH/ g, functionality = 4.3)	100.0
Catalysts	1.0
Surfactant	2.5
Blowing agent (water, M _w = 18 g/mole, functionality = 2)	2.0
PMDI (MR-200), NCO indexes of 100, 130, 150 and 170	?

$$\text{Equivalent weight of raypol 4221} = \frac{56.1}{440} \times 1000 = 127.5$$

$$\text{Equivalent weight of water} = \frac{18}{2} = 9.0$$

Note: Surfactants and catalysts are neglected in stoichiometric calculations because they do not react with NCO groups.

$$\text{Number of equivalent in formulation} = \frac{\text{parts by weight (pbw)}}{\text{equivalent weight}}$$

Equivalent in the above formulation:

$$\text{Polyol (Raypol 4221)} = \frac{100}{127.5} = 0.784$$

$$\text{Water (blowing agent)} = \frac{2.0}{9.0} = 0.222$$

$$\text{Total equivalent weight} = 1.006$$

For stoichiometric equivalence, PMDI pbw is total equivalent \times equivalent weight because PMDI reacts with polyol and water.

thus:

$$\text{PMDI (pbw)} = 1.006 \times \frac{\text{PMDI molar mass}}{\text{functionality}} = 1.006 \times \frac{366.99}{2.7} = 136.7$$

Note: 136.7 defines the isocyanate quantity at 100 index

where;

$$\text{Isocyanate index} = \frac{\text{actual amount of isocyanate}}{\text{theoretical amount of isocyanate}} \times 100$$

thus:

$$\# \text{ Isocyanate index} = 100;$$

$$\text{Isocyanate actual} = \frac{136.7}{100} \times 100 = 136.7 \text{ pbw}$$

$$\# \text{ Isocyanate index} = 130;$$

$$\text{Isocyanate actual} = \frac{136.7}{100} \times 130 = 177.8 \text{ pbw}$$

$$\# \text{ Isocyanate index} = 150;$$

$$\text{Isocyanate actual} = \frac{136.7}{100} \times 150 = 205.1 \text{ pbw}$$

$$\# \text{ Isocyanate index} = 170;$$

$$\text{Isocyanate actual} = \frac{136.7}{100} \times 170 = 232.5 \text{ pbw}$$

Table A1 Isocyanate quantity at different NCO indexes in the above formulations

Formulations (pbw)	NCO index			
	100	130	150	170
Polyol (Raypol [®] 4221)	100	100	100	100
Catalysts	1.0	1.0	1.0	1.0
Surfactant	2.5	2.5	2.5	2.5
Blowing agent	2.0	2.0	2.0	2.0
PMDI (MR-200)	137	178	205	233

NCO conversion calculation

The NCO conversion can be calculated by FTIR method, defined as the ratio between isocyanate peak area at time t and isocyanate peak area at time 0, following equation:

$$\text{Isocyanate conversion (\%)} = \left[1 - \frac{\text{NCO}^f}{\text{NCO}^i} \right] \times 100$$

where;

NCO^f is the area of isocyanate absorbance peak area at time t

NCO^i is the area of isocyanate absorbance peak area at time 0

Quantity of free NCO in RPUR foams were normalized by aromatic ring absorption band at 1595 cm^{-1} .

Table A2 Free NCO absorbance peak area in PMDI (MR-200) from ATR-IR

PMDI (MR-200) spectra	NCO Absorbance peak area Normalized @ 1.0 Ar-H peak area
1	98.886
2	97.547
3	97.274
Average (NCO^i); ATR-IR	97.9

Example Calculate the conversion of isocyanate (α) and PIR: PUR of rigid polyurethane foams catalyzed by Cu(pentaen) catalyst at NCO index 100

Conversion of isocyanate (%)Data at **Table A2**Absorbance peak area of initial NCO = 97.9 = NCOⁱ

The data from **Table A4** at NCO index 100, absorbance peak area of free NCO was normalized by aromatic ring quantity:

Absorbance peak area of final NCO = 0.330 = NCO^f

thus,

$$\begin{aligned} \text{Conversion of isocyanate (\%)} &= \left[1 - \frac{\text{NCO}^f}{\text{NCO}^i} \right] \times 100 \\ &= \left[1 - \frac{0.330}{97.9} \right] \times 100 \end{aligned}$$

$$\% \text{ NCO conversion} = 99.7$$

PIR:PUR

Absorbance peak area of PIR (polyisocyanurate) = 0.862

Absorbance peak area of PUR (polyurethane) = 4.739

$$\text{thus, PIR:PUR} = \frac{0.862}{4.739} = 0.182$$

Table A3 NCO conversion of RPUR foam catalyzed by DMCHA at different NCO indexes

NCO indexes	Peak Area					NCO conversion (%)	PIR/PUR
	NCO 2277 cm ⁻¹	Ar-H 1595 cm ⁻¹	PIR 1415 cm ⁻¹	PUR 1220 cm ⁻¹	NCO ^f (Ar-H=1.0)		
100	0.604	1.928	1.055	5.618	0.313	99.7	0.188
130	0.946	2.094	1.118	5.304	0.452	99.5	0.211
150	1.556	2.295	1.129	5.013	0.678	99.3	0.225

Table A4 NCO conversion of RPUR foam catalyzed by Cu(pentaen) at different NCO indexes

NCO indexes	Peak Area					NCO conversion (%)	PIR/PUR
	NCO	Ar-H	PIR	PUR	NCO ^f		
	2277 cm ⁻¹	1595 cm ⁻¹	1415 cm ⁻¹	1220 cm ⁻¹	(Ar-H=1.0)		
100	0.621	1.883	0.862	4.739	0.330	99.7	0.182
130	0.868	1.887	0.816	4.146	0.460	99.5	0.197
150	1.723	1.807	0.887	4.096	0.954	99.0	0.217

Table A5 NCO conversion of RPUR foam catalyzed by Cu(pentaen):Zn(pentaen) at different NCO indexes

NCO indexes	Peak Area					NCO conversion (%)	PIR/PUR
	NCO	Ar-H	PIR	PUR	NCO ^f		
	2277 cm ⁻¹	1595 cm ⁻¹	1415 cm ⁻¹	1220 cm ⁻¹	(Ar-H=1.0)		
100	0.472	1.901	1.023	5.986	0.248	99.7	0.171
130	0.73	1.66	0.813	3.991	0.440	99.6	0.204
150	1.067	1.587	0.790	3.475	0.672	99.3	0.227

Table A6 NCO conversion of RPUR foam catalyzed by Zn(pentaen) at different NCO indexes

NCO indexes	Peak Area					NCO conversion (%)	PIR/PUR
	NCO	Ar-H	PIR	PUR	NCO ^f		
	2277 cm ⁻¹	1595 cm ⁻¹	1415 cm ⁻¹	1220 cm ⁻¹	(Ar-H=1.0)		
100	0.629	1.513	0.732	3.947	0.416	99.6	0.185
130	1.159	1.774	0.858	4.163	0.653	99.3	0.206
150	1.416	1.816	0.896	4.020	0.780	99.2	0.223

Table A7 NCO conversion of RPUR foam catalyzed by W_Cu(pentaen) at different NCO indexes

NCO indexes	Peak Area					NCO conversion (%)	PIR/PUR
	NCO	Ar-H	PIR	PUR	NCO ^f		
	2277 cm ⁻¹	1595cm ⁻¹	1415cm ⁻¹	1220cm ⁻¹	(Ar-H=1.0)		
100	0.728	1.862	0.903	4.765	0.391	99.6	0.190
130	0.974	1.443	0.791	3.588	0.675	99.3	0.220
150	2.034	1.827	0.947	4.217	1.113	98.9	0.225

Table A8 NCO conversion of RPUR foam catalyzed by W_Cu(pentaen):Zn(pentaen) at different NCO indexes

NCO indexes	Peak Area					NCO conversion (%)	PIR/PUR
	NCO	Ar-H	PIR	PUR	NCO ^f		
	2277 cm ⁻¹	1595 cm ⁻¹	1415 cm ⁻¹	1220 cm ⁻¹	(Ar-H=1.0)		
100	0.984	1.596	0.896	4.746	0.617	99.4	0.189
130	1.073	1.443	0.702	3.573	0.744	99.2	0.196
150	2.243	1.989	0.902	4.376	1.128	98.8	0.206

Table A9 NCO conversion of RPUR foam catalyzed by W_Zn(pentaen) at different NCO indexes

NCO indexes	Peak Area					NCO conversion (%)	PIR/PUR
	NCO	Ar-H	PIR	PUR	NCO ^f		
	2277 cm ⁻¹	1595 cm ⁻¹	1415 cm ⁻¹	1220 cm ⁻¹	(Ar-H=1.0)		
100	0.853	1.621	0.759	3.988	0.526	99.5	0.190
130	1.085	1.445	0.701	3.539	0.751	99.2	0.198
150	1.779	1.711	0.841	4.090	1.040	98.9	0.206

Appendix B

Compression Curves and Data

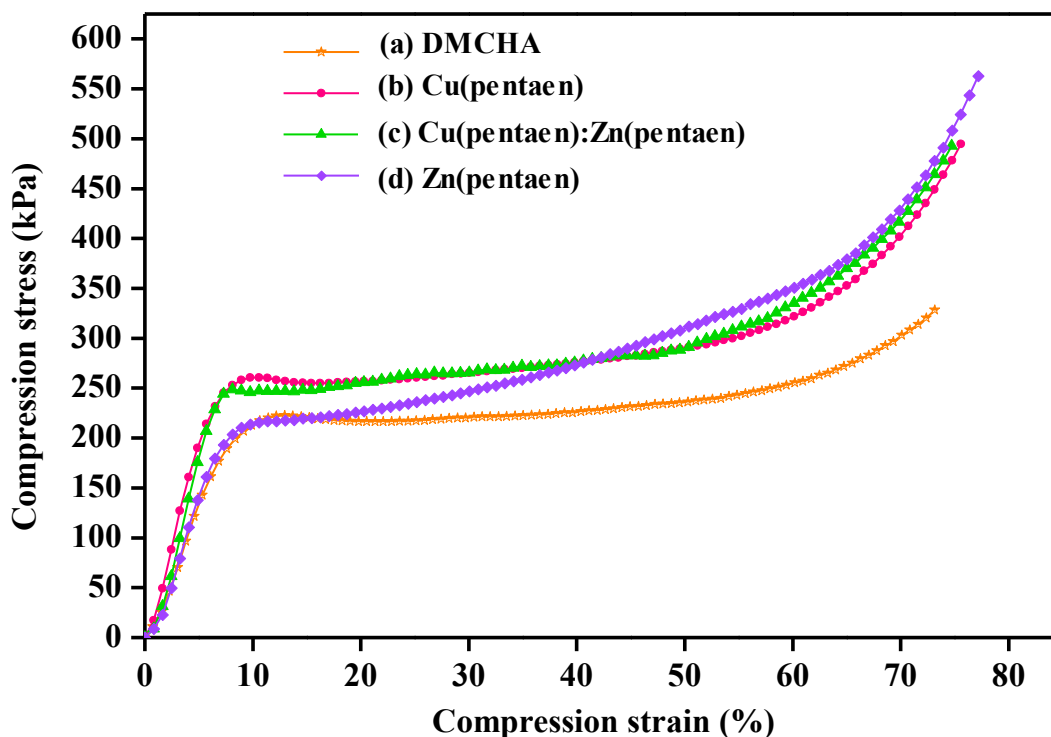


Figure B1 Perpendicular compression stress-strain curve of RPUR foams catalyzed by different catalysts at NCO index of 150

Table B1 Reaction times and physical properties of RPUR foams catalyzed by metal acetate and amine

Formulations (pbw)	Starting materials at NCO index of 100			
	Cu(OAc) ₂	Zn(OAc) ₂	pentaen	Non-catalyst
<i>Reaction times</i>				
Cream time (min.)	1:21	1:10	-	1:12
Gel time (min.)	2:47	2:44	-	2:57
Tack free time (min.)	24:13	20:25	-	27:21
Rise time (min.)	18:32	15:10	-	17:03
<i>Density (kg/m³)</i>	63.4	57.9	-	-
<i>External appearance</i>	Low blowing	Low blowing	-	Brittle foam

Table B2 Formulations, reaction times, physical and mechanical properties of RPUR foams catalyzed by different metal complexes

Formulations (pbw)	Catalysts at different NCO indexes											
	DMCHA (Ref.)						Cu(pentaen)					
	100		130		150		100		130		150	
Raypol [®] 4221	100		100		100		100		100		100	
Catalysts	1.0		1.0		1.0		1.0		1.0		1.0	
B8460	2.5		2.5		2.5		2.5		2.5		2.5	
H ₂ O	2.0		2.0		2.0		2.0		2.0		2.0	
MR-200	137		178		205		137		178		205	
Efficiency parameters	Data	S.D.	Data	S.D.	Data	S.D.	Data	S.D.	Data	S.D.	Data	S.D.
<i>Reaction times</i>												
Cream time (min.)	0:22	0.6	0:23	0.6	0:24	0.6	0:28	0.6	0:29	1.0	0:30	0.6
Gel time (min.)	0:32	0.6	0:36	1.0	0:41	0.6	0:45	1.0	0:50	1.0	0:57	0.6
Tack free time (min.)	3:01	1.0	3:35	1.0	4:02	1.0	2:08	1.5	2:19	1.5	2:28	1.5
Rise time (min.)	2:21	1.5	2:40	1.0	3:05	1.0	2:25	2.5	2:32	2.5	2:40	2.0
<i>Density</i>												
Density (kg/m ³)	39.7	0.5	43.4	0.7	46.7	0.8	42.4	0.5	46.3	0.5	49.1	0.7
<i>Mechanical properties</i>												
// Compressive strength (kPa)	197.2	-	250	-	285.8	-	-	-	-	-	353.2	-
// Compressive modulus (kPa)	-	-	-	-	217.5	-	-	-	-	-	260.7	-

Table B3 Formulations, reaction times, physical and mechanical properties of RPUR foams catalyzed by different metal complexes

Formulations (pbw)	Catalysts at different NCO indexes											
	Cu(pentaen):Zn(pentaen)						Zn(pentaen)					
	100		130		150		100		130		150	
Raypol [®] 4221	100		100		100		100		100		100	
Catalysts	1.0		1.0		1.0		1.0		1.0		1.0	
B8460	2.5		2.5		2.5		2.5		2.5		2.5	
H ₂ O	2.0		2.0		2.0		2.0		2.0		2.0	
MR-200	137		178		205		137		178		205	
Efficiency parameters	Data	S.D.	Data	S.D.	Data	S.D.	Data	S.D.	Data	S.D.	Data	S.D.
<i>Reaction times</i>												
Cream time (min.)	0:27	0.6	0:28	0.6	0:29	0.6	0:25	0.6	0:26	0.6	0:27	0.6
Gel time (min.)	0:53	1.0	1:00	1.0	1:07	1.0	0:57	1.5	1:05	1.0	1:13	1.0
Tack free time (min.)	2:51	1.5	3:03	1.0	3:13	1.5	3:58	1.0	4:14	1.5	4:32	1.5
Rise time (min.)	3:07	2.1	3:12	2.0	3:20	2.5	3:42	2.5	3:57	2.1	4:18	2.5
<i>Density</i>												
Density (kg/m ³)	40.8	0.9	44.7	0.7	47.5	0.6	38.6	1.0	42.7	1.0	45.5	0.8
<i>Mechanical properties</i>												
// Compressive strength (kPa)	228.0	-	288.6	-	321.5	-	-	-	-	-	280.8	-
// Compressive modulus (kPa)	-	-	-	-	247.4	-	-	-	-	-	215.8	-

Table B4 Formulations, reaction times and physical properties of RPUR foams catalyzed by different metal complexes

Formulations (pbw)	Catalysts at different NCO indexes											
	DMCHA (Ref.)						W_Cu(pentaen)					
	100		130		150		100		130		150	
Raypol [®] 4221	100		100		100		100		100		100	
Catalysts	1.0		1.0		1.0		1.0		1.0		1.0	
B8460	2.5		2.5		2.5		2.5		2.5		2.5	
H ₂ O	2.0		2.0		2.0		2.0		2.0		2.0	
MR-200	137		178		205		137		178		205	
Efficiency parameters	Data	S.D.	Data	S.D.	Data	S.D.	Data	S.D.	Data	S.D.	Data	S.D.
<i>Reaction times</i>												
Cream time (min.)	0:22	0.6	0:23	0.6	0:24	0.6	0:26	0.6	0:27	0.6	0:28	0.6
Gel time (min.)	0:32	1.0	0:36	1.0	0:41	1.0	0:39	1.0	0:45	1.0	0:50	1.0
Tack free time (min.)	3:01	1.5	3:35	1.5	4:02	1.5	1:47	1.5	1:58	1.5	2:08	1.5
Rise time (min.)	2:21	2.1	2:40	2.1	3:05	2.0	2:03	2.1	2:11	2.0	2:11	2.1
<i>Density</i>												
Density (kg/m ³)	39.7	0.7	43.4	1.0	46.7	0.6	41.8	0.8	45.5	0.7	48.6	1.0

Table B5 Formulations, reaction times and physical properties of RPUR foams catalyzed by different complexes

Formulations (pbw)	Catalysts at different NCO indexes											
	W_Cu(pentaen):Zn(pentaen)						W_Zn(pentaen)					
	100		130		150		100		130		150	
Raypol [®] 4221	100		100		100		100		100		100	
Catalysts	1.0		1.0		1.0		1.0		1.0		1.0	
B8460	2.5		2.5		2.5		2.5		2.5		2.5	
H ₂ O	2.0		2.0		2.0		2.0		2.0		2.0	
MR-200	137		178		205		137		178		205	
Efficiency parameters	Data	S.D.	Data	S.D.	Data	S.D.	Data	S.D.	Data	S.D.	Data	S.D.
<i>Reaction times</i>												
Cream time (min.)	0:25	1.0	0:26	1.0	0:27	1.0	0:23	1.0	0:24	1.0	0:25	1.0
Gel time (min.)	0:47	1.0	0:53	1.0	1:01	1.0	0:50	1.0	0:58	1.0	1:06	1.0
Tack free time (min.)	2:30	1.5	2:44	2.0	2:58	1.5	3:41	2.0	3:57	2.0	4:12	2.0
Rise time (min.)	2:48	2.0	3:01	2.5	3:14	2.5	3:30	2.0	3:42	2.0	4:06	2.5
<i>Density</i>												
Density (kg/m ³)	40.1	0.8	43.8	1.0	47.1	0.8	37.8	0.7	42.0	0.7	44.8	0.8

Table B6 Formulations, reaction times and physical properties of RPUR foams catalyzed by different complexes

Formulations (pbw)	Catalysts at NCO index 100											
	Added Ethylenediamine (en)						Added Triethylenehexamine (trien)					
	Cu(pentaen)		Zn(pentaen)		Cu:Zn(pentaen)		Cu(pentaen)		Zn(pentaen)		Cu:Zn(pentaen)	
RaypoI [®] 4221	100		100		100		100		100		100	
Catalysts	1.0		1.0		1.0		1.0		1.0		1.0	
B8460	2.5		2.5		2.5		2.5		2.5		2.5	
H ₂ O	2.0		2.0		2.0		2.0		2.0		2.0	
MR-200	137		137		137		137		137		137	
Efficiency parameters	Data	S.D.	Data	S.D.	Data	S.D.	Data	S.D.	Data	S.D.	Data	S.D.
<i>Reaction times</i>												
Cream time (min.)	0:26	0.6	0:23	0.6	0:25	1.0	0:27	1.0	0:24	1.0	0:26	0.6
Gel time (min.)	0:39	1.0	0:48	1.0	0:44	1.0	0:43	1.0	0:51	1.0	0:48	1.0
Tack free time (min.)	1:48	1.5	3:35	1.5	2:28	2.0	1:58	1.5	3:46	1.5	2:47	1.5
Rise time (min.)	2:05	2.5	3:20	2.0	2:43	2.0	2:11	2.1	3:32	2.0	2:58	2.1
<i>Density</i>												
Density (kg/m ³)	37.3	0.9	34.7	1.0	36.5	0.7	38.1	0.8	35.7	1.0	37.6	0.8

VITAE

Name : Miss Ruchuon Promnimit
Date of birth : May 2, 1986
Nationality : Thai
Address : 157, Moo 12, Chuaplerng, Prasat, Surin, 32140
University Education : Bachelor's Degree from Department of Chemistry, Faculty of Science, Srinakarinwirot University, 2006-2009

Master's Degree from Program in Petrochemistry and Polymer Science, Faculty of Science, Chulalongkorn University, 2009-2011

Conference attendance: Poster presentation "Preparation of Rigid Polyurethane Foam catalyzed by using Mixed Metal Complexes and Pentaethylenhexamine as Catalysts" at The 20th Thaksin University Annual Conference: Thai Society Development With Creative Research in J.B. Hotel Hat-Yai, Songkhla, Thailand.

